PETROLOGY AND SEDIMENTATION OF THE ARCHEAN QUETICO METASEDIMENTS IN THE ATIKOKAN-MINE CENTRE AREA, NORTHWESTERN ONTARIO

A THESIS
SUBMITTED TO THE FACULTY OF THE GRADUATE SCHOOL
OF THE UNIVERSITY OF MINNESOTA

BY
FRANK PEZZUTTO

IN PARTIAL FULFILLMENT OF THE REQUIREMENTS
FOR THE DEGREE OF
MASTER OF SCIENCE

DECEMBER, 1988

ABSTRACT

Petrology and Sedimentation of the Archean Quetico Metasediments in the Atikokan-Mine Centre Area, Northwestern Ontario

The Quetico Subprovince in the Atikokan-Mine Centre region of Northwestern Ontario comprises an Archean gneiss-granite superbelt between the Wabigoon and the Wawa-Shebandowan Subprovinces to the north and south, respectively. A one-to two-kilometer wide marginal zone of low-grade metasedimentary rocks parallels the Quetico fault along the northern portion of the Quetico Subprovince in the study area. These metasediments are dominated by the resedimented facies association of greywacke, pebbly sandstone, mudstone and conglomerate. The metagreywackes are regularly bedded and graded and display sedimentary features typical of turbidite deposition.

The stratigraphic nomenclature in the Rainy Lake area which was established at the beginning of the century by A.C. Lawson can still be applied, although the stratigraphic relationships have been reversed. Poulsen and others (1980) have shown unequivocally that the Coutchiching Series (of which the Quetico Metasediments may be correlative) is not the oldest unit in the area because it overlies the Keewatin metavolcanic unit. However, the relationships between the Quetico metasediments, the Seine Series, and the Steep Rock Series still need to be resolved and and zircon geochronology should help in correlating these units.

All rocks in the Quetico Subprovince have undergone at least greenschist facies metamorphism. The metasediments have been deformed, progressively metamorphosed southward and migmatized toward a central axis so that the original textures and most of the sedimentary features have been obliterated. The core of the Quetico Subprovince is made up of metasedimentary migmatite remnants, amphibolite, and granitic intrusives, many of anatectic origin.

Bedding stikes east and dips are nearly vertical. Two episodes of folding have been recognized in the eastern and central portions of the study area. Three sets of folds have been recognized along the western margin. An initial folding episode produced recumbent folds with an associated early shistosity (S_1). This early schistosity was modified by a second generation of tight to isoclinal folds which produced a penetrative and almost perfectly planar schistosity (S_2). Lineations found in the bedding planes trace the attitudes of fold axes and plunge moderately to steeply to the east and west. Along the western margin of the study area, kinks and small chevron folds are related to the folding of the S_2 schistosity around steeply dipping S_3 axial fold surfaces.

In the eastern half of the study area, relatively thick, graded metagreywacke beds are prominent; thirty kilometers to the west along Highway 11, turbidite beds become thinner and more silt-and mud-rich. In the western half of the study area, interlaminated siltstone and mudstone packages are more common, as are Bouma B and DE sequences. Areal variations in the relative proportions of lithologic types and in the character of Bouma sequences all indicate a general east to west facies transition from proximal near Atikokan (mid-fan), to distal (lower-fan) near Mine Centre.

Modal analyses of 41 metagreywacke and pebbly sandstone samples reveal that reworked rhyolite-dacite volcanic rocks and coeval tonalitic intrusives were major sediment sources. Mafic volcanics, chert, slate, minor potassic granite and possibly basement were additional sources and point to a mixed provenance as confirmed by QmFLt plots. QFL plots indicate an orogenic source for much of the detritus but this inference is suspect. A dissected magmatic arc is the logical choice to explain a mixed provenance.

The sediments may have been derived by the rapid erosion of unconsolidated material on volcanic edifices and associated coeval tonalitic plutons. Transportation of detritus to unstable basin margins was likely accomplished by high velocity streams. The temporary clastic piles were likely jarred loose and transported downslope into back-arc or fore-arc environments.

Heavy mineral analysis reveals the vast majority of the heavy minerals present to be metamorphic species such as biotite, apatite, actinolite and epidote. A zircon varietal study reveals dominantly pink to purple (hyacinth) and brown (malacon) zircons. Most zircons appear as short stubby simple prisms with pyramidal ends. Length to width ratios are commonly equal to or less than 2. Unzoned varieties are more common than those that are zoned or contain a dark core.

U-Pb geochronology has provided an absolute time framework for deposition of the Quetico Metasediments. Zircons recovered from the Blalock pluton define a 2688 +4/-3 Ma minimum age for sediment deposition. The youngest detrital zircons from the Quetico Metasediments are in the range of 2700 +/-3 Ma; the oldest zircons are approximately 3004 Ma. These two dates roughly bracket the age of sediment deposition although it is likely that most sedimentation took place in the range of 2700 to 2750 Ma because this is the time of extensive volcanism and plutonism in this part of the Superior Province. Preliminary U-Pb analyses from adjacent greenstone and batholithic terranes have yielded age dates that correlate with those determined from detrital zircons recovered from the Quetico Metasediments. These units must be regarded as possible sediment sources.

ACKNOWLEDGEMENTS

The author would like to express his feelings of gratitude to the many individuals who have given freely of their time and knowledge in helping to make this thesis possible. To each, I extend my sincere thanks for the cooperation that was so vital to the progress and completion of this study. I regret that each cannot be cited individually, but I trust that each will find a real measure of reward in the knowledge that they shared in this undertaking.

Funding for this study was provided through a research grant from the Geological Survey of Canada, Project Code 850014. The author would like to thank Dr. Richard W. Ojakangas of the University of Minnesota, Duluth, and Dr. Kenneth D. Card of the Geological Survey of Canada for their field guidance and constructive criticism. The author is also indebted to Dr. J.C. Nichol, Dr. D.G. Darby and Dr. T.B. Holst of the University of Minnesota, Duluth for being members of the thesis committee. Capable field assistance was provided by D. Aspie, D. Williams and R. Vecchio. Sincere thanks goes to G.C. Patterson, C.E. Kemp, J. Giguere, M. Engle, S. Hauck, J.J. Heine, and J.S. Walker for research assistance. Dr. D.W. Davis of the Royal Ontario Museum, Toronto was very generous in providing geochronologic data. Special thanks goes to Laura Marie Sjogren for her patience and support. Finally, I would like to dedicate this thesis to my parents, whose love and encouragement are forever inspiring.

TABLE OF CONTENTS

LIST OF FIGURES

LIST OF TABLES

LIST OF PLATES

Chapter 1

INTRODUCTION

Sedimentation on the Canadian Shield during Archean time was dominated by the resedimented (turbidite) facies association of greywacke, mudstone-siltstone and conglomerate (Ojakangas, 1985). In the Superior Province, deposition of these immature sediments took place in the greenstone belts of the Abitibi, Wawa-Shebandowan, Wabigoon, Uchi and Sachigo Subprovinces. In addition, similar sediments may have been deposited in distal environments in what are now the English River, Pontiac and Quetico Gneiss Subprovinces.

The study of Archean rocks is complicated by deformation, metamorphism and faulting. Most metasedimentary sequences are metamorphosed to greenschist and locally to amphibolite facies, but macroscopic sedimentary structures such as bedding and grading are commonly preserved. Most original sedimentary textures and structures have been obliterated in the gneiss belts. Faults commonly parallel the trends of the rock units; strike-slip faults are a common feature along subprovince boundaries. Along these major east-west fault zones there is commonly a juxtaposition of high-grade and low-grade terranes; this, coupled with contrasting structural styles and trends makes correlation between blocks difficult (Card and Ciesielski, 1986). In addition, metasedimentary sequences are commonly intruded by diapirs of granite (Ayres, 1978).

The study of Archean sedimentation has numerous aspects. Of great importance is the determination of the depositional environment based

upon original textures, stratigraphic relationships, sedimentary structures, and geometry. Also of great importance is the determination of provenance based upon petrographic (modal) analyses complemented by geochemical and paleocurrent data. Both provenance and paleocurrent direction are a function of tectonic setting.

Detailed interpretations of detrital modes in clastic sediments can yield insights into geologic history that can be gained in no other way (Dickinson, 1970). The composition of clastic sediments can be used to estimate crustal composition as well as provenance and can be employed as a constraint on models of crustal evolution and synthesis through geologic time (Sawyer, 1986).

The identification of detrital grains, especially fine-grained lithic fragments, is of great importance because their relative proportions are direct guides to the nature of the source rocks in the study area. This is especially true in areas of active volcanism where source terranes have undergone rapid erosion and deposition.

In the Superior Province, studies of supracrustal rocks have yielded insights into the nature of the composition, tectonism and development of the Archean crust. Studies of volcanic-granitic and metasedimentary-gneiss terranes have been successful in integrating the history of the Superior Province into a regional synthesis (Percival and Stern, 1984).

The objective of this study is to do a sedimentological analysis of the Quetico Metasediments in one part of the Quetico gneissic subprovince. Detrital zircon geochronology has been successfully

applied to metavolcanic belts of the western Superior Province (Davis and Edwards, 1982), permitting correlation of the Wabigoon and Wawa-Shebandowan metavolcanic subprovinces. Zircon assemblages of the Quetico Metasediments are now being age-dated in order to correlate with adjacent terranes. This investigation will enhance the understanding concerning the origin of the Quetico metasediments, characteristics of the source rocks and early crustal interactions in this portion of the Superior Province.

In order to address these objectives, fieldwork was carried out in 1986 in an area of low-grade metasediments in the northern part of the Quetico Subprovince adjacent to the Wabigoon Volcanic-Plutonic Subprovince. It is located near the town of Atikokan, approximately 250 km west of Thunder Bay, Ontario. The study area covers approximately 350 km^2 bounded by latitude 48° 42' to 48° 46'N and longitude 91° 10' to 92° 10'W (Fig. 1.1).

Outcrops along Highways 11 and 11B and along lakes and streams of the Seine River system were investigated in detail; rock type, bed thickness, grain-size and data pertaining to Bouma sequences were recorded at each outcrop. These data, along with local structural information and younging directions, were utilized in constructing six stratigraphic sections. More than 100 samples were collected for petrographic analysis, and six bulk samples were collected for heavy mineral separation.

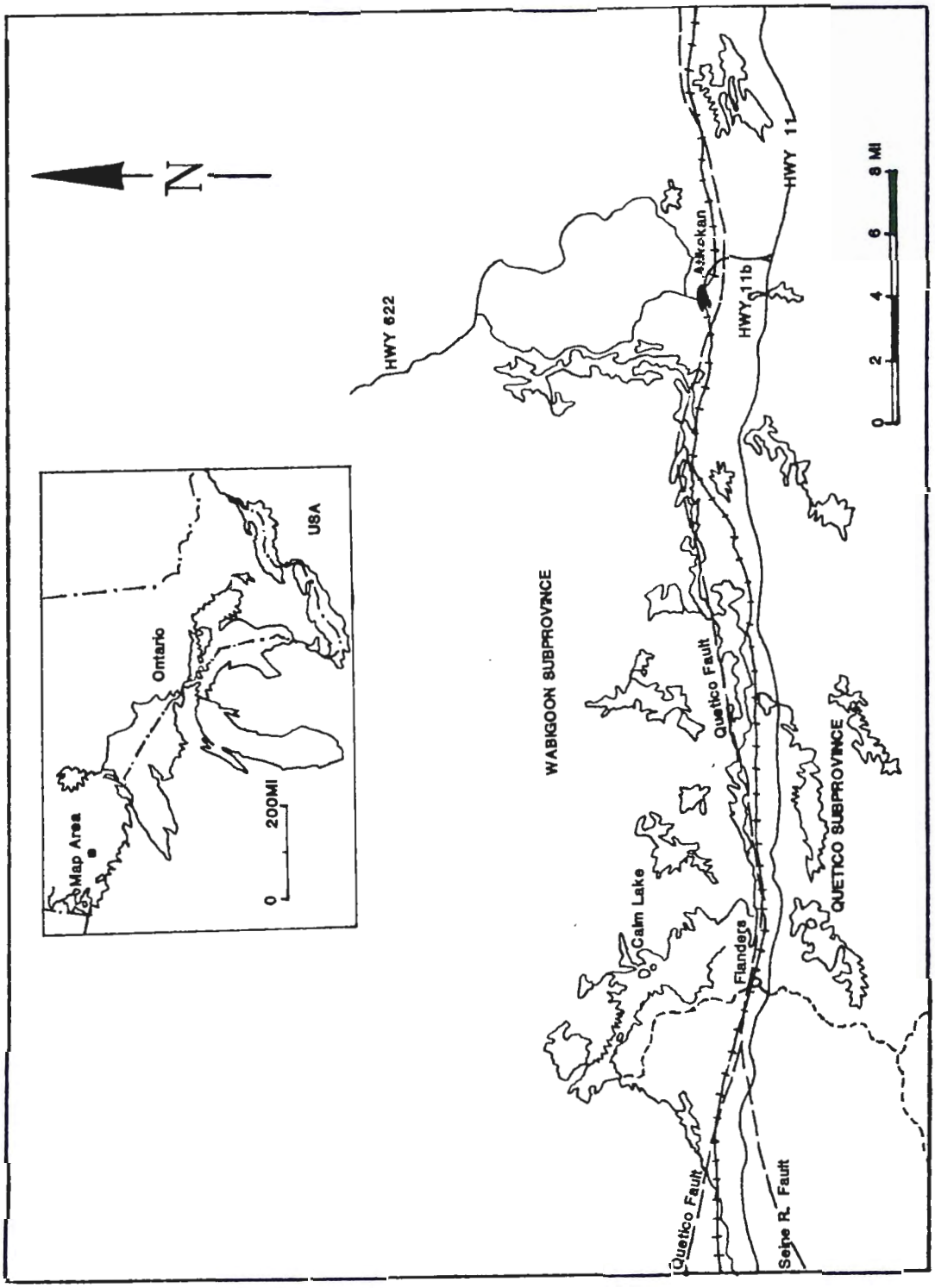

Figure 1.1 Location map of the study area.

Regional Geology

The Superior Province with an area of more than two million km^2 surrounding James Bay and southern Hudson Bay, contains most of the Archean (>2500 Ma) rocks of the Canadian Shield. The Superior Province has been subdivided into ten east-trending linear subprovinces (Fig. 1.2) on the basis of combinations of structural trends and styles, lithologies, absolute and relative ages of rock units, tectonic events, metallogenesis, metamorphic grade and geophysical characteristics (Goodwin, 1972; Card and Ciesielski, 1986). These criteria have led to the recognition of two different types of lithotectonic domains. Greenstone belts of volcanic-sedimentary rocks with granitic plutons have been classified as volcanic-granite superbelts or subprovinces. Gneiss belts and their associated granitic plutons have been grouped into gneiss-granite superbelts or subprovinces. These represent the many crustal components assembled in late Archean time to form the Superior Province.

Metasedimentary terranes, the gneiss-granite superbelts (the Quetico, the English River and the Pontiac Subprovinces), may represent major turbidite sedimentary basins that are possibly peripheral to the volcanic-granite superbelts (Sawyer, 1983). These metasedimentary (i.e., paragneiss) terranes are less widespread than the volcanic-granite superbelts and are characterized by amphibolite and locally by granulite facies metamorphism (Blackburn et al., 1985).

The 20 to 100 km wide Quetico Subprovince of the Canadian Shield comprises a major Archean metasedimentary superbelt between the

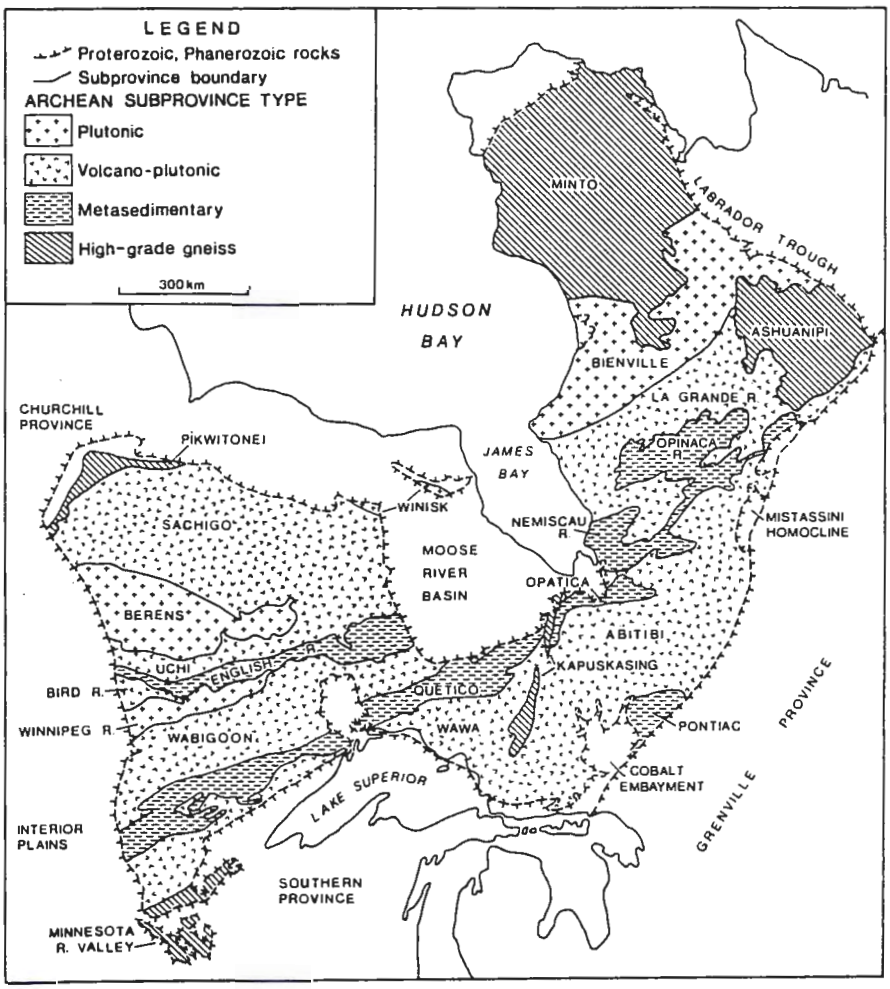

Figure 1.2 Subdivisions of the Superior Province showing subprovince type and location (From Card and Ciesielski, 1986).

Wabigoon and the Wawa-Shebandowan superbelts to the north and south, respectively. The Quetico superbelt extends at least 1200 km from beneath cover in the Fort Frances, Ontario area, to the Kapuskasing Structural Zone, and may extend 800 km further to the east as the Opatica belt.

In the study area, two major faults, the Quetico fault and the Rainy Lake-Seine River fault, separate three areas of different lithology, structural style and metamorphic grade (Fig. 1.1). These faults, which form subprovince boundaries, are representative of a major east-west dextral transcurrent fault system that extends through much of the Superior Province (Card and Ciesielski, 1986). Between the Quetico and the Rainy Lake-Seine River faults is a sequence of low-grade metavolcanic rocks (Keewatin of Lawson, 1887), intruded by anorthosite and gabbro which in turn are intruded by granitic rock (Laurentian of Lawson). All are unconformably overlain by conglomerate and immature sandstone (Seine Series of Lawson). In the Seine Conglomerate, volcanic cobbles and pebbles of felsic to intermediate composition are common. According to Frantes (1987), the Seine sedimentary sequence consists of poorly sorted conglomerate and interbeds of immature sandstone which suggest an alluvial fan merging into a braided fluvial environment.

North of the Quetico fault are gneisses, and large granitic masses separated by metavolcanic belts of the Wabigoon Subprovince. In the Wabigoon Subprovince, volcanism occurred mainly between 2750 and 2690 Ma, followed by major plutonism and metamorphism at 2700 to 2660 Ma

(Card, 1985). The oldest rocks in the study area are mafic tonalites which occur as xenoliths within tonalite in the Marmion Lake area (approximately 10 km north of the town of Atikokan); radiometric dating indicates the mafic tonalite crystallized approximately 2990 Ma (Don Davis, personal communication). Metamorphic grade in the Wabigoon Subprovince is generally subgreenschist to greenschist in the central part of greenstone belts and increases to low-pressure amphibolite facies in the surrounding granites and gneisses.

Supracrustal rocks of the Steep Rock Series lie unconformably above the Marmion tonalite (Smyth, 1891; Jolliffe, 1955). The basal member of the Steep Rock Series is an arkosic conglomerate and is exposed intermittently along the Marmion tonalite. The arkosic conglomerate is overlain by bedded limestone and dolomite which contains the hematitic ore zone of the Steep Rock and Caland iron mines. Fossil stromatolites are present in the limestone. Mafic lapilli tuffs overlie the carbonate unit, followed by mafic pillowed flows and intermediate to felsic flows, tuffs and breccias. Gabbroic sills and dykes transect the metavolcanic rocks and tonalitic basement. Small units of clastic metasediments (wacke, argillite, conglomerate, and arkose), occur intermittently throughout the Wabigoon Subprovince and appear to generally post-date volcanic intrusives (Stone, et al., 1986). The youngest rocks in the Atikokan area are granite and granodiorite such as the large, spherical Eye-Dashwa granite pluton located 10 km northwest of Atikokan. Potassium-argon radiometric age data indicate that this pluton cooled about 2650 Ma

(Kamineni and Stone, 1983).

South of the Quetico fault in the study area and south of the Seine River fault further west are the metasedimentary rocks of the Quetico Subprovince which are now largely biotite schists. The rocks have been deformed, progressively metamorphosed southward and migmatized towards a central axis so that the original textures and most of the sedimentary features have been obliterated except a marginal zone a few kilometers wide along the northern edge of the subprovince (Pirie and Mackasey, 1978).

The core of the Quetico Subprovince is made up of metasedimentary migmatite remnants, amphibolite schists, paragneisses and granitic intrusions, many of anatectic origin (Percival, 1983; Percival and Stern, 1984).

Structural trends differ greatly in the Wabigoon and Quetico Subprovinces in the study area. In the Wabigoon Subprovince, schistose metavolcanic sequences are intruded by syntectonic diapirs (Blackburn, 1980). This resulted in the isoclinal folding of volcanic strata about vertical axes and the wrapping of strata around mushroom-like intrusions of tonalite. Post-tectonic metamorphic gradients cross-cut axial-fold surfaces and there is no consistent tectonic trend on the regional scale (Borradaile, 1982).

In the adjacent Quetico belt, tectonic trends are consistently east-west. Metagreywacke and schist are very tightly or isoclinally folded with curving fold hinges and coplanar axial surfaces with an invariable east-west strike. The succession as a whole becomes younger

to the ENE. Isograds are parallel to the east-west axial traces, suggesting syntectonic metamorphism (Borradaile, 1982).

In the study area, the margin of the Wabigoon and Quetico Subprovinces is marked by the Quetico fault, a relatively late, major strike-slip fault. To the west, this margin is marked by the Rainy River-Seine River fault. The boundary between the two subprovinces is not always distinct and in some cases it exists as a diffuse transitional zone obscured by metamorphism (Kehlenbeck, 1976). Fumerton (1982) has proposed that the Quetico fault is not continuous in the Calm Lake area, but rather that the Rainy Lake-Seine River fault is continuous with the fault presently referred to as the Quetico fault to the east (Fig. 1). Fumerton suggested that as the Quetico fault approaches Calm Lake from the east, it continues to the south along what is now known as the Rainy Lake-Seine River fault. Consequently he proposed that the northern fault (presently referred to as the Quetico fault) be renamed the Little Turtle fault and the Rainy Lake-Seine River fault be renamed the Quetico fault. In order to avoid confusion, the author proposes to retain the older and established nomenclature.

Previous Work and Stratigraphy

Stratigraphic studies in the Atikokan Mine-Centre area have a complex and controversial history. The relative ages and spatial relationships among the Coutchiching, Seine, and Steep Rock Series, the Quetico Metasediments, the Keewatin lava flows, and various intrusive rocks represent a formidable geologic problem. A discussion of previous research is given here.

Mineral exploration in the Rainy Lake area dates back to the 1880's. There was an influx of prospectors between 1887 and 1900 due to the completion of the Canadian Pacific Railroad which provided access to Rainy Lake. In addition, there was an overflow of prospectors from a gold rush in northern Minnesota.

The Steep Rock Series located immediately north of the town of Atikokan was first described by Smyth in 1891. Smyth observed that the metasediments in the Steep Rock Series were not in contact with the "southern series" (the metasediments situated south of the Quetico fault in the Atikokan area) even though they are situated within a few kilometers of each other. Spurred by interest in the area, Smith and McInnes conducted the first systematic mapping here in 1897.

The Archean stratigraphic nomenclature for rocks of the Rainy Lake area was established by A.C. Lawson in 1888, and it quickly became internationally accepted. Lawson's oldest division was the Laurentian orthogneiss, upon which sediments were deposited. Lawson designated this metagreywacke and slate unit in the southern part of the Wabigoon Subprovince as the Coutchiching Series. Lawson observed the

Coutchiching Series to lie unconformably beneath the thick sequence of felsic to mafic rocks (Keewatin Series). Unconformably overlying the Keewatin Series is conglomerate and subarkosic arenite which Lawson assigned to the Seine Series.

In 1904, an international committee (Van Hise and others, 1905), studied the area and concluded that the Coutchiching Series overlies rather than underlies the Keewatin Series. Lawson revisited the area in 1913 and restated his original convictions about the relative position of the Keewatin and Coutchiching Series. The stratigraphic position of the "southern sediments" south of the Quetico fault has been the focus of considerable controversy ever since.

Lawson regarded the metasediment in the study area as part of the Seine Series, and younger than the Steep Rock Series. This view was later expressed in a classic paper by Hawley (1930). After completing a regional study, Hawley indicated the metasediments to be of the Seine Series with a fault separating them from the older Steep Rock Series. Although the Steep Rock Series and the Seine Series contain similar conglomerates, the Steep Rock Series contains algal stromatolites, dolomites, and iron formations, whereas the Seine Series is nearly completely composed of clastic sediments with minor iron formations. Hawley (1930), inferred that the Seine Series is younger because it is not intruded by gabbros as is the Steep Rock Series.

Lawson (1913), noted that the north-south trending folds of the Steep Rock Series and those in the Keewatin flows on the north side of the Quetico fault do not match the east-trending fold axes of the

Quetico Metasedimentary sequences. Hawley (1930) proposed that two separate directions of folding were caused by stresses related to an east-west dextral shearing with the north block moving eastward and the south block moving to the west. Tanton (1929), assigned the "southern sediments" as pre-Keewatin (i.e., Coutchiching). Moore (1940), considered the Steep Rock Series and the Seine Series as contemporaneous.

More recent mapping has resulted in the production of the Atikokan-Lakehead Sheet (Pye and Fenwick, 1965), and Kenora-Fort Frances Sheet (Blackburn, 1981) Compilation Maps at 1 to 253,440. With regard to localized studies, Young (1960) mapped the Bennet-Tanner area to the northeast of the present study area. Other closely studied localities in the vicinity include the Finlayson Lake area by Fenwick (1976), the Steep Rock Lake area by Shklanka (1972), and the Righteye Lake area by Fumerton (1980). Borradaile (1982) reviewed structural trends in Bennet and Tanner Townships in the Calm Lake area.

Poulsen (1982) has postulated a fault boundary for rocks in the Rainy Lake area which are situated between the Wabigoon Subprovince to the north and the Quetico metasediments to the south. The Coutchiching Series of Rainy Lake has previously been correlated with the Seine Series (Wood, 1980), but Poulsen's (1982) interpretation of a strike-slip fault separating the Wabigoon and Quetico Subprovinces makes this correlation suspect. Strongly supporting Poulsen's argument are geochronological data which demonstrate a 40 Ma year age difference between the Coutchiching Series and the Seine Series (Davis and Corfu,

1985). Davis and Corfu based their assertations on geochronological detrital zircon data. Therefore the notion that the Seine type alluvial-fluvial rocks are a transitional facies between Wabigoon volcanics and Quetico turbidites finds little support due to strike-slip faulting.

Discussion

The interpretation of the stratigraphic succession in the Rainy Lake area has long been contentious. The stratigraphic nomenclature which was established at the beginning of the century by Lawson can still be applied, although the stratigraphic relationships have been reversed. Significant modifications to the stratigraphy were first presented by Grout in 1925 (Table 1.1). Table 1.2 presents an inferred sequence of events just to the west of this study area.

Recent work by Poulsen (1984), indicates that the oldest supracrustal rocks along the southern boundary of the Wabigoon Subprovince boundary are metavolcanics of the Keewatin Series. His work is summarized in Figure 1.3. In the Rice Bay Dome area (west of the study area), the Keewatin Series is dominated by mafic flows. In the Mine Centre area, the Keewatin Series consists of intermediate to felsic flows, with pyroclastic units and amygdaloidal flows: mafic flows occur along its base in the area. Poulsen et al. (1980), have shown unequivocally that the Coutchiching Series which Lawson contended to be older than the Keewatin Series is younger than the Keewatin Series.

The Coutchiching Series (dominantly immature metasandstone),

	LAWSON (1913)	GROUT (1925)	HARRIS (1974)
Youngest			
	Keweenawan Dykes		Felsic and Intermediate Intrusives
	Algoman Granites	Algoman Granites	Early Intrusives
	Seine Series	Huronian Metasediments	Metasediments
	Laurentian Tonalites	Laurentian Granite-Gneiss	
	Keewatin	Archean Greenschist	Metavolcanics
	Coutchiching		Lower Metasediments
Oldest			

Table 1.1 General statigraphic interpretations of the Rainy Lake area by several workers. Some units are time equivalent and named differently, others were not observed by the workers (From Frantes, 1987).

Time (Ma)	Volcanism and sedimentation	Plutonism	Tectonism and metamorphism
>2100		diabase dykes	regional fracturing uplift, faulting, local cataclasis, regional cooling
2600-2700		Algoman granitic plutons, granite dykes and pegmatites	folding and regional metamorphism (greenschist to amphibolite facies)
		Rocky Islet Bay Complex	
	deposition of Seine Series		uplift and folding
		Rice Bay sills, Laurentian tonalites, gabbro and related rocks	
	Keewatin volcanism		
	deposition of Coutchiching (multiple sources and unknown basement)		

Table 1.2 Inferred sequence of events of the Rainy Lake area (After Goldich and Peterman, 1980).

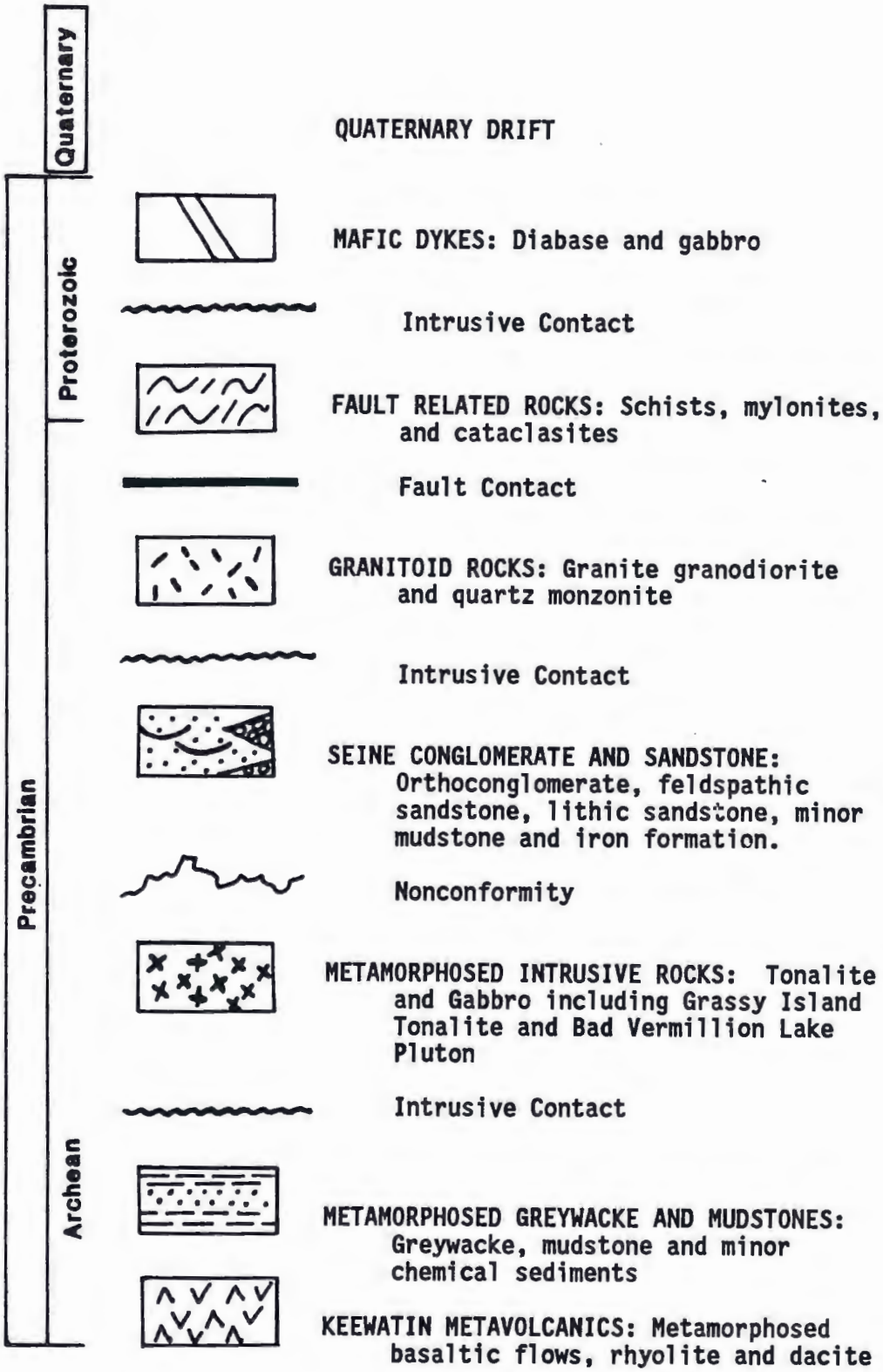

Figure 1.3 Poulsen's (1984) generalized stratigraphy of the Rainy Lake area (From Frantes, 1987).

occurs in three areas: two are in the Rice Bay Dome area of Rainy Lake, and the third is within the Quetico Subprovince, south of the Rainy Lake-Seine River fault. In the Quetico Subprovince, rocks which some believe to be Coutchiching equivalents, are referred to as the Quetico Metasediments and form most of the Quetico Subprovince. It should be noted that Lawson's Rice Bay Dome sediments are in the Wabigoon Subprovince, whereas the possibly related metasediments in the study area are situated in the Quetico Subprovince.

The Seine Series is the youngest supracrustal sequence in the Mine Centre area, and unconformably overlies both the Keewatin volcanics and a felsic pluton. There is still controversy as to whether the metasedimentary rocks in the Atikokan area are distal members of the Coutchiching or Seine Series, or an unrelated sequence. Therefore, the author proposes that the term Quetico Metasediments be used in this report to avoid unjustified implications of correlation with metasediments in the Rainy Lake area. Certainly more work is needed to clarify the relationships between the Coutchiching Series, the Seine Series and the Quetico metasediments.

Chapter 2

FIELD DESCRIPTIONS OF LITHOLOGIC TYPES

Field study was restricted to the Quetico metasediments south of the Quetico fault between Atikokan and the area east of Mine Centre. Much of the area is heavily wooded or covered by lakes and swamps. Outcrop is poor except along rivers and major roadways. Thus, the vast majority of fieldwork took place along Highways 11 and 11B and along the Seine River shorelines because these places were easily accessible and amenable to the cleaning of outcrops by scrubbing and bleaching. Megascopic analyses on outcrops were conducted along traverses perpendicular to the bedding across weathered surfaces. Field studies of the metasediments included measurement of bed thickness, determination of internal Bouma sequences and top determinations.

Stratigraphic sections were constructed in areas with a high percentage of exposure. On each outcrop, individual beds were studied consecutively up-section until the entire outcrop was measured and all pertinent information recorded. Outcrops were tied in using a compass, metal chain and Jacob's staff. Gaps in the stratigraphic section were also recorded using the metal chain. A summary of the lithologies present as well a summary of sedimentary structures present is given below.

METAGREYWACKE

General Field Description

Metagreywacke is the most abundant metasedimentary rock found in the study area, commonly interbedded with slate and uncommonly with

pebbly metasandstone. Bedding is very pronounced and regular with good lateral continuity (Fig. 2.1). The fine-to medium-grained metagreywacke beds are commonly graded. The bases of most beds are perfectly flat. Most metagreywackes have a schistose fabric. Bouma beds are generally of the AB, A, B, DE and ABE type. Fresh surfaces are dark green to black; weathered surfaces are brown to light green. Sand-to-silt ratios in the sequences is high, generally greater than 2 to 1.

The light-green to dark-green matrix accounts for 30-75% of the rock volume and is composed of chlorite and sericite; biotite is common in rocks of higher metamorphic grade. Also visible are poorly sorted clasts which consist of quartz, feldspar and lithic fragments 0.5 to 1.5 mm in diameter. Disseminated pyrite and quartz-carbonate veins are also common.

Macroscopic Bedding Characteristics

In the eastern half of the study area near the town of Atikokan, the metagreywacke beds studied in four stratigraphic sections are generally 10 to 40 cm thick (with occasional beds up to 60 cm thick, Table 2.1). A high percentage (86 to 98) of the metagreywacke beds are graded, and 90 to 100% of the metagreywacke beds here contain a basal A unit in Bouma AB, A, and ABE sequences (Table 2.2).

In the western half of the study area, the metagreywacke beds are generally 10 to 15 cm thick, and grading ranges from 81 to 95%. Basal A units are still dominant, but Bouma B and DE sequences are much more common.

Figure 2.1 Metagreywacke-slate sequence showing prominent lateral continuity. Location 3.5 km west of Lerome Lake along HWY 11.

Stratigraphic Section	1A	1B	2	3	4	5	
Total Thickness (m)	523	537	656	236	275	334	
Exposure %	76.9	46.6	55.6	60.6	49.5	47.1	
# of Beds Counted	112	78	140	102	187	1101	Total 1720
# of Beds that are greywacke (GW)	99	73	140	91	173	570	1046
% of Beds that are greywacke (GW)	88.5	94.0	100.0	89.2	92.5	51.8	Average 86.0
% Graded Beds (GW)	85.6	98.0	86.8	95.7	81.1	94.6	92.3
% Siltstone-Mudstone packages	5.3	1.3	0.0	0.0	7.5	48.2	7.2
% Pebbly Sandstone	6.2	5.1	0.0	8.8	0.0	0.0	1.2
% Conglomerate	0.0	0.0	0.0	2.0	0.0	0.0	0.1
Ave. Thick. AB (cm)	14.8	41.9	16.5	16.0	11.5	10.8	13.6
Ave. Thick. A (cm)	16.9	46.0	3.3	11.0	--	--	8.4
Ave. Thick. B (cm)	13.2	--	6.2	--	11.5	8.2	9.2
Ave. Thick. ABE (cm)	10.0	9.3	9.2	--	6.6	11.2	9.7
Ave. Thick. DE (cm)	8.8	6.5	3.7	--	7.3	4.9	5.5
" " Siltstone-Mudstone packages	2.1	62.0	--	--	19.4	48.2	40.9
" " Pebbly SS (cm)	49.1	81.0	--	160.9	--	--	106.1
" " Conglom. (cm)	--	--	--	62.5	--	--	62.5

Table 2.1. Details for stratigraphic sections arranged east (left) to west (right). Location of the six stratigraphic sections is given in Figure 6.6.

Bouma Divisions of a Complete Turbidite Bed

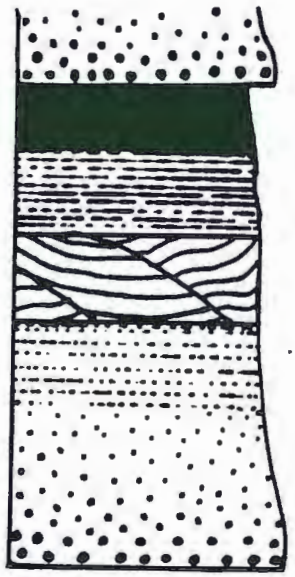

E-Pelitic division, partly turbidity current, partly hemipelagic

D-Parallel laminations of silt and mud

C-Rippled cross-bedded or convoluted

B-Parallel laminated sandstone

A-Graded or massive sandstone

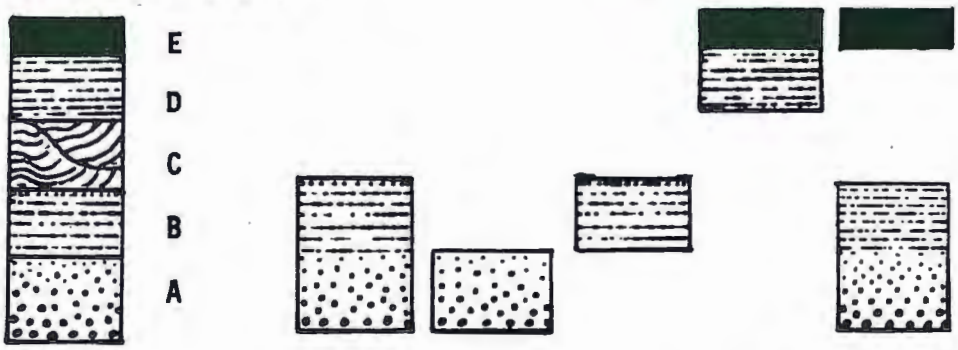

	AB	A	B	DE	ABE
# of Greywacke beds counted	99	73	140	173	570
Stratigraphic Section 1A	77.8%	5.1%	8.0	8.0	1.1%
Stratigraphic Section 1B	43.6%	1.4%	0.0%	9.6%	45.4%
Stratigraphic Section 2	77.5%	5.0%	7.5%	5.0%	5.0%
Stratigraphic Section 3	76.9%	23.1%	0.0%	0.0%	0.0%
Stratigraphic Section 4	42.2%	0.0%	3.5%	48.0%	6.3%
Stratigraphic Section 5	20.8%	0.0%	15.8%	41.7%	21.7%

Table 2.2 Chart showing the percentages of Bouma sequences present in the six stratigraphic sections. Stratigraphic sections arranged from east (top) to west (bottom).

Sedimentary Structures

In the study area, the metagreywackes exhibit most of the primary structures attributable to turbidites. The sedimentary structures typical of turbidite sequences are described in the literature (e.g., Ojakangas, 1968; Middleton and Hampton, 1973).

Graded bedding is the most common feature observed in individual beds (Fig. 2.2). Sediment carried in turbulent suspension is subjected to internal sorting processes. When the flow ceases, the sorting may be preserved as a texture called graded bedding. In distribution (typical) grading, the entire grain size distribution progressively shifts from the bottom to the top of the bed as a response to the decay of turbulence in the gravity current. Grain sizes in the Quetico Metagreywackes range from coarse sand at the base to fine sand or silt at the top. Megascopic grading in the six stratigraphic sections ranges from 81 to 98% of the beds studied (Table 2.1).

The turbidite Bouma sequence (Bouma, 1962) represents the standard or typical sediment accumulation from a turbidity current. It is characterized by five components which occur in a predictable sequence, with each sequence representing deposition by a single turbidity current. The five divisions of the Bouma sequence are as follows (Table 2.2): A-graded or massive sandstone; B-parallel laminated sandstone; C-rippled cross-bedded or convoluted; D-parallel laminations of silt and mud; E-pelitic divisions, partly turbidity current and partly hemipelagic (Walker, 1984). The metagreywacke beds in the eastern half of the study area are typically AB sequences (65%),

Figure 2.2 Graded bedding in several medium-grained metagreywacke beds. Beds become finer-grained to the top (south). Photo taken along HWY 11B, 1 km north of the junction into Atikokan.

with lesser amounts of Bouma A, B, DE and ABE sequences (Table 2.2). Metagreywacke sequences in the western half of the study area are more silt-and mud-rich; many are Bouma AB beds (21 to 42%), but B and DE sequences are more abundant here than to the east.

Cross-bedding, which results from traction currents, is a rare feature almost exclusively restricted to the pebbly sandstone (Fig. 2.3). Both trough and planar cross-bedding types were observed, with cross-bed sets ranging from 1 to 3 cm in thickness and from 10 to 50 cm in length.

Typical turbidites show some ripple cross-lamination which forms the "C" division in a typical Bouma bed. Climbing ripples are a result of a combination of traction and rapid fall-out of suspended matter. The "C" division was rarely observed in the Quetico metasediments, likely due in part to obliteration by metamorphism.

Flame structures form along the sand and mud interface in sand beds that are deposited rapidly on a soft substratum. Because the density and viscosity of the mud are less than that of the overlying sand, deformation along this interface is common and is marked by "flames" of mud extending upward into the sand. Flame structures represent high rates of deposition which are common in turbidites (Fig. 2.4). Flame structures are locally present in the Quetico metasediments and project 5 to 25 cm into the disturbed bed.

Soft-sediment slumps occur when large masses of sediment move downslope due to the shear within the mass. Earthquakes, oversteepened slopes, excessive pore-pressure in the sediment and sudden sediment

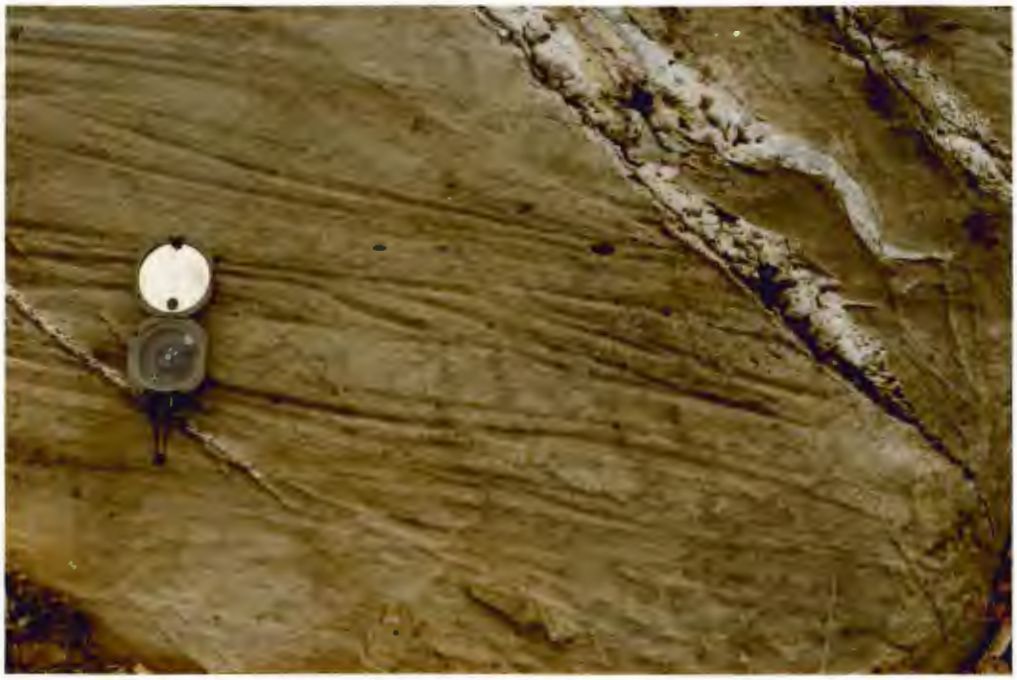

Figure 2.3 Cross-bedding in medium-grained metagreywacke. Photo taken on HWY 11, 2 km west of junction with HWY 11B.

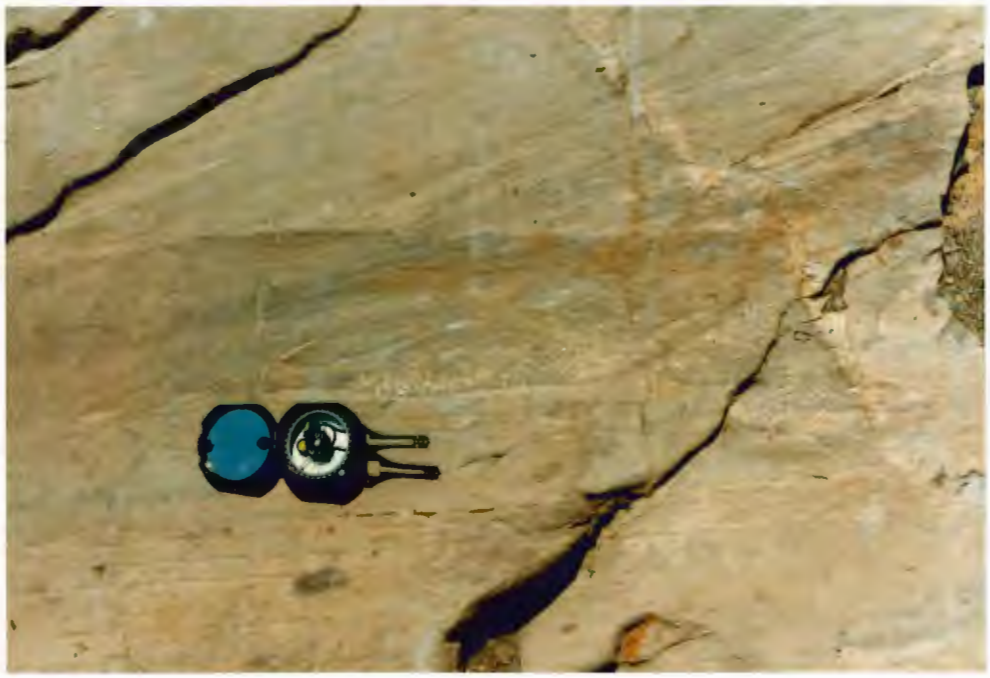

Figure 2.4 Flame structures at the base of a coarse-grained meta-greywacke. These have been strongly accentuated by the schistosity. Photo taken along HWY 11B, 1 km north the junction with HWY 11.

loading may trigger slumps (Clari and Ghibaudo, 1979). These bodies, if they are large enough, generally retain their internal coherence, including stratification. Soft-sediment slump features are present in the Quetico metasediments in the form of gently convoluted strata, thickened strata, occasional pulled-apart strata and overturned bedding. Slumps may be confused with tectonically deformed beds but the two may be differentiated in cases where slumped beds have undeformed beds above and below.

Scours are sedimentary structures produced by erosion of beds by currents. These megascopic erosional features are present in the Quetico metasediments and are recognized by the infilled coarse sediment. The scour features are rarely more than 10 to 15 cm deep and 20 to 40 cm across. Scours may indicate the origin of major erosive currents such as those generated at river deltas or submarine fans. However, the lack of three-dimensional exposures made paleocurrent measurements from scours nearly impossible to obtain but preliminary field observations indicate a possible paleocurrent direction from the NE.

Although turbidites are theoretically a non-erosive mode of sediment transport (Middleton and Hampton, 1973), in reality erosion takes place at the head as is evidenced by the presence of sole-marks and rip-up clasts in many turbidites. According to Hendry (1978), mud-chips represent penecontemporaneous erosion of underlying mud-rich beds. Mud-chips are frequently observed in the Quetico metasediments (Fig. 2.5), and occur as 0.5 to 2 cm long light grey clasts near the

Figure 2.5 Mud-chips in a medium-grained metagreywacke. Photo taken on the north side of HWY 11 near boat-launch at Lerome Lake.

bases of individual beds.

SLATE (METAMORPHOSED MUDSTONE)

General Field Description

Light grey to black slate with minor amounts of interbedded siltstone, is a major constituent of the metasediments, especially in the western half of the study area. The individual slate beds are 0.4 to 10 cm thick but generally fall in the 1 to 5 cm range (Table 2.1). Metamorphosed couplets of siltstone and mudstone are common (Fig. 2.6), and form packages as thick as 210 cm. The siltier beds are light grey in colour, whereas the mud-rich beds are light-green to black in colour giving the packages a striking striped appearance. Beds are of even thickness and are laterally continuous for up to 100 metres. The slates have an extremely well developed cleavage that has been termed continuous cleavage by Borradaile et al., (1982).

PEBBLY METASANDSTONE

General Field Description

Pebbly metasandstone comprises between 0 to 8.8% of the beds counted in the six stratigraphic sections, with the greatest concentration occurring near the junction of HWY 11 and 11B (Table 2.1). The pebbly metasandstone commonly occurs as a transitional rock type between metagreywacke and metaconglomerate (Fig. 2.7). Clast sizes in the metaconglomerate range from 2 to 12 cm in diameter. Pebbly metasandstone also occurs as thick, regularly bedded, amalgamated sequences up to 10 metres thick. The medium-to coarse-grained beds are usually graded (especially distinct at the

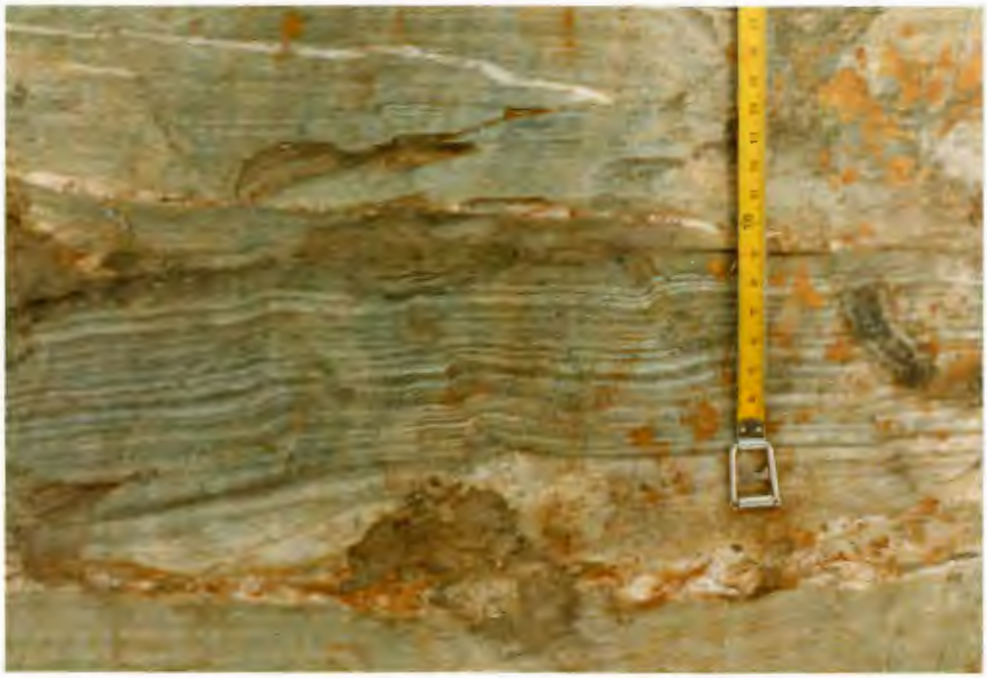

Figure 2.6 Interbedded siltstone-mudstone. Note the fine laminations. Photo taken on HWY 11, 0.5 km east of the gravel road leading to Gehl Lake.

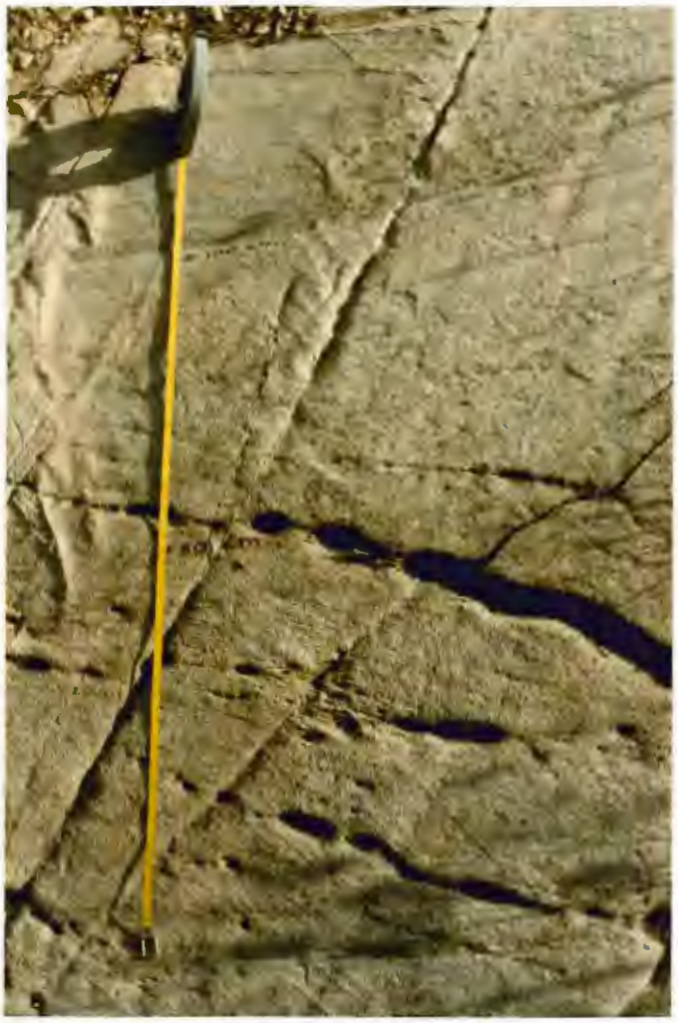

Figure 2.7 Thick, cross-bedded, amalgamated pebbly metasandstone beds. This sequence of thick pebbly metasandstone units appears to be continuous up-section for 21 metres and is associated with conglomerate. Photo taken on HWY 11, 2 km west of junction 11B into Atikokan.

tops), flat based and laterally continuous. Beds are generally 40 to 80 cm thick with occasional beds up to 2 metres thick . The beds appear to be channeled and occasionally cross-bedded. Both planar and trough cross-bedding types are observable in individual beds. Shale partings are rare or absent; sand to shale ratios in the sequences are high, greater than 10 to 1.

Fresh pebbly metasandstone surfaces are dark grey in colour; weathered surfaces appear light grey. Differential weathering is prominent between clasts and matrix. The fine-to medium-grained schistose matrix makes up 50 to 80% of the rock volume. The largest framework grains are concentrated at the bases of beds; field observation identifies them as quartz and feldspar fragments, with lesser amounts of granitic and felsic volcanic fragments. The coarser pebbly metasandstone beds show faint imbrication.

Pebbly metasandstone cannot be described using the Bouma model. Using Mutti and Lucchi's (1972) classification scheme, the pebbly metasandstone appears to be transitional between facies "A4" (organized pebbly sandstone), and facies "B2" (massive sandstone without dish structures). Mutti and Lucchi's (1972) classification scheme and its implications to the environment of deposition will be elaborated upon in Chapter 6.

BIOTITE SCHIST

General Field Description

The development of biotite in the study area increases south of the biotite isograd which is roughly parallel to and is located two

kilometers south of the Quetico fault throughout the study area except along the western margin where the biotite isograd crosses HWY 11, as does the Quetico fault. These rocks are the higher grade equivalents of the metagreywackes and slates as evidenced by the presence of relict primary textures and sedimentary structures. Bedding and grading are usually preserved; argillaceous layers are now recognizable as biotite-rich beds. Amphibolites and migmatites are present southward where the metamorphic grade has increased.

Fresh surfaces are dark-green to black and feature a distinct schistosity. Weathered surfaces are light-grey to brown, limonite-stained, and extremely fissile.

In the medium-grained schists, ragged laths of biotite wrap around larger, more competent quartz and feldspar grains. Some lithic clasts are deformed and help define the fabric. The schistosity is defined by the preferred crystallographic orientation of the phyllosilicates and by the preferred dimensional orientation of larger clasts. A typical biotite schist is illustrated in Figure 2.8.

METACONGLOMERATE: PARACONGLOMERATE

General Field Description

Metaconglomerate beds are volumetrically less abundant than any of the rock types and are generally restricted to outcrops near the intersection of HWY 11 and 11B. Five paraconglomerate beds were observed, usually associated with pebbly metasandstone; the two rock types are transitional with each other. The clasts are matrix supported, make up 10 to 20% of the rock and range from 0.5 to 10 cm ,

Figure 2.8 Biotite schist. Photo taken along the western margin of study area on HWY 11, 0.5 km east of dirt road to Gehl Lake.

in diameter. The clasts are angular to subrounded and are dominantly of tonalite and felsic volcanics. Also present are clasts of chert and quartz. The matrix consists of a dark grey to dark green, fine-to medium-grained wacke (Fig. 2.9). Individual beds vary in thickness from 30 cm to 1.1 m, and are rarely laterally continuous.

The absence of grading, imbrication and stratification is characteristic of facies "A1" (disorganized conglomerate) from the classification scheme of Mutti and Lucchi (1972).

METACONGLOMERATE: ORTHOCONGLOMERATE

General Field Description

Only one orthoconglomerate occurrence was noted in the study area, on the south side of HWY 11, three kilometers west of the HWY 11 turnoff into Atikokan. The bed is entirely clast-supported. It has an abrupt top and bottom, is interbedded with graded metagreywacke beds (Fig 2.10), and ranges in thickness from 40 to 60 cm. It is laterally continuous for at least 40 meters. The orthoconglomerate appears to be a lenticular intraformational body.

The clasts in the unit are of various lithologies and range in diameter from 1 to 18 cm. The matrix makes up approximately 35% of the rock volume and consists of metagreywacke and pebbly metasandstone. The clasts are dominantly of granitic-tonalitic composition. Fine-grained felsic volcanics, mafic volcanics, chert, quartz, and metasedimentary (likely slate) clasts are also present.

The matrix is highly schistose and wraps around more competent grains. The tonalitic clasts tend to be rounder and less deformed than

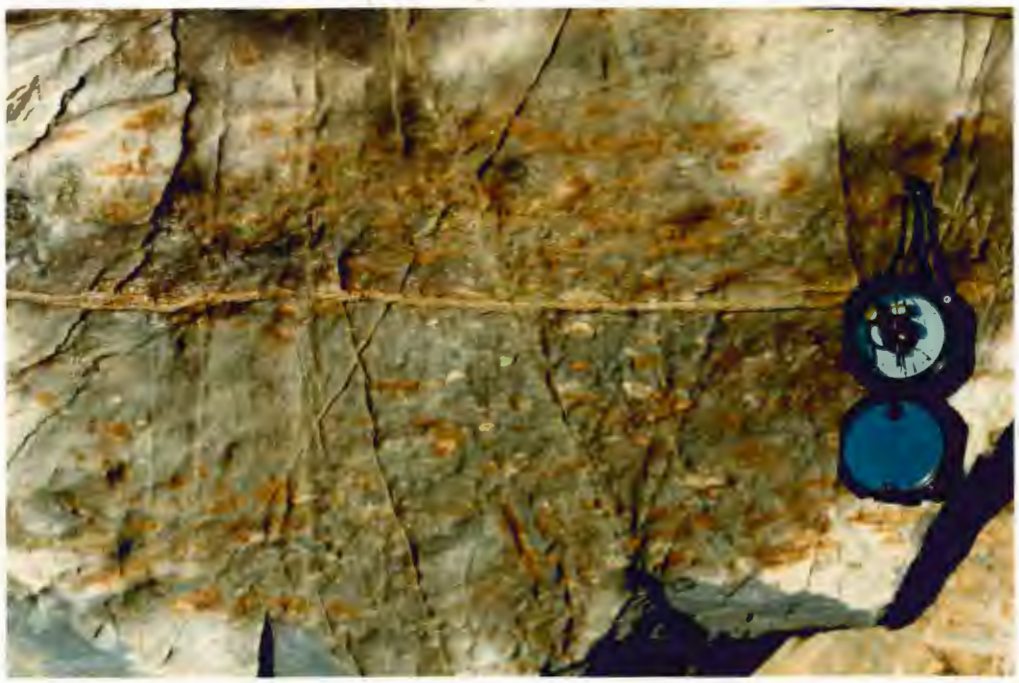

Figure 2.9 Paraconglomerate located on the south side of HWY 11, 0.5 km west of the junction of HWY 11B into Atikokan. Pebbles are felsic volcanics, chert and mud-chips.

Figure 2.10 Orthoconglomerate bed located on HWY 11, 1.5 km west of the junction of HWY 11B into Atikokan. Clasts are flattened parallel to bedding.

than the clasts composed of volcanic or metasedimentary material. It is common to see less competent clasts wrap around more competent tonalite clasts.

Rocksaw cuts allow a three-dimensional view of the orthoconglomerate. The clasts are elongated in two directions and shortened in the third. They have a flattened pancake-like appearance parallel to bedding.

The presence of crude horizontal stratification with clasts set in a sandy matrix indicates the presence of a facies "A2" organized conglomerate as defined by Mutti and Lucchi (1972).

Chapter 3

PETROGRAPHY

Prior to this study, little quantitative petrographic work had been conducted on the Quetico Metasediments of the study area. A comprehensive modal analysis of the Quetico Metasediments should prove useful in interpreting the provenance and sedimentary history. Metamorphic recrystallization has obliterated most of the original clastic textures, transforming the rocks into low-grade schists, commonly with porphyroblasts of biotite and, in higher grade rocks, porphyroblasts of garnet, cordierite and amphibole. Fortunately, relatively low-grade exposures are present along Highways 11 and 11B, and from the Seine River System; 108 samples were collected for thin section analysis. Forty-one thin sections (representing coarse-grained metagreywackes and pebbly metasandstones) were selected for point-counting. In each point-count, traverses were conducted normal to the bedding until 600 points were identified. Results are given in Tables 3.1a, 3.1b, 3.1c, 3.1d and 3.1e. Table 3.1e also provides the average for the modal components.

Grains were examined and categorized using established guidelines of previous workers (e.g., Dickinson, 1970). A summary of the criteria used for detrital grain classification (operational definitions) is given below. All percentages given in the descriptions are for rock volume unless otherwise indicated.

OPERATIONAL DEFINITIONS

Quartz

SAMPLE #	2B1	3A1	3A2	3A3b	3AZ	3BZ	4A1	4DZ	4D1
Total Quartz	21.0	20.8	17.7	23.2	22.9	13.3	29.5	26.7	28.3
Common Monoxline	2.5	2.5	3.0	3.0	4.5	5.0	4.5	3.7	6.2
Common Undulose	8.7	11.0	7.8	12.7	14.5	6.8	13.0	16.0	9.8
Polycrystalline	2.0	1.8	0.7	1.8	2.7	0.7	2.5	4.7	2.8
Volcanic	0.0	0.0	0.0	0.0	0.0	0.2	0.0	0.2	0.0
Stretch/Schist.	0.0	0.0	0.0	0.0	0.0	0.2	0.0	0.0	0.0
Recrystallized Chert	7.7	5.0	6.2	5.7	1.0	0.3	9.5	2.2	9.5
Total Feldspar	5.5	9.2	7.0	6.3	8.7	13.9	6.2	8.8	6.0
Plagioclase	5.5	8.8	6.8	5.8	7.7	15.7	5.8	8.3	6.0
Orthoclase	0.0	0.3	0.2	0.5	1.0	0.2	0.5	0.5	0.0
Microcline	0.0	0.0	0.0	0.0	0.0	0.0	0.0	0.0	0.0
Total Lithic Frag.	10.3	12.5	13.5	7.2	10.5	17.1	7.2	10.3	16.2
Felsic Volcanic	1.2	3.5	1.3	2.5	1.0	3.7	0.2	1.7	4.8
Fel. Int. Volc.	6.0	4.8	3.8	2.0	9.0	12.5	4.5	7.7	8.2
Int. Mafic Volc.	0.0	0.7	0.0	0.3	0.0	0.0	0.0	0.0	0.2
Mafic Volcanic	0.0	0.0	0.0	0.0	0.0	0.0	0.0	0.0	0.0
Plut. Plag/Qtz	2.3	0.7	1.5	1.0	0.2	0.7	1.3	1.0	1.2
Plut. Ortho/Qtz	0.8	1.3	1.2	1.0	0.3	0.2	1.2	0.0	1.3
Plutonic Mafic	0.0	1.5	0.0	0.3	0.0	0.0	0.0	0.0	0.5
Slate	0.0	0.0	5.7	0.0	0.0	0.0	0.0	0.0	0.0
Total Misc. Grains	2.8	5.3	4.8	4.3	4.1	7.2	4.7	3.0	7.3
Muscovite	0.0	0.0	0.0	0.0	0.0	0.0	0.0	0.0	0.0
Opaques	1.7	2.0	2.0	1.5	2.2	3.0	1.0	1.5	1.8
Zircon	0.0	0.0	0.0	0.0	0.0	0.0	0.0	0.0	0.2
Apatite	0.2	0.5	0.0	0.3	0.2	0.7	0.7	0.2	0.2
Epidote	1.0	2.8	2.8	2.5	1.7	3.5	3.0	1.3	5.2
Total Cem./Matrix	60.2	52.2	57.0	59.0	53.9	46.7	52.5	51.2	42.2
Hematite Cement	0.2	0.0	0.0	0.0	0.0	1.0	0.0	0.5	0.0
Calcite Cement	0.5	2.8	1.3	2.8	0.0	4.0	1.2	0.0	1.2
Sericite	0.0	0.0	0.0	0.0	0.2	0.9	0.0	4.2	0.7
Chlorite	1.7	6.3	4.5	8.7	7.3	32.6	5.3	20.0	12.2
Tremolite/Act.	0.0	0.0	0.0	0.0	0.0	0.0	0.0	0.0	0.0
Biotite	23.5	30.1	36.5	37.0	31.6	0.5	31.7	11.5	18.2
Qtz-Feld Matrix	34.5	13.0	14.6	10.5	14.8	7.7	14.3	15.0	10.0

Table 3.1a Modal analyses of medium-grained metagreywackes and pebbly metasandstones expressed in percent (600 point-count). Values add up to 100. Samples are arranged east to west.

SAMPLE #	5C2	6A2	6C1	6C2	7A2	11AZ	13A2	15C1	15CZ
Total Quartz	27.4	19.0	20.5	18.8	12.2	20.5	21.5	17.0	13.5
Common Monoxline	5.2	4.2	3.8	2.8	1.5	3.5	3.8	3.0	4.5
Common Undulose	13.7	7.3	9.0	8.3	6.8	12.7	6.8	8.2	12.7
Polycrystalline	3.5	2.2	1.7	1.3	0.8	3.5	2.5	2.8	4.3
Volcanic	0.0	0.0	0.0	0.0	0.0	0.2	0.0	0.0	0.0
Stretch/Schist.	0.0	0.0	0.0	0.0	0.0	0.0	0.0	0.0	0.0
Recrystallized	4.8	5.3	6.0	6.3	3.0	0.7	8.3	3.0	2.0
Chert	0.2	0.0	0.0	0.0	0.0	0.0	0.0	0.0	0.0
Total Feldspar	16.3	10.0	11.0	10.8	11.2	10.3	3.6	6.7	10.8
Plagioclase	15.0	9.8	10.8	9.8	11.0	9.7	3.5	6.2	9.8
Orthoclase	1.3	0.2	0.2	1.0	0.0	0.7	0.2	0.5	1.0
Microcline	0.0	0.0	0.0	0.0	0.2	0.0	0.0	0.0	0.0
Total Lithic Frag.	8.3	9.0	7.9	8.2	8.2	16.3	7.8	6.1	10.3
Felsic Volcanic	3.0	2.5	1.3	1.7	1.3	0.3	0.5	0.5	1.7
Fel. Int. Volc.	1.2	2.8	2.0	2.8	3.2	15.8	4.2	1.7	6.8
Int. Mafic. Volc.	0.3	0.3	0.2	0.0	0.2	0.0	0.0	0.0	0.0
Mafic Volcanic	0.0	0.0	0.2	0.0	0.2	0.0	0.0	0.0	0.0
Plut. Plag/Qtz	2.8	1.7	1.7	2.0	2.2	0.0	2.2	2.3	1.2
Plut. Ortho/Qtz	0.7	1.3	1.5	1.2	0.7	0.2	1.0	1.6	0.7
Plutonic Mafic	0.3	0.3	1.0	0.5	0.5	0.0	0.0	0.0	0.0
Slate	0.0	0.0	0.0	0.0	0.0	0.0	0.0	0.0	0.0
Total Misc. Grains	4.5	3.2	4.3	4.8	7.3	3.8	4.7	2.8	2.7
Muscovite	0.0	0.2	0.0	0.2	0.2	0.0	0.0	0.0	0.0
Opaques	2.0	1.0	3.5	2.3	2.0	1.7	2.5	1.3	1.7
Zircon	0.0	0.0	0.0	0.0	0.0	0.5	0.0	0.2	0.0
Apatite	0.0	0.0	0.0	0.0	0.0	0.7	0.0	0.0	1.0
Epidote	2.5	2.0	0.8	2.3	5.2	1.0	2.2	1.2	0.0
Total Cem./Matrix	43.5	58.8	56.3	57.3	60.9	48.7	62.3	67.5	52.7
Hematite Cement	0.0	0.0	0.0	0.0	0.0	0.0	0.0	0.0	0.0
Calcite Cement	5.3	7.2	5.3	2.7	5.7	4.0	0.0	0.8	0.0
Sericite	6.4	5.5	5.5	4.5	0.0	0.2	0.0	0.0	0.0
Chlorite	27.8	36.3	34.8	35.0	29.3	3.7	6.3	10.5	12.3
Tremolite/Act.	0.0	0.0	0.0	0.0	0.0	0.0	0.0	0.0	0.0
Biotite	0.8	0.0	0.0	0.0	11.2	27.2	37.0	30.2	28.8
Qtz-Feld Matrix	3.3	9.8	10.7	15.2	14.7	13.7	19.0	26.0	11.5

Table 3.1b Modal analyses of medium-grained metagreywackes and pebbly metasandstones expressed in percent (600 point-count). Values add up to 100. Samples are arranged east to west.

SAMPLE #	19D1	24A1	24A2	27BZ	29B1	30C1	33AZ	35BZ	36CZ
Total Quartz	23.3	22.5	28.7	20.2	22.2	21.3	12.7	19.7	11.8
Common Monoxline	2.2	3.7	4.5	2.5	1.2	2.8	4.2	4.3	1.8
Common Undulose	13.5	12.0	11.5	8.7	11.8	2.2	3.8	10.0	3.5
Polycrystalline	3.0	2.8	3.5	5.3	1.2	13.0	2.7	2.7	2.2
Volcanic	0.0	0.2	0.0	0.0	0.0	0.0	0.0	0.0	0.0
Stretch/Schist.	0.0	0.0	0.0	0.0	0.5	0.0	0.0	0.0	0.0
Recrystallized	4.7	3.7	9.2	3.7	7.5	3.3	0.8	2.0	4.3
Chert	0.0	0.2	0.0	0.0	0.0	0.0	1.2	0.7	0.0
Total Feldspar	8.0	12.7	9.0	11.5	13.8	21.8	10.2	11.5	7.7
Plagioclase	7.8	12.3	8.5	11.2	12.8	20.6	10.0	10.8	7.2
Orthoclase	0.2	0.3	0.5	0.3	1.0	1.0	0.2	0.5	0.5
Microcline	0.0	0.0	0.0	0.0	0.0	0.2	0.0	0.2	0.0
Total Lithic Frag.	6.2	12.0	11.0	11.2	15.7	16.0	17.2	19.0	15.2
Felsic Volcanic	1.7	2.3	2.2	2.0	5.2	6.3	6.7	8.0	2.8
Fel. Int. Volc.	1.0	2.7	3.3	6.2	2.5	6.3	5.2	8.8	9.5
Int. Mafic. Volc.	0.0	0.2	0.3	0.2	1.2	0.0	1.2	0.8	0.0
Mafic Volcanic	0.0	0.2	0.0	0.0	0.0	0.0	0.2	0.0	0.0
Plut. Plag/Qtz	2.2	1.7	1.8	1.5	4.3	1.8	2.3	1.0	1.0
Plut. Ortho/Qtz	1.0	1.7	1.8	0.8	1.2	1.7	0.8	0.3	1.8
Plutonic Mafic	0.3	3.0	1.5	0.5	0.8	0.0	0.8	0.0	0.0
Slate	0.0	0.3	0.0	0.0	0.5	0.0	0.0	0.0	0.0
Total Misc. Grains	3.3	4.0	3.2	3.8	10.0	1.0	6.7	2.3	1.8
Muscovite	0.0	0.2	0.2	0.0	0.0	0.0	0.0	0.0	0.0
Opaques	1.6	2.5	2.0	1.5	2.3	0.8	4.5	1.2	1.8
Zircon	0.0	0.0	0.0	0.0	0.0	0.0	0.2	0.0	0.0
Apatite	0.2	0.0	0.0	0.0	0.0	0.0	0.0	0.0	0.0
Epidote	1.5	1.3	1.0	2.3	7.7	0.2	2.0	1.2	0.0
Total Cem./Matrix	60.6	48.8	48.2	53.3	38.6	40.0	53.3	47.7	63.4
Hematite Cement	0.0	0.0	0.0	0.0	0.0	0.0	0.0	0.0	0.0
Calcite Cement	1.2	9.5	1.3	1.3	3.5	6.3	7.8	4.8	0.8
Sericite	0.0	3.8	2.2	2.5	0.0	10.5	1.7	0.5	0.0
Chlorite	17.6	28.0	33.2	27.5	4.7	13.2	12.7	24.5	6.0
Tremolite/Act.	0.0	0.0	0.0	0.0	0.0	0.0	0.0	0.0	9.2
Biotite	28.0	0.0	3.0	10.2	17.3	0.0	23.2	9.7	28.3
Qtz-Feld Matrix	13.8	7.5	8.5	11.7	13.0	9.8	7.8	8.2	19.3

Table 3.1c Modal analyses of medium-grained metagreywackes and pebbly metasandstones expressed in percent (600 point-count). Values add up to 100. Samples are arranged east to west.

SAMPLE #	37BZ	41C1	44B1	44C1	45CZ	101BZ	101DZ	101EZ	103BZ
Total Quartz	13.7	16.8	17.4	21.8	14.5	16.3	11.0	19.0	12.1
Common Monoxline	1.7	4.2	1.7	1.3	2.3	4.0	2.2	4.0	1.0
Common Undulose	3.5	10.0	13.3	15.0	7.5	6.0	5.8	8.2	4.2
Polycrystalline	2.2	1.7	0.7	0.7	2.7	4.2	2.2	3.8	1.2
Volcanic	0.0	0.0	0.0	0.0	0.0	0.0	0.0	0.0	0.0
Stretch/Schist.	0.0	0.2	0.0	0.2	0.0	0.0	0.0	0.0	0.5
Recrystallized	5.8	0.7	1.7	4.5	1.8	2.0	0.7	2.8	5.2
Chert	0.0	0.2	0.0	0.2	0.2	0.2	0.2	0.2	0.0
Total Feldspar	6.8	15.0	8.8	8.8	9.6	11.8	11.3	10.2	6.0
Plagioclase	6.3	14.0	8.7	8.3	9.6	11.3	10.8	10.0	5.3
Orthoclase	0.5	1.0	0.2	0.5	0.0	0.5	0.5	0.2	0.6
Microcline	0.0	0.0	0.0	0.0	0.0	0.0	0.0	0.0	0.0
Total Lithic Frag.	9.8	14.7	8.8	10.2	12.8	9.5	11.7	10.5	43.2
Felsic Volcanic	2.3	4.0	2.3	3.5	1.7	1.8	1.2	1.8	10.7
Fel. Int. Volc.	4.0	9.8	2.5	4.2	6.3	4.7	5.7	6.7	5.3
Int. Mafic. Volc.	0.0	0.0	1.2	0.2	0.0	0.3	0.0	0.0	23.3
Mafic Volcanic	0.0	0.0	0.0	0.0	0.0	0.0	0.0	0.0	0.5
Plut. Plag/Qtz	2.7	0.7	0.8	1.2	3.8	0.8	3.0	0.5	2.0
Plut. Ortho/Qtz	0.8	0.2	1.2	0.0	1.0	1.8	1.3	1.3	0.3
Plutonic Mafic	0.0	0.0	0.7	1.2	0.0	0.0	0.0	0.0	0.5
Slate	0.0	0.0	0.2	0.3	0.0	0.0	0.5	0.0	0.5
Total Misc. Grains	2.0	3.3	4.5	4.3	3.0	4.5	1.3	9.2	6.7
Muscovite	0.0	0.0	0.0	0.0	0.0	0.0	0.0	0.0	0.0
Opaques	1.0	2.7	2.0	3.0	2.8	3.5	1.3	5.8	1.7
Zircon	0.0	0.0	0.0	0.0	0.2	0.0	0.0	0.2	0.0
Apatite	0.2	0.2	0.2	0.0	0.0	0.0	0.0	0.0	0.0
Epidote	0.8	0.5	2.3	1.3	0.0	1.0	0.0	3.2	5.0
Total Cem./Matrix	68.0	50.0	60.0	54.3	60.0	57.9	64.7	51.2	32.3
Hematite Cement	0.2	0.0	0.0	0.0	0.0	0.2	0.3	2.2	0.0
Calcite Cement	0.2	7.3	4.7	7.7	4.7	4.5	6.0	6.0	4.5
Sericite	0.0	4.2	0.0	6.2	0.0	2.5	3.3	3.7	1.5
Chlorite	0.5	25.2	10.8	34.5	10.8	38.0	43.3	29.5	23.0
Tremolite/Act.	13.5	0.0	0.0	0.0	0.0	0.0	0.0	0.0	0.0
Biotite	20.6	4.7	25.3	0.0	25.3	0.3	0.0	0.2	0.0
Qtz-Feld Matrix	33.2	8.6	19.2	6.0	19.2	12.3	11.7	9.7	3.3

Table 3.1d Modal analyses of medium-grained metagreywacke and pebbly metasandstone expressed in percent (600 point-count). Values add up to 100. Samples are arranged east to west.

SAMPLE #	103C1	103C2	104AZ	202I	206I	AVERAGE
Total Quartz	16.8	12.7	11.8	18.0	20.3	19.7
Common Monoxline	2.2	1.8	1.8	1.7	1.7	3.1
Common Undulose	10.8	3.0	6.3	11.0	15.0	9.7
Polycrystalline	0.5	6.2	1.8	0.3	0.3	2.6
Volcanic	0.0	0.0	0.0	0.0	0.0	Trace
Stretch/Schist.	0.0	0.0	0.0	0.0	0.0	Trace
Recrystallized	3.0	1.7	1.8	4.3	3.3	4.1
Chert	0.3	0.0	0.0	0.7	0.0	0.1
Total Feldspar	6.8	16.0	8.5	9.8	5.7	10.0
Plagioclase	6.7	14.3	8.2	7.8	3.2	9.4
Orthoclase	0.2	1.7	0.3	2.0	2.3	0.6
Microcline	0.0	0.0	0.0	0.0	0.2	Trace
Total Lithic Frag.	8.5	14.8	10.3	12.0	5.8	12.2
Felsic Volcanic	2.2	6.0	3.2	5.0	1.5	2.9
Fel. Int. Volc.	3.3	4.8	5.2	2.3	1.8	5.2
Int. Mafic. Volc.	0.8	0.8	0.3	2.3	0.2	0.9
Mafic Volcanic	0.3	0.3	0.0	0.2	0.7	0.1
Plut. Plag/Qtz	0.5	1.5	0.7	1.0	1.0	1.6
Plut. Ortho/Qtz	0.7	1.3	1.0	0.8	0.7	1.0
Plutonic Mafic	0.5	0.0	0.0	0.3	0.0	0.4
Slate	0.2	0.0	0.0	0.0	0.0	0.2
Total Misc. Grains	7.0	2.3	9.8	5.8	9.0	5.5
Muscovite	0.0	0.2	0.0	0.0	0.0	Trace
Opaques	2.3	1.3	4.3	3.0	1.5	2.2
Zircon	0.0	0.0	0.0	0.0	0.0	Trace
Apatite	0.0	0.0	0.0	0.0	0.0	0.1
Epidote	5.7	0.8	5.5	2.8	7.5	2.6
Total Cem./Matrix	53.6	54.4	59.5	54.3	58.1	55.4
Hematite Cement	0.0	0.0	0.0	0.0	0.0	0.1
Calcite Cement	3.2	9.0	5.8	9.7	2.5	3.9
Sericite	3.0	2.8	4.7	7.0	4.8	2.4
Chlorite	31.8	31.3	39.0	30.7	42.3	21.8
Tremolite/Act.	0.0	0.0	0.0	0.0	0.0	0.6
Biotite	4.8	0.0	0.0	0.0	0.0	13.6
Qtz-Feld Matrix	10.9	11.3	10.0	7.0	9.5	13.2

Table 3.1e Modal analyses of medium-grained metagreywacke and pebbly metasandstone expressed in percent (600 point-count). Values add up to 100. Average modal value for the point counts is given at end. Samples are arranged east to west.

1) Common plutonic quartz occurs as large singular grains, or as aggregates of 2 or 3 grains, most with undulose extinction. Some grains are cataclasized and have numerous tiny crystals on the grain margins. Common plutonic quartz is the most abundant quartz type and consistently averages approximately 9.7% of the rock volume. Composite quartz grains consisting of at least four large crystals are also present and account for 2.6% of the rock volume. These grains are likely plutonic in origin.

2) Volcanic quartz, unit grains with embayments filled with volcanic material, is uncommon.

3) Polycrystalline quartz grains are of three types: schistose, stretched and recrystallized. Minor amounts of schistose and stretched quartz were encountered and likely indicate minor derivation from a metamorphic protolith. Stretched and schistose quartz comprise less than 1% of the rock volume. Recrystallized quartz (4.1% rock volume) appears as a mosaic of minute polygonal grains.

4) Uncommon chert grains were recognized by typical pin-point extinction of polycrystalline grains. Some of the chert may have recrystallized and is no longer identifiable as such.

These four quartz types are responsible for approximately 19.7% of the rock volume.

Feldspar

To corraborate orthoclase modes (much of the plagioclase appears untwinned), heels of point-counted samples were stained for K-feldspar using sodium-cobaltinitrite.

1) Uncommon fresh orthoclase appears as single grains with low birefringence, distinct cleavage and rare Carlsbad twins.
2) Altered orthoclase has similar characteristics as those above but is cloudy and saussuritized. Edges appear tattered with sericite and chlorite alteration which blends into the matrix. Altered orthoclase comprises 0.6% of the rock volume.
3) Fresh plagioclase is uncommon and occurs as single grains with polysynthetic twinning.
4) Altered plagioclase (albite) is identified by polysynthetic twinning, a cloudy appearance and saussuritization. Sericite, chlorite and carbonate are common alteration minerals. Plagioclase comprises approximately 9.4% of the rock volume.
5) Microcline is readily identified by Tartan twinning, although it is extremely rare.

Feldspar averages 10% of the metagreywackes by volume. The percentage may have been higher but alteration and saussuritization appear to have reduced its abundance.

Lithic Clasts

Classification of various volcanic and plutonic clasts in the metagreywacke and pebbly sandstone is based upon grain-size, fabric, and relative amounts of K-feldspar, plagioclase and quartz. There are limitations to this type of study in that some of the plagioclase is untwinned and much of the K-feldspar occurs as fine-grained groundmass in felsic volcanics. These problems were solved by staining for K-feldspar using sodium-cobaltinitrite. Estimation of the percentages

of volcanic and plutonic clasts was aided by visually estimating the amount of K-feldspar staining on heels using a binocular microscope. This system, coupled with textural and mineralogical data, provided general accuracy in determining the composition of clasts.

1) Felsic volcanic fragments are identified by the presence of fine-grained quartz and orthoclase. Phenocrysts of K-feldspar and quartz are common in these clasts; hornblende and plagioclase phenocrysts occur less frequently. On stained heels, felsic volcanic clasts stand out as bright yellow grains. Felsic volcanic fragments (identified as rhyolite or rhyodacite) are relatively significant, averaging 2.9% of the rock volume and 23% of all lithic fragments.

2) Felsic to intermediate volcanic fragments are characterized by phenocrysts of twinned plagioclase, quartz and hornblende set in a fine-grained K-feldspar and plagioclase-rich matrix. Most clasts are porphyritic and some fragments exhibit trachytic texture. Fragments of this type are stained a faint but distinct yellow on heels. Felsic-intermediate clasts (essentially dacite) constitute 5.2% of the rock volume and 43% of all lithic fragments.

3) Intermediate to mafic volcanic fragments are characterized by needle-like plagioclase laths, with occasional plagioclase phenocrysts and altered hornblende set in a fine-grained green to brown chlorite-rich matrix. Laths are either randomly oriented or pilotaxitic with distinct flow-banding. There is a lack of K-feldspar staining in these clasts. They represent 0.9% of the rock volume and 9% of all lithic fragments.

4) Mafic volcanic clasts under plane-polarized light are distinguished by white needle-like plagioclase laths within a dark green to dark brown chlorite-rich matrix. The plagioclase laths are usually randomly oriented. These clasts are likely altered basalt. Some fine-to medium-grained fragments exhibit ophitic texture and are likely altered diabase fragments. Mafic clasts are rare and comprise only 1% of all lithic fragments; their paucity is likely due to high weatherability.
5) Plutonic rock fragments are identified by medium-to coarse-grained textures. Three types of plutonic rock fragments are identified: plagioclase and quartz (P-Q), orthoclase and quartz (K-Q), and mafic plutonic clasts.

Plagioclase-quartz clasts account for 1.6% of the rock volume (13% of all lithic fragments), whereas orthoclase-quartz fragments are slightly less common and average 9% of all lithic fragments. The amount of orthoclase-quartz fragments may be slightly overestimated because some of the orthoclase component may be untwinned plagioclase.

Mafic plutonic fragments are rare and account for less than 1% of the rock volume and only 2% of all lithic clasts. They are identified by coarse plagioclase crystals associated with a matrix of fibrous chlorite.

6) Slate fragments are uncommon, comprising approximately 1% of all lithic fragments. Slate is identified by the presence of silt-sized quartz, oriented sericite and pale green chlorite.

Other Detrital Minerals

Opaque minerals average 1 to 3% of the rock volume. Pyrite,

hematite and magnetite were recognized under reflected light. Detrital zircon is rare but pleochroic halos in biotite flakes are credited to its presence. Large, ragged and seemingly broken muscovite flakes with strong birefringence are rare. These grains are likely detrital in origin.

Metamorphic "Matrix-Cement" and Textures

Metamorphic recrystallization has obliterated much of the original texture and has transformed the primary silty and clayey matrix into a polymineralic assemblage.

Lower greenschist facies metagreywackes typically have a matrix assemblage of silt-sized quartz and feldspar, chlorite, sericite carbonate and epidote. Biotite is found south of the biotite isograd and is associated with epidote and chlorite. Actinolite-tremolite and biotite are the stable metamorphic minerals south of the amphibole isograd. In general, the metamorphic minerals, especially phyllosilicates, exhibit a high degree of preferred orientation parallel to the axial traces of major folds. A large percentage of the matrix consists of silt-sized quartz and feldspar fragments. The amount of such matrix can be overstated because it is commonly difficult in these highly foliated rocks to distinguish comminuted felsic lithic fragments and heavily altered and saussuritized feldspar from original matrix.

1) Chlorite is a ubiquitous metamorphic mineral occurring as fine-grained, pale green laths and as fibers enclosing framework grains. In greenschist facies rocks, chlorite comprises approximately

36% of the rock volume, whereas in biotite-grade metasediments, it constitutes 17% of the rock volume.

2) Biotite is the second most common metamorphic mineral in the study area, particularly in the biotite schists. It occurs as pleochroic brown to green porphyroblasts of various sizes. There are two ages of biotite (Dutka, 1982), and in some cases, younger synkinematic biotite laths were observed to wrap around older prekinematic biotite. Biotite averages up to 25% of the rock volume in the biotite schist.

3) Sericite is common throughout the matrix in the low-grade samples, and is present as minute, colourless, elongate crystals with strong birefringence. Sericite accounts for 4% of the rock volume in the greenschist grade metasediments but is uncommon in biotite-grade metasediments.

4) Epidote is easily recognized by its high relief and anomalous interference colours. It usually appears as tiny subhedral tabular crystals in quantities of 1 to 3%. Some rock samples near the Quetico fault contain 6 to 8% epidote.

5) Calcite occurs as a cloudy and tattered alteration product and as a replacement of both plagioclase and matrix. It is also encountered as thin and irregular stringers. Carbonate exhibits extreme interference colours, twinning and a change of relief upon rotation. Between 3.5 and 6% of the rock volume is carbonate.

6) Hematite-limonite cement is present as rust-coloured halos around pyrite grains and as fillings between cleavage planes.

Hematite-limonite cement constitutes less than 1% of the rock volume.

7) Apatite is present in quantities of less than 1%. It is recognized by hexagonal outline, moderate relief and weak birefringence. It is likely metamorphic in origin.

8) Amphibole (actinolite-tremolite) is found at four localities within the study area, the most accessible being the Highway 11B turnoff. The randomly oriented lath-shaped amphiboles are poikiloblastic with inclusions of quartz. Where present, 10% of the rock volume is made up of this mineral. The presence of amphibole has been instrumental in redefining the amphibole isograd in the area.

9) Muscovite is observed in thin section as colourless laths with strong birefringence. Muscovite is evenly distributed throughout the rock matrix but also occurs in layers in phyllites. Large, ragged anhedral flakes of muscovite are also present, and may represent detrital grains.

10) Metamorphic albite is ubiquitous in all rocks. Low anorthosite content (An_{0-10}), albite twinning and relief less than balsam identifies the plagioclase as albite.

Petrographic Description of Rock Types

Metagreywacke

Thin section examination of metagreywackes reveals them to be compositionally and texturally immature. They are fine-to medium-grained and poorly sorted with angular to subrounded clasts. The clasts range from 0.05 to 2 mm in diameter, commonly with their long axes parallel to the schistosity as defined by the alignment of the phyllosilicates. Graded-bedding is observable in thin section.

Quartz is the most abundant constituent in the metasediments. Common monocrystalline plutonic quartz is the most common quartz type and constitutes 10% of the rock volume. Recrystallized quartz is fairly common; volcanic, stretched and schistose quartz occur infrequently. Chert is rare. The various quartz types constitute approximately 20% of the metagreywacke by volume.

Feldspar is the next most abundant mineral type and occurs as both untwinned (dominantly untwinned plagioclase) and as twinned grains. The twinned grains are usually smaller. Much feldspar has been saussuritized and altered to chlorite, sericite and carbonate. Modal study reveal an average of 10% feldspar, with 9.4% plagioclase and 0.6% orthoclase.

Rock fragments average 12.2% of the metagreywacke by volume and comprise 22.4% of the framework grains. Felsic and felsic-intermediate volcanics are the most abundant of the lithic clasts. They are also the most deformed of the clasts; such labile clasts often blend into the matrix. Intermediate-mafic and mafic clasts are uncommon but are

easily distinguished by chloritic alteration. Plutonic clasts, consisting dominantly of aggregates of quartz and plagioclase with lesser amounts of quartz and orthoclase, occur in amounts of 1 to 2% in coarser metagreywackes. Mafic plutonic clasts are rare.

The matrix comprises 55 to 75% of the rock volume and consists of very fine-grained quartz, predominantly sodic-feldspar, chlorite, sericite, epidote, apatite, pyrite and other opaques. Carbonate is common in some metagreywackes. The proportion of clasts to matrix is highly variable; clasts account for 25 to 75% of the rock. Often the matrix-clast boundary is gradational or diffuse due to similarity in composition and due to metamorphic alteration. The standard limit of 0.02 mm was used to distinguish between clasts and matrix.

Subhedral to euhedral crystals of chlorite, sericite, muscovite and biotite occur with a preferred crystallographic orientation, imparting a distinct continuous schistosity to the rocks. In some cases, phyllosilicates are observed to bend and wrap around more competent clasts.

In general, the metagreywackes of this study fall within the broad range of lithic arkosic wacke and lithic subarkosic wacke, using the classification scheme of Pettijohn et al., (1973; Fig. 3.1). Figures 3.2, 3.3 and 3.4 provide microscopic views of the modal components in the metagreywackes.

Biotite Schist

The biotite schists in the study area are the higher grade metamorphic equivalents of the phyllites, slates and metagreywackes.

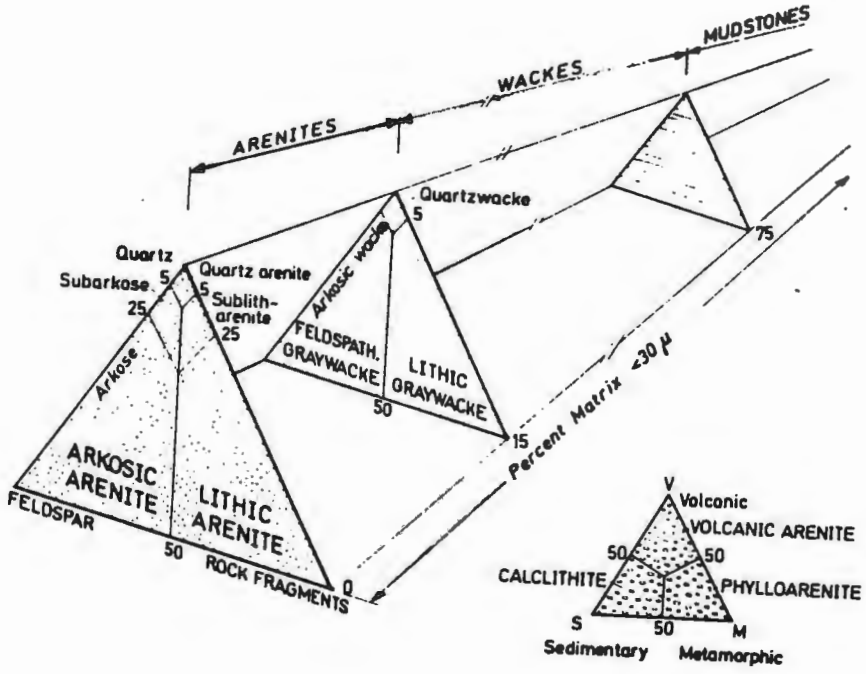

Figure 3.1 Dott's (1964) modified terrigenous sandstone classification scheme (From Pettijohn et al., 1973).

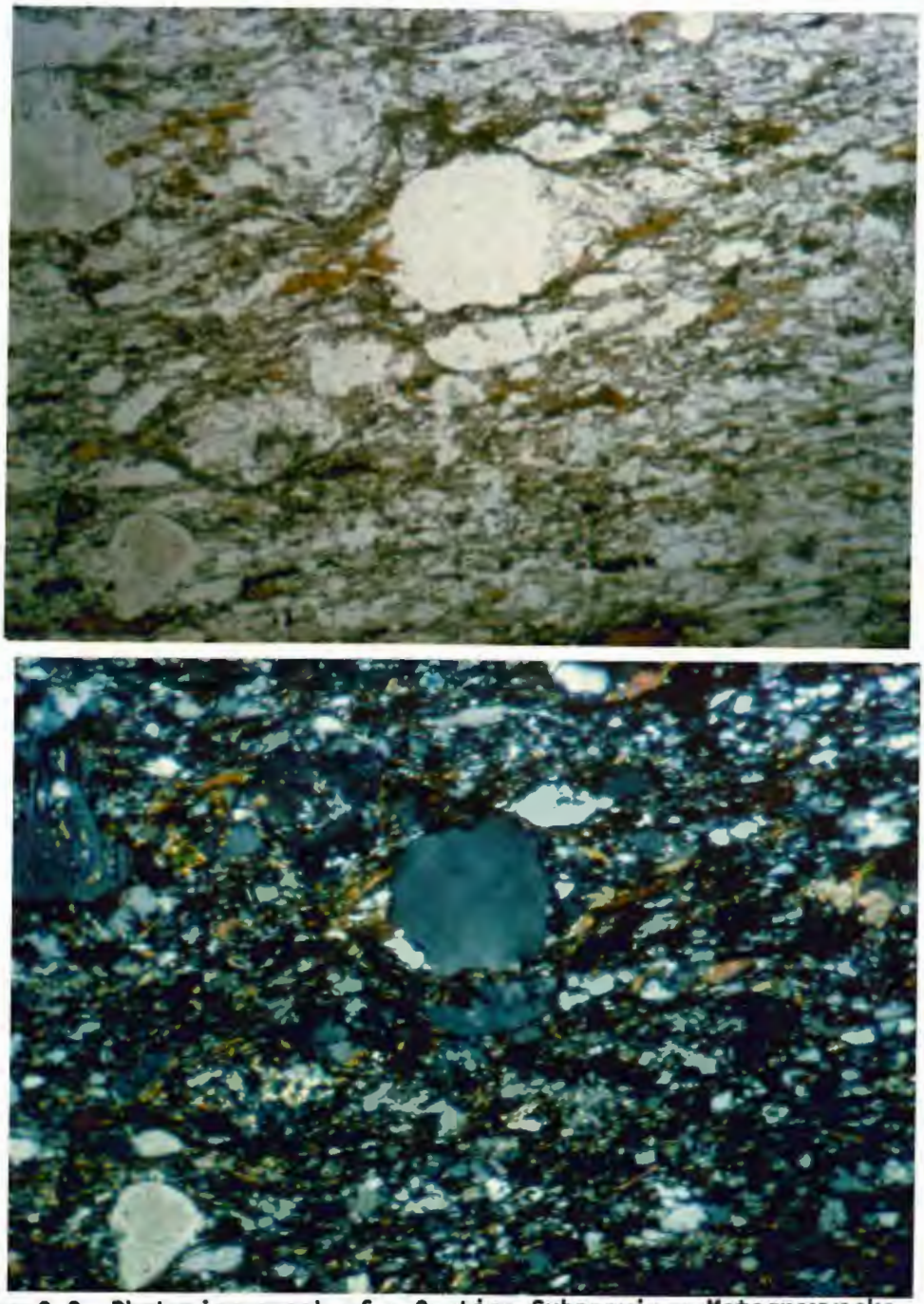

Figure 3.2 Photomicrograph of a Quetico Subprovince Metagreywacke (Sample 27BZ) exhibiting common quartz grain at centre, and plagioclase clasts at top and bottom right. Note how the stretched felsic volcanic clast at the bottom left blends into the matrix which consists of fine-grained quartz, feldspar, chlorite and biotite. Field of view is 1.2 mm wide. (A) is uncrossed nicols, (B) is crossed nicols.

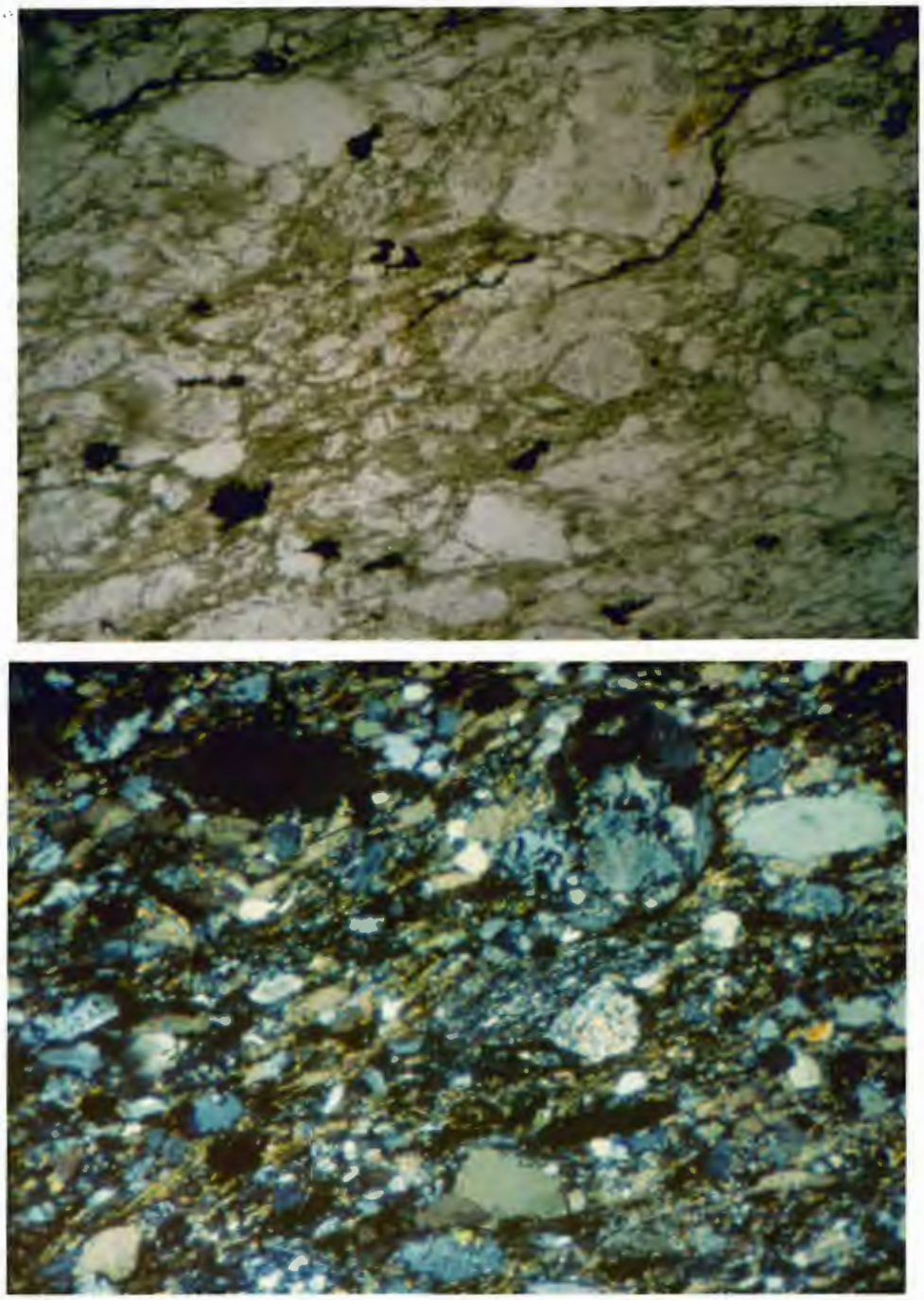

Figure 3.3 Photomicrograph of a Quetico Subprovince Metagreywacke (Sample 24A1) displaying a plutonic clast with myrmekitic texture at upper centre, felsic volcanic clast at centre, and quartz and feldspar framework grains set in a matrix of chlorite and sericite. Field of view is 1.2 mm wide. (A) is uncrossed nicols, (B) is crossed nicols.

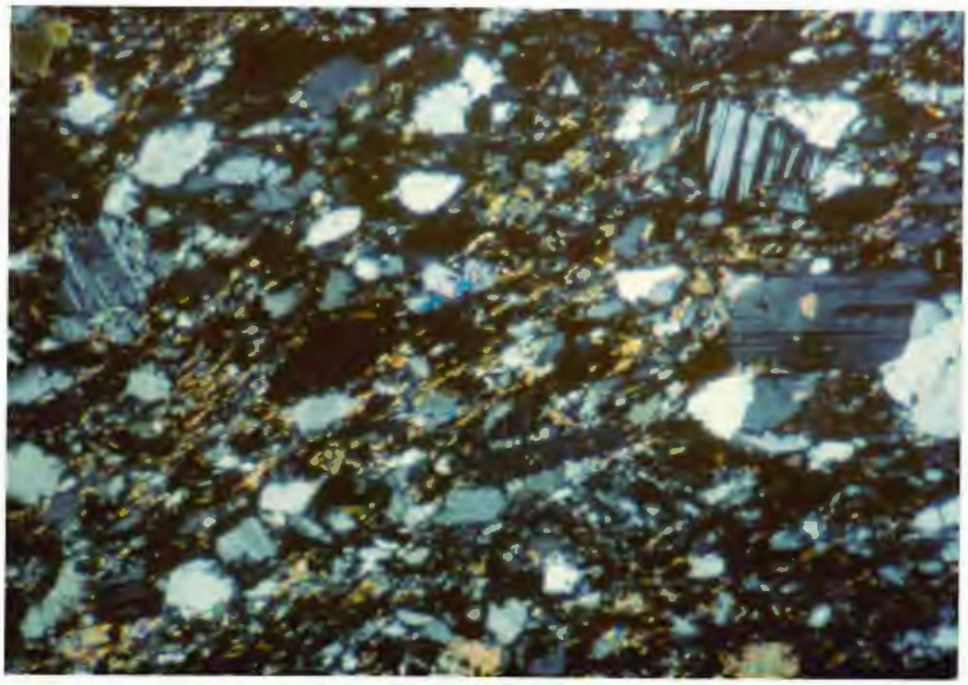

Figure 3.4 Photomicrograph of a Quetico Subprovince subarkosic metagreywacke (Sample 5CII) dispaying abundant plagioclase, polycrystalline quartz and common undulose quartz set in a matrix of chlorite and sericite. Field of view is 1.2 mm wide.

Thus, the detrital components in the biotite schists are comparable to their lower-grade counterparts.

In thin section, biotite is the most abundant mineral present and averages 12 to 38% of the rock volume. The medium-grained poikiloblastic ragged biotite laths (up to 2.5 mm long) wrap around larger more competent clasts of subangular quartz, feldspar, volcanic and uncommon plutonic fragments. The biotite is of two ages, and in some cases, younger synkinematic biotite deflects around older prekinematic biotite (Dutka, 1982).

The matrix consists of a fine-grained assemblage (in decreasing order) of quartz, feldspar, chlorite, epidote, sericite, apatite and opaques. Muscovite is uncommon; carbonate is a major constituent locally.

Plutonic quartz is the most abundant quartz type; recrystallized quartz is also common. Feldspar is extensively saussuritized, making compositional determination difficult using microscopic techniques. Lithic fragments are dominantly aphanitic to porphyritic volcanics of felsic to intermediate composition. They are commonly flattened and deformed, blending into the matrix.

The dimensional orientation of deformed clasts and the preferred orientation of the phyllosilicates helps to define the schistosity. Figures 3.5 and 3.6 are microphotographs of typical biotite schists.

Pebbly Metasandstone

The pebbly metasandstone is made up of poorly-sorted angular to subrounded, fine-to coarse sand and granules of volcanic and

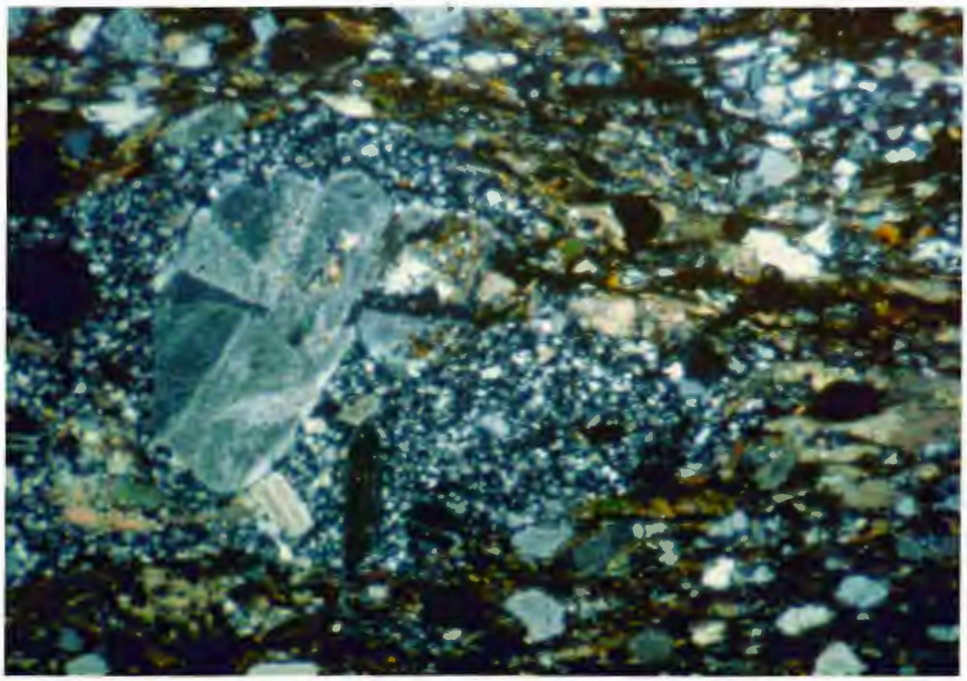

Figure 3.5 Photomicrograph of a Quetico Subprovince biotite schist (Sample 35BZ) dispaying a large porphyritic dacite clast at centre and a chert clast at the upper right. Schistosity is defined by the crystallographic orientation of biotite. Field of view is 1.2 mm wide.

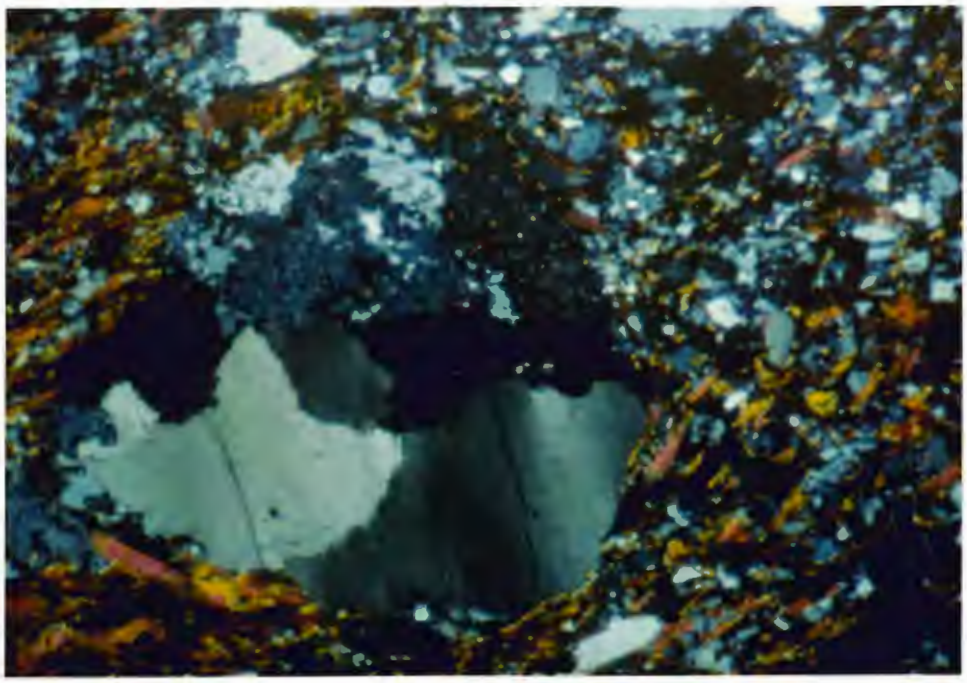

Figure 3.6 Photomicrograph of a Quetico Subprovince biotite schist (Sample 13A2) displaying a large plutonic quartz-plagioclase clast set in a matrix of flaky biotite and fine-grained quartz and feldspar. Field of view is 1.2 mm wide.

plutonic rock fragments with clasts in variable amounts of common and polycrystalline quartz, plagioclase and minor amounts of orthoclase, chert and slate. The framework grains are set in a fine-to medium-grained schistose matrix and average 42% of the rock volume.

Modal analysis of six thin sections indicates their composition to be similar to that of metagreywacke. Lithic fragments average 11.6% of the rock by volume, 75% of which are felsic to intermediate volcanic in composition. Other important constituents include 9.0% feldpar (dominantly plagioclase), and approximately 20% quartz, most of which is common plutonic quartz. Feldspar grains are saussuritized and altered. Most lithic fragments are deformed; the most unstable grains blend into the matrix. The matrix-supported grains are concentrated at the bases of beds. Pebbly metasandstone beds usually merge into metagreywacke. The matrix of the pebbly metasandstone consists of silt-to sand-sized quartz, feldspar, chlorite, sericite (biotite in higher grade metasediments), epidote, apatite, magnetite and pyrite. The matrix averages 58% of the rock volume.

There is a preferred clast alignment in the pebbly metasandstones, likely from strain. The clast alignment is parallel to the schistosity and makes a three to six degree angle with the bedding plane. The schistosity is outlined by the planar orientation of clasts and phyllosilicates. Typical pebbly metasandstones are shown in Figures 3.7 and 3.8.

Metamorphosed Mudstone and Siltstone

Slate commonly occurs interbedded with metagreywacke in the study

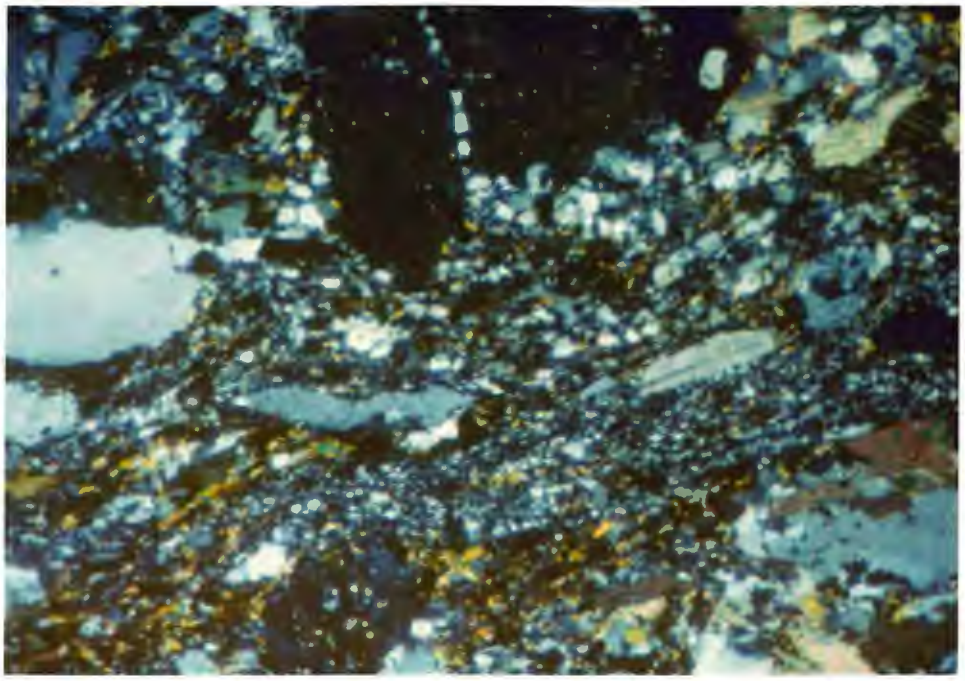

Figure 3.7 Photomicrograph of a Quetico Subprovince pebbly metasandstone (Sample 29BI). Two stretched felsic clasts are situated at centre. A tonalitic fragment is situated at the bottom right; a composite quartz grain is situated at the left and a quartz-plagioclase grain is situated at the top centre. Field of view is 1.2 mm wide.

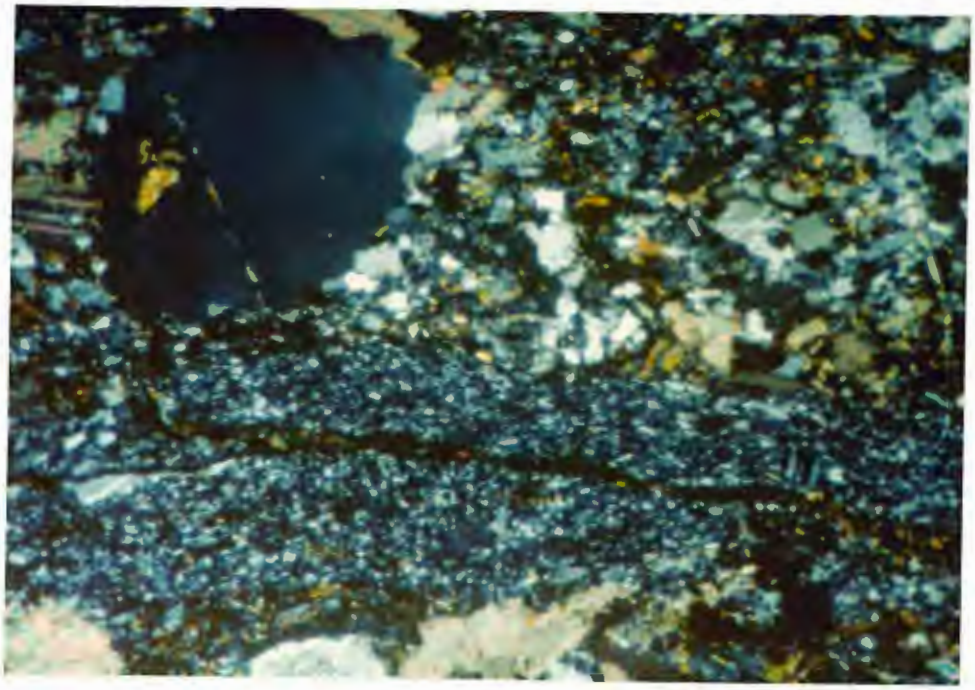

Figure 3.8 Photomicrograph of a Quetico Subprovince pebbly metasandstone (Sample 29BI) displaying two felsic volcanic clasts at bottom and a large common quartz grain at the top left. Field of view is 1.2 mm wide.

area.

Slate clasts are composed of fine-to very-fine grained subrounded quartz. Appreciable amounts of plagioclase and lesser amounts of orthoclase are present in some slides. Modal analyses were not conducted but visual estimates indicate the presence of 35% quartz, 10% feldspar and 3% opaques. The clasts are set in a very fine-grained matrix of chlorite, sericite, muscovite, epidote, quartz and feldspar. Approximately 50% of the rock is made up of matrix. Carbonate is locally present and occurs as patches or as irregular veinlets. Much of the slate has a banded appearance due to the compositional banding of chlorite, sericite and muscovite on a millimeter scale. Chlorite predominates in the darker layers along with lesser amounts of epidote, sericite and muscovite. Lighter coloured bands are composed primarily of minute interlocking quartz and feldspar grains with variable amounts of muscovite and carbonate. Compositional banding is likely due to the metamorphism of mud-rich tops which may represent both the distal deposits of normal turbidity currents and pelagic deposition.

As with all other metasediments studied, the slate has a distinct schistosity as defined by the crystallographic orientation of phyllosilicates. A typical slate is shown in Figure 3.8.

Metamorphosed Orthoconglomerate

Petrographic modal studies were not conducted on the metamorphosed orthoconglomerate in the study area because it is not volumetrically important. In thin section, the polymictic orthoconglomerate contains granules, pebbles and cobbles of many different lithologies.

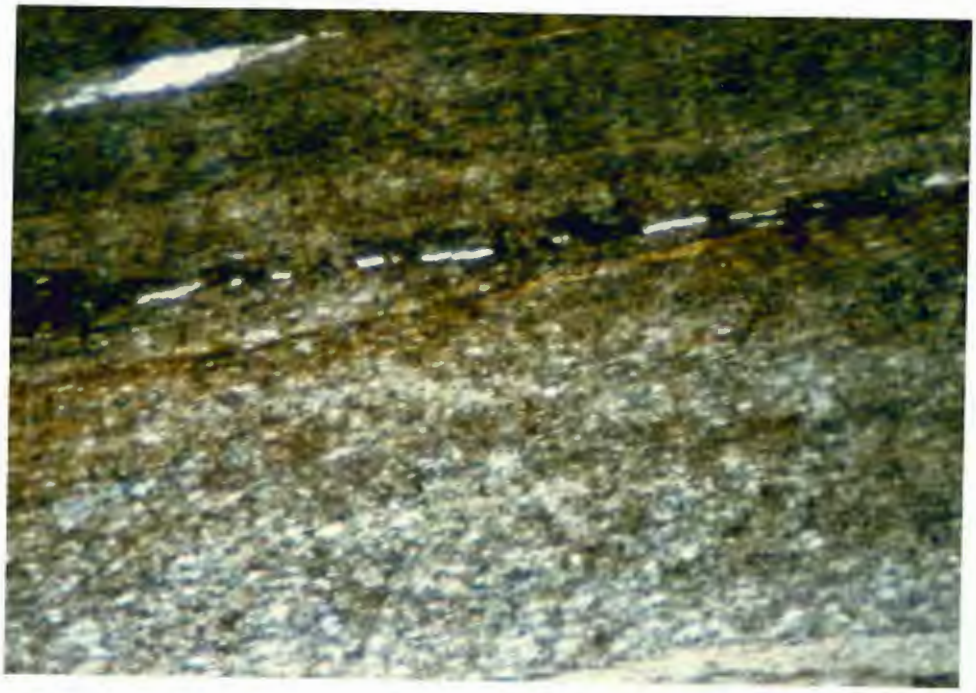

Figure 3.9 Photomicrograph of a Quetico Subprovince slate (Sample 211-I). Note how the quartz-rich silt bottom grades into a dark fine-grained top consisting of chlorite and epidote. Field of view is 1.2 mm wide.

Tonalitic and related felsic intrusives, metachert and felsic to intermediate volcanic fragments (most with porphyritic textures), are the dominant clast types. Quartz pebbles, slate and mafic clasts with hornblende and chlorite alteration are also common.

The conglomerate matrix is made up of angular to sub-rounded fine-to medium-grained sand and granule-sized volcanic fragments, intrusive fragments, feldspar, quartz and chert, all set in a much finer assemblage of quartz, sericite, chlorite and opaques. The matrix percentage is difficult to estimate due to metamorphism and deformation of the clasts but appears to comprise about 25% of the rock. The matrix is highly schistose and wraps around more competent grains and clasts.

The deformation and elongation of the clasts depends upon their composition. Plutonic rocks such as tonalite are more rounded and less deformed than those of metasedimentary material. Volcanic clasts are also deformed; mafic clasts are more deformed than those of felsic composition. The clasts are aligned parallel to the bedding plane and subparallel to the foliation. The clasts are elongated in two directions, and shortened in another, representing a pancake-like ellipsoid shape. Figure 3.8 is a photomicrograph of the orthoconglomerate.

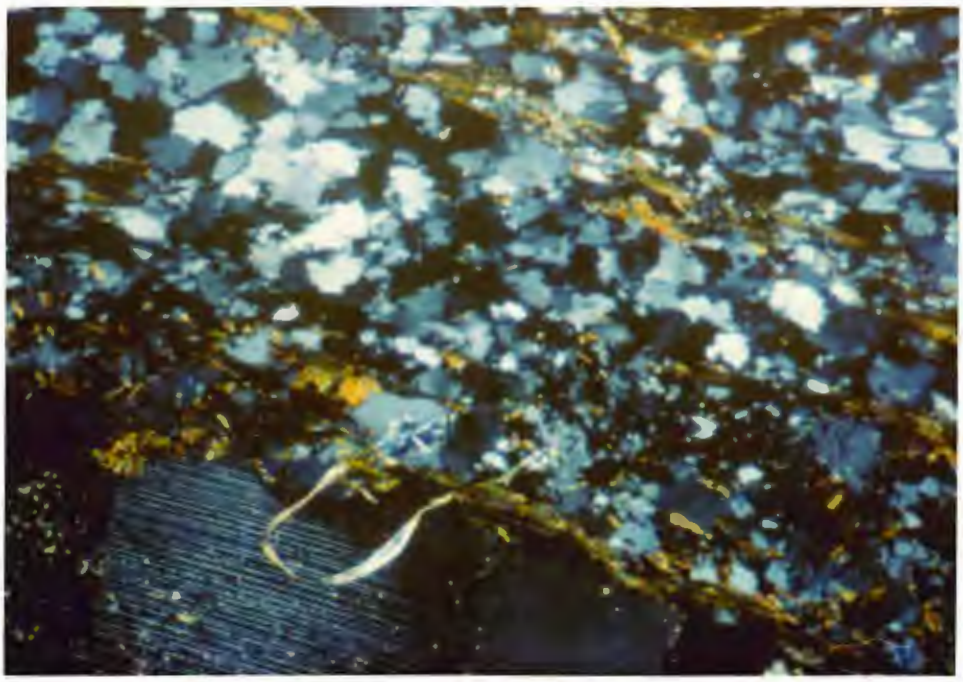

Figure 3.10 Photomicrograph of a Quetico Subprovince orthoconglomerate (Sample 13BIb). The field of view is dominated by chert clasts at centre and upper right and a tonalite clast at lower left. Field of view is 1.2 mm wide.

HEAVY MINERAL ANALYSES

Heavy minerals, so called because their specific gravities are higher than those of major framework grains, are volumetrically minor components of sandstones, usually comprising less than 1% of the rock volume. However, because of their diversity (over 30 transluscent detrital species are of common occurrence), and often characteristic paragenesis, heavy minerals have always played a key role in the interpretation of sediment provenance (Poldervaart, 1955). There has been a severe decline in the popularity of heavy mineral study after it became apparent that post-depositional processes such as dissolution and authigenic precipitation commonly take place. Nevertheless, heavy minerals remain extremely sensitive indicators of provenance and are important in paleogeographic reconstuction.

Certain heavy mineral species, especially zircons, display a high resistivity in the sedimentary process. Zircon's relative stability in the sedimentary cycle is attributed to its resistance to chemical attack, small size and lack of cleavage.

Heavy minerals were separated from samples by crushing and sieving, followed by densimetric (tetrabromoethane), magnetic and electromagnetic methods as outlined by Hutton (1950), and Poldervaart (1955). Initially, 5 to 10 kg of rock was placed in a jaw crusher and later passed through a U.S. Standard 60 mesh (0.25 mm) sieve. The number of zircons broken is surprisingly small. The powder was then placed in beakers, water added and the mixture stirred, then left to stand for three or four minutes, and the water carefully decanted.

This process was repeated until the water no longer appeared turbid. The sample was then dried and weighed. The mixture was then transferred to 1000 cc pear-shaped separatory funnels half-filled with tetrabromoethane. The mixture was then stirred at various depths with a glass rod at two to four hour intervals. The separation was usually complete within 24 hours, after which the heavy fraction was filtered off, washed with acetone, and dried.

A hand-held magnet was used to remove most of the magnetite, after which the sample was transferred to an isodynamic separator. The strongly magnetic fraction (mainly pyrite and iron-rich biotite) was quicky recovered and set aside. The less magnetic fraction was repeatedly run slowly through the separator at appropriate settings until a clean separation was obtained. The heavy separation was then divided into smaller units using a microsplitter, and mounted in Canada Balsam on 4.5x2.5 cm slides. Dr. Don W. Davis of the Geochronology Laboratory, Royal Ontario Museum, Toronto, also conducted some heavy mineral separations.

In order to obtain quantitative heavy mineral data, three types of point-counts were conducted on heavy mineral suites extracted from four different samples. In the first point count, the percentage of the opaque and magnetically susceptible material was calculated. This practice was abandoned after it became apparent that 94% of the minerals identified were opaques and metamorphic minerals such as biotite, actinolite, epidote and apatite. The type of point-count was conducted on relatively nonmagnetic fractions in order to determine

the percentages of non-opaque and nonmagnetic minerals such as zircon, tourmaline and rutile. Finally a varietal study was conducted on unbroken zircons, subdividing them according to colour, internal features, shapes and length-width ratios. Results are given in Tables 3.2, 3.3 and 3.4.

Apatite is the dominant non-magnetic heavy mineral present, averaging 80% of the grains identified. Zircon is second in abundance and averages between 10 and 20% of the grains. Biotite, epidote and chlorite are next in abundance, rarely exceeding 2% of the grains counted. Other heavy minerals observed include actinolite, anatase, andalusite, enstatite, hornblende, rutile and tourmaline (Table 3.2).

Purple-pink (hyacinth) zircon is the most common zircon type noted, followed in abundance by brown (malacon), dark brown-black (metamict), colourless and yellow varieties. The majority of the zircons are unzoned regardless of colour. The most common internal feature observed was zoning; 2 or 3% of the zircons have a dark core although zoning is more common in hyacinths. The majority of the grains studied are subhedral or idiomorphic in shape. Rounded or eye-shaped varieties are uncommon. Length to width ratios rarely exceed 2. Needle-like zircons are extremely rare likely due to their fragility (Table 3.3 and 3.4).

HEAVY MINERAL TYPE IDENTIFIED	SAMPLE 4DZ	SAMPLE 11AZ	SAMPLE 45CZ	SAMPLE 101BZ
Actinolite	0.0	0.0	0.0	0.7
Anatase	0.0	0.0	0.0	0.3
Andalusite	0.0	0.0	0.0	0.3
Apatite	86.3	71.7	78.3	81.3
Biotite	2.0	3.0	0.7	0.7
Chlorite	0.0	0.7	0.3	1.7
Enstatite	0.0	0.0	0.0	0.7
Epidote	1.0	2.3	1.0	2.7
Hornblende	0.0	0.3	0.0	0.0
Rutile	0.7	0.3	1.7	1.7
Tourmaline	0.7	0.3	0.3	0.7
Zircon	9.3	21.3	17.6	10.3

Table 3.2 Percentages of relatively non-magnetic heavy minerals (300 grain counts). All samples contain minor amounts of opaques. Samples are arranged east to west.

ZIRCON COLOUR & INTERNAL FEATURE	SAMPLE 4DZ			SAMPLE 11AZ		
	Euhedral	Subhed.	Rounded	Euhedral	Subhed.	Rounded
Brown (Malacon)						
Zoned	3.7	5.7	0.3	3.7	3.7	1.7
Unzoned	3.0	11.0	2.7	3.3	10.0	7.7
Dark Core	0.3	0.3	0.7	0.7	1.7	0.7
Purple-Pink (Hyacinth)						
Zoned	6.3	15.0	1.0	7.3	6.3	2.0
Unzoned	6.3	16.7	7.7	4.3	15.0	6.3
Dark Core	0.7	1.3	0.0	0.0	1.7	0.0
Dark Brown-Black (Metamict)						
Zoned	0.3	1.7	0.0	0.7	0.7	0.0
Unzoned	0.7	6.7	1.7	2.0	2.3	4.0
Dark Core	0.0	1.0	0.3	0.3	0.7	0.7
Colourless						
Zoned	0.0	0.0	0.0	0.7	1.0	0.0
Unzoned	0.7	2.3	0.0	2.7	3.0	1.3
Dark Core	0.0	0.7	0.0	0.0	0.3	0.0
Yellow						
Zoned	0.3	0.0	0.0	0.7	0.0	0.0
Unzoned	0.0	0.3	0.3	2.3	2.0	1.7
Dark Core	0.0	0.0	0.0	0.3	0.0	0.0

Table 3.3 Varietal study of unbroken zircon grains (300 grain counts, expressed in percent).

ZIRCON COLOUR & INTERNAL FEATURE	SAMPLE 45CZ			SAMPLE 101BZ		
Brown (Malacon)	Euhedral	Subhed.	Rounded	Euhedral	Subhed.	Rounded
Zoned	3.3	6.7	1.0	3.0	3.3	0.0
Unzoned	3.3	8.3	3.0	2.0	0.6	2.0
Dark Core	0.7	1.0	0.3	1.3	0.3	0.3
Purple-Pink (Hyacinth)						
Zoned	9.7	6.0	1.0	13.7	0.7	0.7
Unzoned	9.3	12.0	3.3	11.0	19.0	4.7
Dark Core	1.3	1.3	0.0	9.3	5.3	1.3
Dark Brown-Black (Metamict)						
Zoned	0.3	0.0	0.3	0.0	0.0	0.0
Unzoned	2.3	2.0	3.3	0.7	2.7	0.0
Dark Core	1.0	0.7	2.3	1.3	2.3	0.0
Colourless						
Zoned	1.3	0.3	0.3	0.0	0.0	0.0
Unzoned	2.3	4.0	3.1	0.3	1.0	0.7
Dark Core	0.0	0.3	0.0	1.0	0.0	0.0
Yellow						
Zoned	0.3	0.3	0.0	0.0	0.0	0.0
Unzoned	0.3	1.3	0.3	0.0	0.3	0.3
Dark Core	0.0	0.3	0.0	0.0	0.0	0.0

Table 3.4 Varietal study of unbroken zircon grains (300 grain counts, expressed in percentages).

GEOCHRONOLOGICAL DATA

High precision U-Pb zircon geochronology was conducted by Dr. D.W. Davis at the Jack Satterly Laboratory of the Royal Ontario Museum, Toronto, to provide age dates for detrital zircons recovered from the Quetico Metasediments in the Atikokan-Mine Centre area. High precision zircon analyses result from application of the new air abrasion and high gradient magnetic separation technique of Krough (1982). Zircon grains were hand picked under the microscope in order to select clear and uncracked specimens.

The resulting age dates can be used in the interpretation of volcanic-plutonic-sedimentary relationships, stratigraphic succession, and more generally, the evolution of the Archean crust (Davis and Edwards, 1982). U-Pb zircon geochronology studies conducted in the Wabigoon Subprovince include: the Wabigoon-Manitou Lakes area (Davis et al., 1982), the Kakagi Lake area (Davis and Edwards, 1982), the Savant Lake-Crow Lake area (Davis and Trowell, 1982), the southern Rainy Lake area (Davis et al., 1986), and the Lumby Lake area (Davis and Jackson, in press). A U-Pb zircon geochronology study was conducted in the Middle Shebandowan Lake area of the Wawa-Shebandowan Subprovince by Corfu and Stott (1985). This work should be useful in correlating across subprovince boundaries and should increase our understanding of the relationships between the Wabigoon, the Quetico and the Wawa-Shebandowan Subprovinces in this portion of the Superior Subprovince.

U-Pb zircon geochronology has provided an absolute time framework

for deposition of the Quetico Metasediments. Zircons recovered from the Blalock pluton which intrudes into the Quetico Metasediments 24 km southwest of the study area, defines a 2688 +4/-3 Ma minimum age for sediment deposition (Davis, Pezzutto and Ojakangas, in preparation). The youngest detrital zircons from the Quetico Metasediments are in the range of 2700+/-3 Ma; the oldest zircons are approximately 3004 Ma (Davis, Pezzutto and Ojakangas, in preparation). These two ages bracket the age of sediment deposition in the Quetico Subprovince. In addition, provenance may be inferred by correlating concordant detrital zircon age values recovered from the Quetico Subprovince with ages of volcanic and plutonic events dated in adjacent subprovinces.

U-Pb analyses of zircons from two felsic tuffs and a quartz porphyry of the Lumby greenstone belt (30 km north of Atikokan), yield ages of 2999 +/-1 Ma for emplacement of these felsic units. Zircons from a unit within the Marmion Lake Tonalite in the same vicinity contains zircons 3003 +/-5 Ma old. These dates correspond with values from the oldest Quetico Subprovince zircons and these units must be regarded as possible provenance sources. Geochronological data from the Marmion Lake Tonalite are also interesting because they provide the first firm evidence for extensive 3000 Ma crust in the southern Superior province (Davis and Jackson, in press).

It is unusual that no ages in the range of 2720-2750 Ma have yet been recovered from the Quetico Metasediments. This time period apparently represents the period of most intense volcanism in the Superior Province, based on dating in the greenstone belts. Perhaps

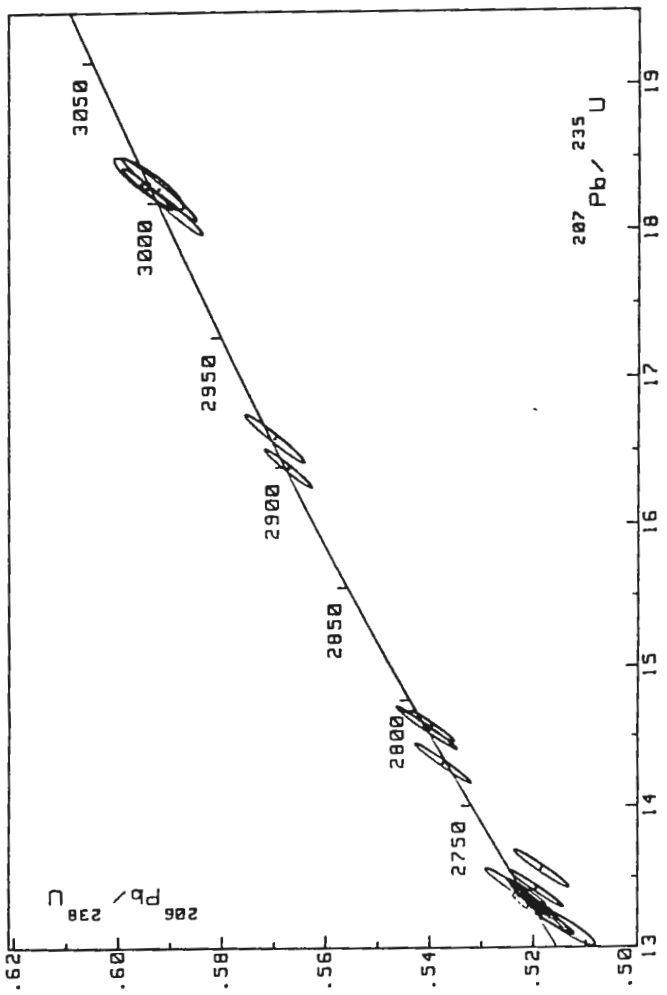

Figure 3.11 U-Pb isotopic data for zircons from the Quetico Metasediments. Error ellipses represent 95% confidence levels (From Davis, Pezzutto and Ojakangas, in preparation).

their absence is a fluke of small sample statistics. The majority of the detrital zircons are younger, with a significant number having ages of 2699 +/-1 Ma. Their source may be a rhyolite tuff from the Boyer Lake sequence in the Wabigoon and Manitou Lakes area which is dated at 2702 +14.6/-4.5 Ma (Davis, Blackburn and Krough, 1982); this felsic tuff is located 80 km north of the study area. A felsic tuff from the Kakagi Lake Group (160 km NW of the study area), was dated at 2711 +1.3/-1.2 Ma, whereas a quartz porphyry of the Berry Creek Complex in the same area gives an age of 2713 +6.0/-4.0 Ma (Davis and Edwards, 1982). Both of these units are similar in age to the bulk of age dates recorded from the Quetico Subprovince which commonly date at about 2710 Ma.

Obviously correlation of this type is tentative since much work in the Quetico Subprovince is still being conducted. In addition, there are numerous volcanic and plutonic units in both the Wabigoon and the Wawa Shebandowan Subprovinces that need to be dated. Geochronological data from the Quetico Subprovince are forthcoming and it is hoped that the results will contain age dates in the 2720-2750 Ma range so that more correlation can be attempted. The results will be published in the future (Davis, Pezzutto and Ojakangas, in preparation).

Chapter 4

METAMORPHISM

The 10 to 100 km wide and 1200 km long broadly symmetrical Quetico metasedimentary belt consists of marginal low-grade metasedimentary rocks, with higher-grade schists, gneisses and plutonic rocks in the interior (Mackasey et al., 1974; Pirie and Mackasey, 1978). The metasedimentary rocks of the Quetico Subprovince are pelitic enough to illustrate the nature of metamorphism from extremely low-grade assemblages through a sequence of fairly low-pressure, medium-grade assemblages characterized by the presence of staurolite, andalusite and garnet, into high-grade assemblages in the core with cordierite, sillimanite, and granites of anatectic origin (Fig. 4.1).

Because this study deals with original mineralogical components and sedimentary features of the Quetico Metasediments, only rocks of greenschist facies and biotite grade metamorphism situated along the Wabigoon and Quetico Subprovince boundary were studied. In the more pelitic beds of the turbidite sequence in rocks of the lowest metamorphic grade, the metamorphic mineral assemblage is sericite, chlorite, quartz, and plagioclase (albite), with minor amounts of carbonate, muscovite and epidote. This assemblage indicates that the metamorphic grade falls into the chlorite zone of the greenschist facies.

A short distance inward (southward) from the northern margin of the Quetico Subprovince, biotite appears while chlorite and sericite decreases in amount and eventually disappear. The presence of

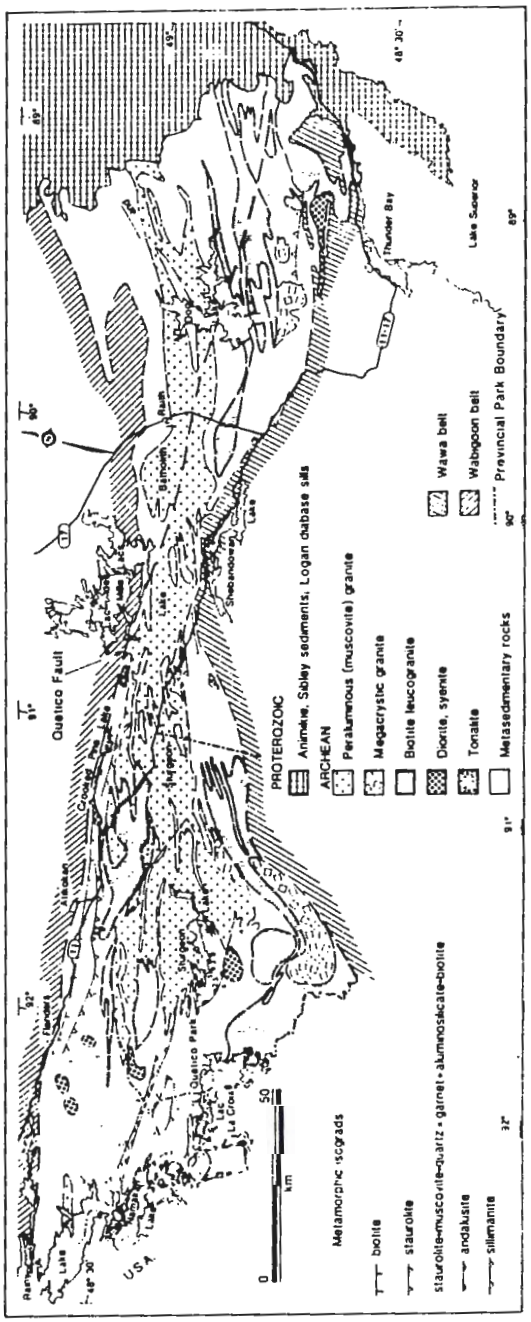

Figure 4.1 Geological map of the western Quetico metasedimentary belt. Data from Kehlenbeck (1976), Lehto (1975), Percival (1983), Percival and Stern (1984), and Pirie and Mackasey (1984). Ornaments on isograd symbols indicate high-grade side (From Percival, Stern and Digel, 1985).

biotite-compatible assemblages roughly flanking Highway 11 suggests the metamorphic grade increases southward from the northern margin to the biotite zone of the greenschist facies.

Petrographic studies of samples obtained near the junction of Highways 11 and 11B reveal the presence of randomly oriented actinolite-tremolite. Previous work in the area (Stone et al., 1984) has resulted in the definition of an amphibole isograd parallel to the biotite isograd. The spatial relationship between the mineral zones is roughly parallel, but this relationship is no doubt controlled by bulk rock composition (Pirie and Mackasey, 1978).

In addition, metamorphic studies in the Spawe-Atikokan area by McIlwaine and Hillary (1974) provide approximate locations of additional metamorphic zones and garnet-andalusite isograds. Fumerton's (1981) work in the vicinity of Calm Lake, resulted in the recognition of similar mineral assemblages near the western margin of the present study area. Across the belt, the metamorphic zonation is symmetrical, with east-west isograds parallel to the main layering and foliation. The relationship suggests that metamorphism may have been syntectonic (Borradaile, 1982). Table 4.1 presents the metamorphic mineral assemblages of the study area.

In Quetico Provincial Park, to the southeast of the study area, metamorphism grades southward from greenschist to amphibolite schist, towards an interior mixture of paragneisses, small leuco-granite bodies of anatectic origin, and the peraluminous Sturgeon Lake granite batholith (Percival, Stern and Digel, 1985).

North boundary of study area:	1) chlorite-sericite
	2) chlorite-sericite-carbonate
	3) chlorite-sericite-muscovite
	4) chlorite-sericite-epidote
	5) chlorite-sericite-epidote-biotite
	6) biotite-chlorite
	7) biotite
South boundary of study area:	8) biotite-tremolite-actinolite-garnet-andalusite

Table 4.1 Compatible metamorphic mineral assemblages in the study area. All assemblages contain quartz and plagioclase. (After Dutka, 1982).

On the basis of metamorphic pelitic assemblages, Percival and Stern (1984) concluded that metamorphism in the marginal schist in the vicinity of Quetico Provincial Park took place under overburden less than 10 km thick as a result of heat transport to the higher structural levels by granitic plutons. Work in the area by Pirie and Mackasey (1978), outlined the relative position of a prograde sequence of events in the pelitic assemblages. Using the P-T diagram of Carmichael, their work indicates a path of regional metamorphism extending from extremely low-grade greenschist conditions along the belt margins through points at 550°C at 3kb and 700° at 4.2kb to a maximum of over 720° at 4.2kb. The significance of the metamorphic assemblages and the significance of their contemporaneity to deformational events will be discussed in Chapter 9 which deals with a tectonic model for the study area.

Chapter 5

STRUCTURAL GEOLOGY

The major structural feature in the study area is the Quetico fault (Fig. 1.1) which is interpreted as an Archean, steeply-dipping, dextral, strike-slip fault. It separates the Wabigoon and Quetico Subprovinces to the north and south respectively, and extends from Lac Des Mille Lacs north of Thunder Bay westward to beyond Rainy Lake, a distance of more than 300 km.

The Quetico Subprovince has a linear form, the product of isoclinal folding and strike-slip faulting (Card and Ciesielski, 1986). According to Borradaile (1982) and Kehlenbeck (1985), two and, in some places, three generations of folds are recognized throughout the Quetico metasedimentary belt. The geometry and orientation of these structures indicate that an early period of gravitational instability in the adjoining Shebandowan Subprovince produced recumbent folds in the Quetico Subprovince with fold axial-surfaces that dipped shallowly to the east or west (Sawyer, 1985). During this folding, a schistosity (S_1) was developed. This early schistosity is evidenced by remnant crenulated biotite-rich laminae in localized areas where the later axial-planar schistosity (S_2) has been less strongly developed. This early schistosity is exposed in samples taken along Highway 11 near Kashabowie, 70 km east of Atikokan (Sawyer, 1983).

In order to construct six stratigraphic sections, the attitudes of various structural elements observed in the field were routinely recorded. These include cleavage, younging directions,

bedding-cleavage relationships and other lineations, and minor fold asymmetry. Plate 1 presents the structural elements in the study area.

The two younging criteria used extensively in the study area are graded-bedding and cross-bedding. Graded-bedding is observable in almost all of the exposures. Cross-bedding is rarely observed but is a reliable local younging indicator. Examples of both graded-bedding and cross-bedding are presented in Chapter 2.

S-Surfaces

There are two planar fabric elements observable in outcrop, bedding and cleavage. Bedding is designated S_0. Bedding is well preserved in the fine-to medium-grained metagreywacke and slate and less so in the metaconglomerate and pebbly metasandstone. The general strike of the strata within the study area ranges from 065-095° and the near-vertical dips vary 15° from vertical (Fig. 5.1). Younging direction is dominantly to the ENE.

One dominant penetrative axial-planar cleavage (S_2) is well-developed, especially in the more argillaceous metasediments (Fig. 5.2). The penetrative cleavage appears as closely spaced discrete parallel surfaces defined by the crystallographic orientation of the phyllosilicates and preferred dimensional orientation of framework grains.

Within the orthoconglomerate, the cleavage is seen to deflect around the larger, more competent clasts. In addition, less competent clasts appear to be aligned with their long and intermediate axes coplanar with the secondary cleavage.

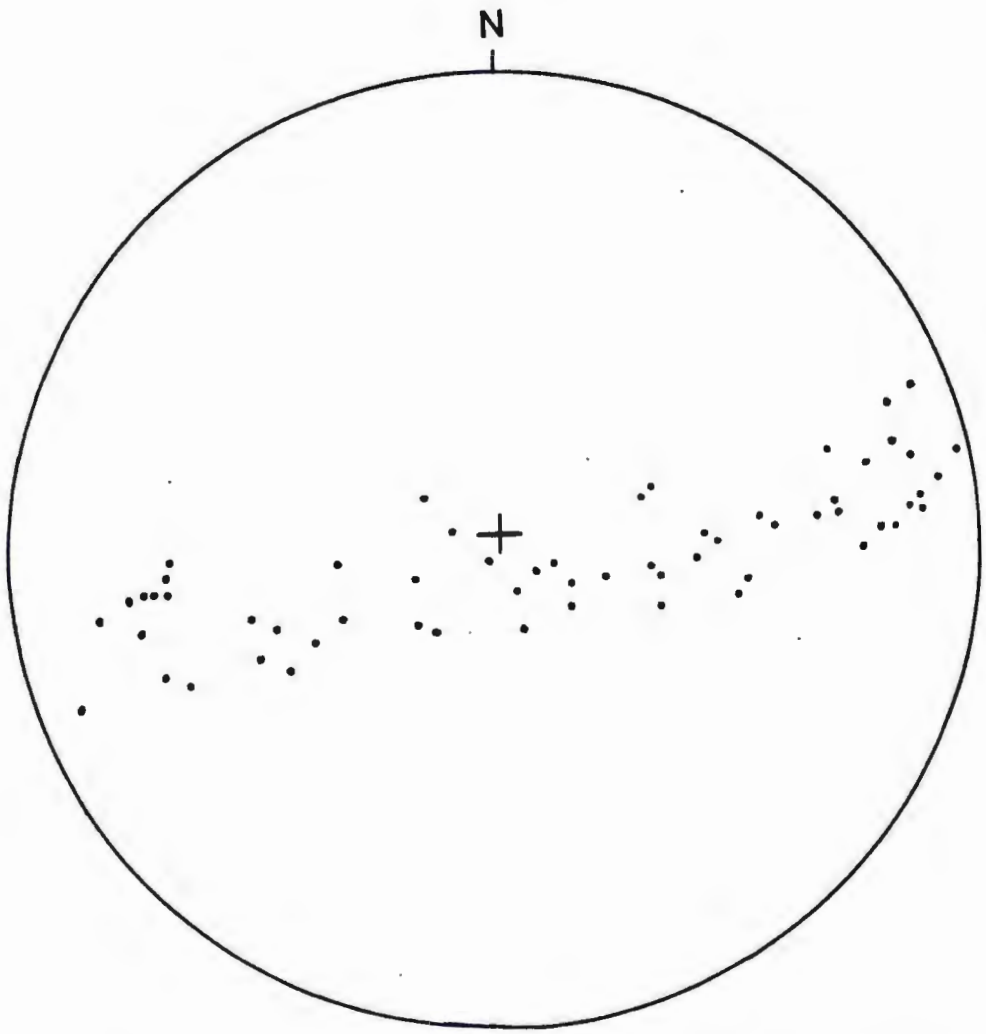

Figure 5.1 Equal area, lower hemisphere stereographic projection of poles to bedding (S_0). Bedding generally strikes to the east and has a steep dip.

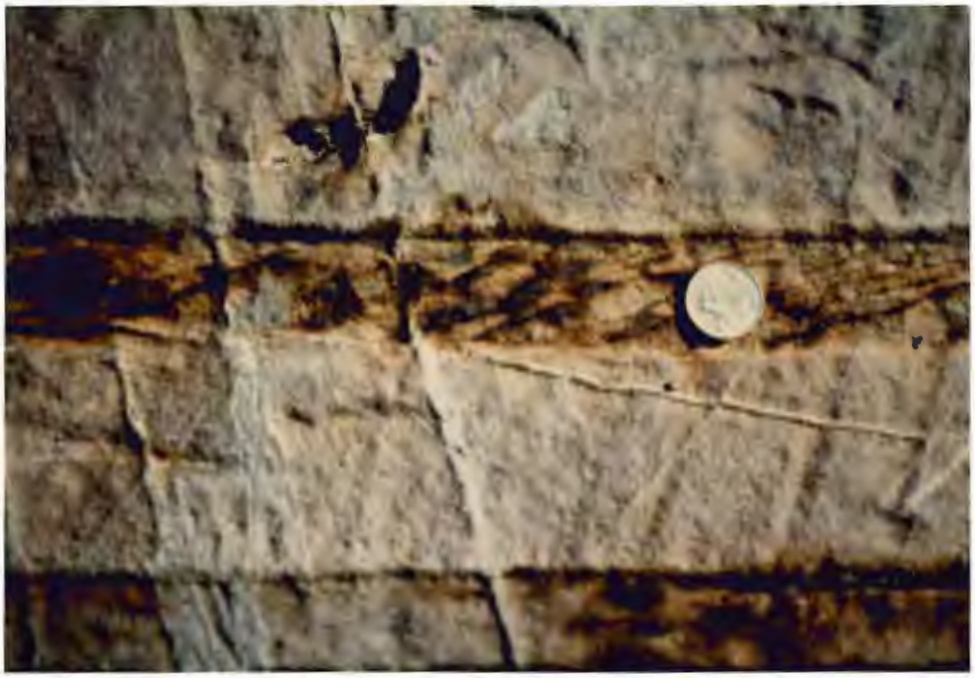

Figure 5.2 Bedding-cleavage (S_0/S_2) relationship readily observable in the argillaceous beds (now slates). Coin is 2.4 cm in diameter. Photo taken on Highway 11, adjacent to the Ministry of Transportation and Communication garage, 4 km west of the junction of Highway 11B into Atikokan.

Lineations

The attitudes of a number of linear fabric elements were observed and recorded. The orientation of cleavage and bedding planes and fold axes were routinely recorded in the field. Bedding and cleavage planes were later plotted as intersections. Stereographic projection of bedding and axial-planar cleavage (S_2) indicates that minor folds in the study area generally plunge shallowly to steeply to the east or west throughout the study area (Fig. 5.3). Along the western margin of the study area, kinks and small chevron folds occur in finely laminated rocks (Fig. 5.4). In these structures, the S_2 schistosity is folded about steeply dipping S_3 axial fold surfaces. The S_3 axial fold surfaces have a variable strike (Fig. 5.5). The size and frequency of chevron and kink folds increase toward the Quetico fault. The development of these folds may be the result of a component of compressive stress acting along the layering in the rock with a previously developed anisotropy (Stewart, 1984). Microscopic examination reveals a crenulation cleavage associated with the kink bands. Spectacular crenulation cleavage (S_3) is observeable on roadcuts along the north side of Highway 11, 4 km east of Flanders road.

Minor Fold Asymmetry

Numerous minor folds were discovered by mapping (Fig. 5.6), and the location of major folds is given in the structural map (Plate 2) contained in the back pocket of this report. The concept of minor fold asymmetry was utilized in determining the relative position of major

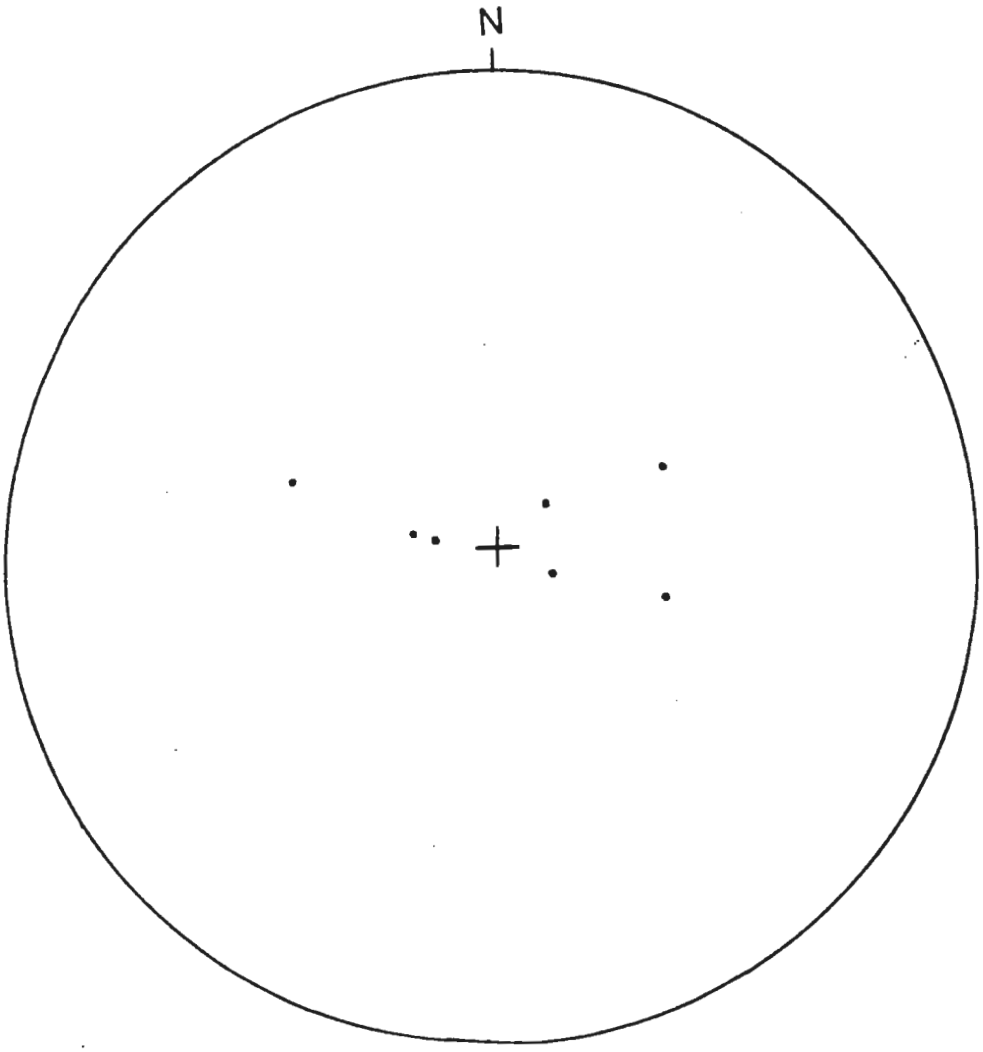

Figure 5.3 Equal area, lower hemisphere stereographic projection of the intersection of bedding and axial-planar cleavage (S_0/S_2). Axial folds have variable plunges east and west.

Figure 5.4 Kink bands (third generation folds) in finely laminated metamorphosed siltstone-mudstone. Photo taken 0.5 km east of Flanders road.

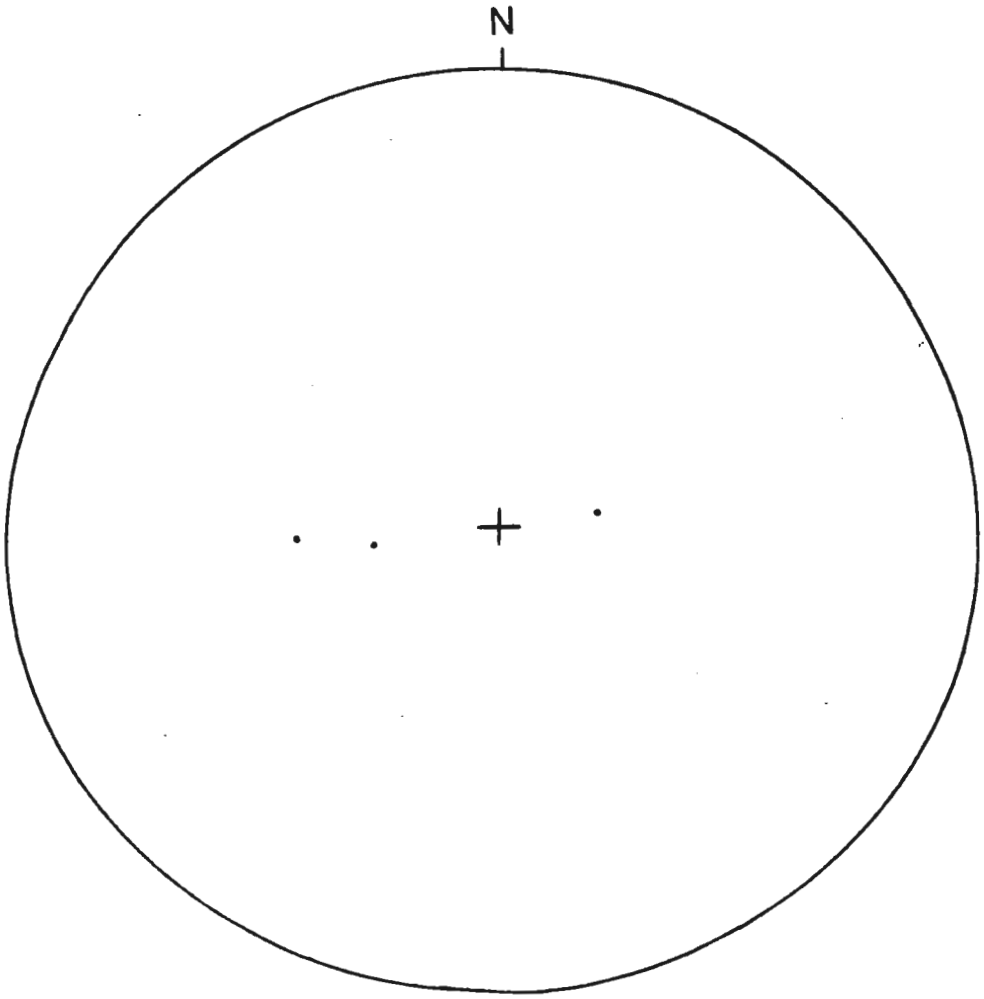

Figure 5.5 Equal area, lower hemisphere stereographic projection of the intersection of bedding and crenulation cleavage (S_0/S_3). The fold axes generally have variable strikes and steep plunges.

folds in the study area. The nomenclature used to describe minor fold asymmetry is presented in Figure 5.7.

The minor folds are the result of the same episode of deformation responsible for the major folds as indicated by the presence of S_2 cleavage which is axial planar to the minor folds. With the understanding of the relationship between bedding and cleavage, and the realization that this similar relationship exists throughout the entire area, local bedding-cleavage relationships found in S, Z, M, or W folds help to indicate the position of major folds in the area.

Second generation (F_2) tight to isoclinal folds are characteristic in the study area. Refolding of earlier folds cause second generation fold structures to be either upward-or downward-facing depending upon the present exposure level (Sawyer, 1983; Fig. 5.8). Only three minor fold closures were observed in the field and their attitudes are presented in Figure 5.9.

Figure 5.6 Minor fold closure (arrow) in tightly folded beds. Fold-hinge plunges to the west (towards bottom of page at 18°). Younging direction is away from the hinge. Photo taken 400 m west of Lerome Lake boat launch along HWY 11.

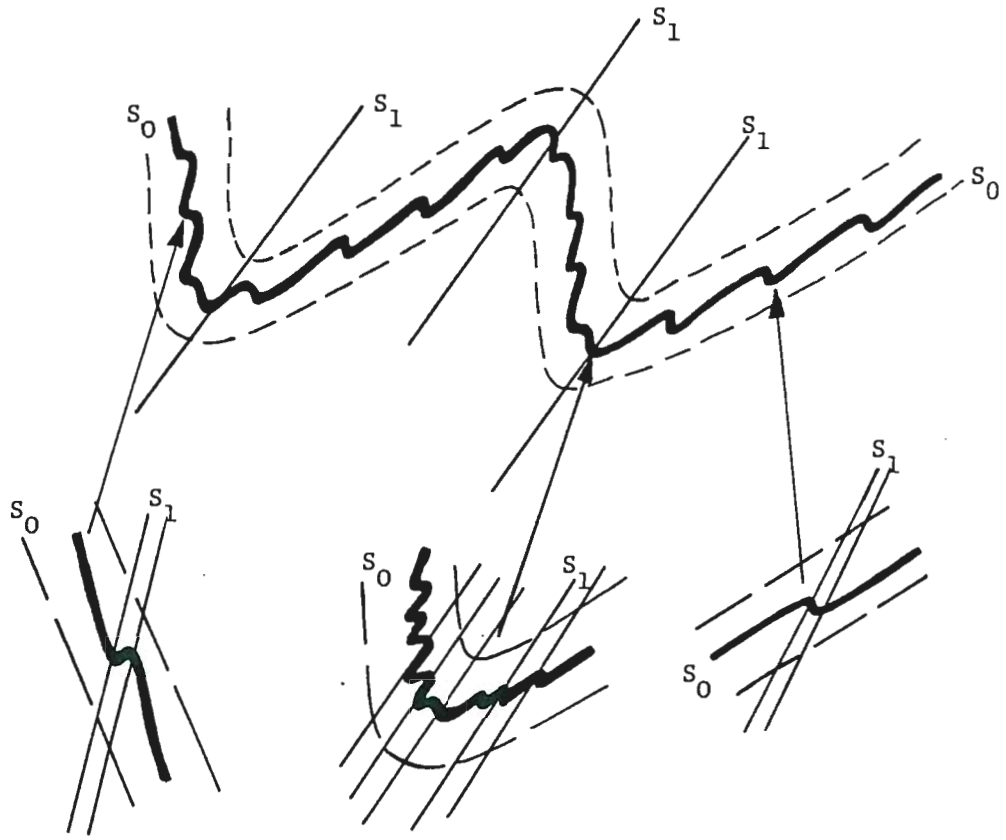

Figure 5.7 Illustration of minor fold asymmetry in relation to major fold structure (Modified from Davis, 1984).

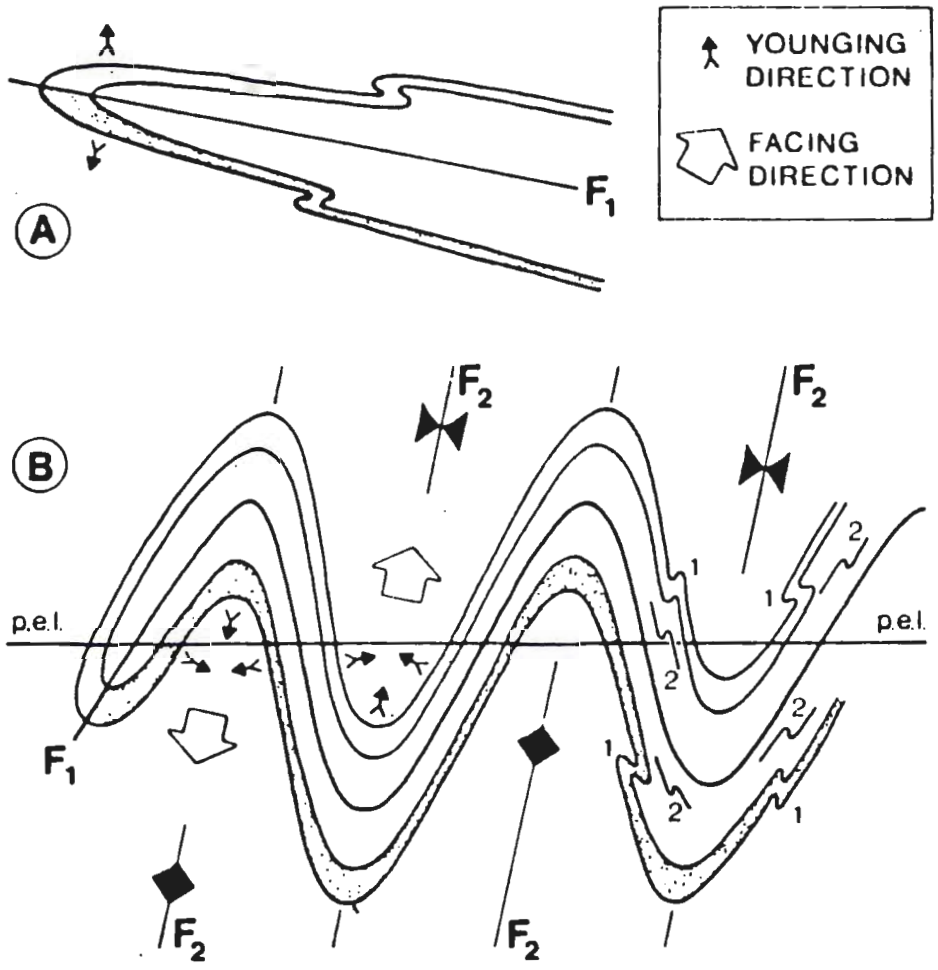

Figure 5.8 (A) F_1 fold showing normal and inverted limbs together with vergence of associated minor folds. (B) F_1 fold refolded by F_2. Note the facing directions depend upon the present exposure level relative to the F_1 axial surface. Both illustrations are cross sections (After Sawyer, 1983).

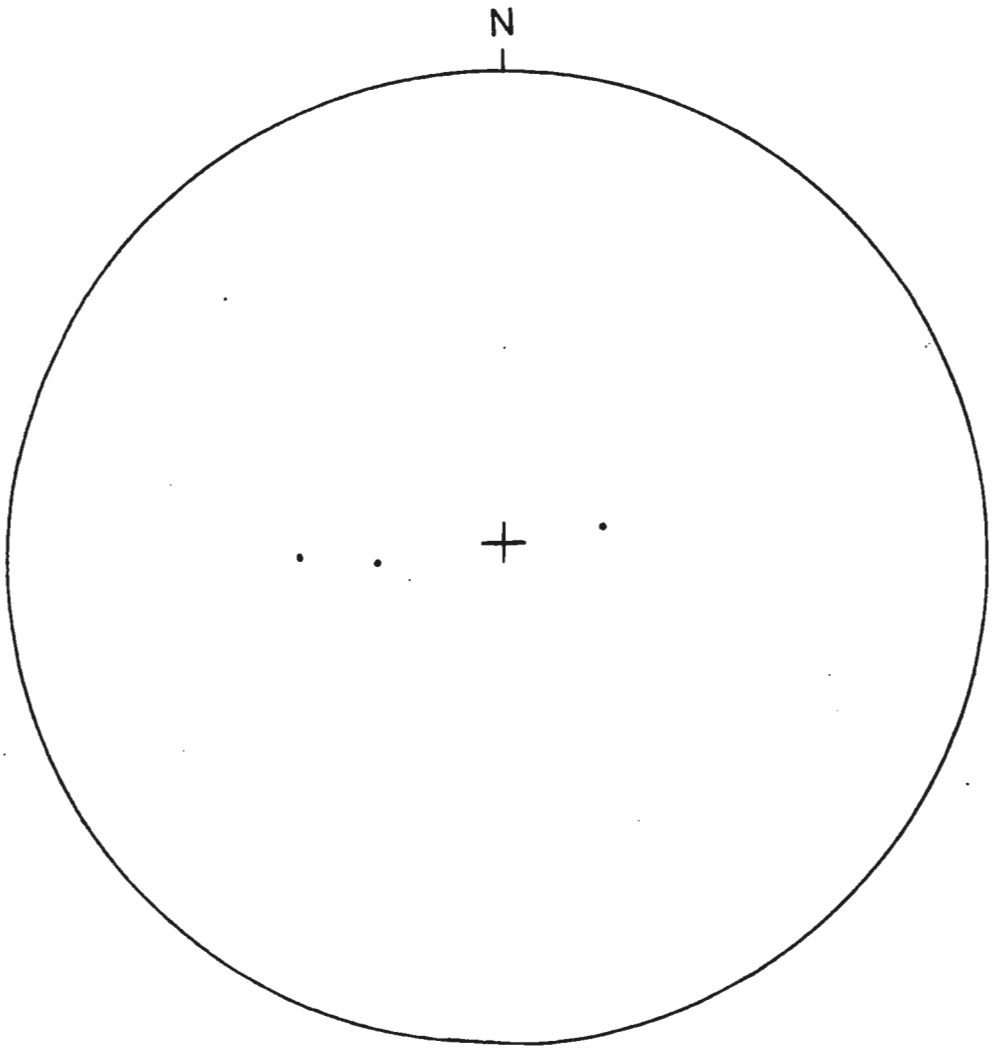

Figure 5.9 Equal area, lower hemisphere stereographic projection of three minor fold axes observed in the study area. The folds plunge steeply to the east and west.

Chapter 6

SEDIMENTATION AND ENVIRONMENT OF DEPOSITION

Turbidity Currents: Mechanics of Flow and Deposition

Mass movements, consisting of sediment travelling down-slope under the influence of gravity, are called sediment gravity flows (mass flows). Sediment gravity flows are distinguished from gravity sliding or slumping because sediment gravity flows contain extensive internal deformation (Dott, 1963). In sediment gravity flows, it is the sediment that is moved by gravity and the sediment motion is responsible for the movement of the interstitial fluid (Middleton and Hampton, 1973).

Sediment gravity flows are recognized by the nature of the dominant sediment support mechanism. Four main categories are recognized: 1) turbidity currents in which the sediment is supported by fluid turbulence, 2) fluidized sediment flows in which sediment is supported by the upward escape of fluid between grains, 3) grain flows, in which the sediment is supported by direct grain collision, and 4) debris flows, in which the larger grains are supported by a mixture of sediment and fluid.

This classification is genetic and some of the proposed mechanisms are hypothetical. In real sediment flows, more than one mechanism is important, making the distinction between flow-types difficult. Although turbidity currents have never been witnessed in a modern marine environment, the resedimented facies association of greywacke and interbedded shales in deep marine conditions can only be explained

by turbidity currents with hemipelagic muds accumulating during the intervals between turbidity currents.

History

The concept of turbidity currents dates back to observations by Forel (1885) on the undercurrent formed by the Rhone River as it enters Lake Geneva. Daly (1936), suggested that turbidity currents might have flowed down the continental shelves and eroded submarine canyons during low sea levels of the Pleistocene. Interest soon changed from their erosive capacity to the capacity of turbidity currents to transport sand and coarser sediments into deeper water, forming graded beds. Kuenen (1950) produced graded beds in his laboratory. He later used the experiments to explain graded beds in the Apennines (Kuenen and Migliorini, 1950). Heezen and Ewing (1950) used turbidity currents to explain broken telecommunication cables in the Atlantic.

Much of the knowledge of sedimentary structures and turbidity facies was summarized by Bouma (1962). The "Bouma Sequence" outlines the five sequences that are typical in a single complete greywacke bed (Table 2.2). Some divisions may be missing from tops or bottoms of individual beds which may start with any division. The proportions of beds starting with the basal "A" sequence is partly influenced by the distance the current has flowed (Walker, 1967). A package of greywackes with a paucity of "A" or "B" sequences may indicate distal environments but care must be taken to ensure that one is not observing overbank deposits.

Mechanics of Deposition

Turbidity currents are surges that are often initiated by a sudden event such as an earthquake or storm. Many turbidity currents originate in submarine canyons and move downslope away from the source. At first they may be confined to canyons or to channels on the fan surface but later the current spreads laterally on distal parts of the submarine fan and basin floor (Middleton and Hampton, 1973).

As turbidity currents travel away from their sources, they develop into flows that are divisible into four parts, each with its own characteristic hydraulic behaviour: the head, the neck, the body and the tail (Fig. 6.1). In a turbidity current, sediment surges forward and upward through the head and back to the tail where it becomes dilute and eventually lost. Thus, the coarsest sediment is progressively concentrated in the head. The head of a turbidity current is a region of both erosion and deposition.

In turbidity currents, the main sediment-support mechanism is turbulence which is generated along the flow boundary; the water moves downslope because the contained sediment makes the current denser than the overlying water. Once an event sets into motion a turbidity current, it is possible that the turbidity current will travel for a long distance because the sediment is held in suspension by turbulence. Turbidity is generated by flow; flow is generated by the downslope action of gravity acting upon a density difference. As a result, there is a complete feedback loop and the turbidity current can travel for hundreds of miles because the energy lost to friction is

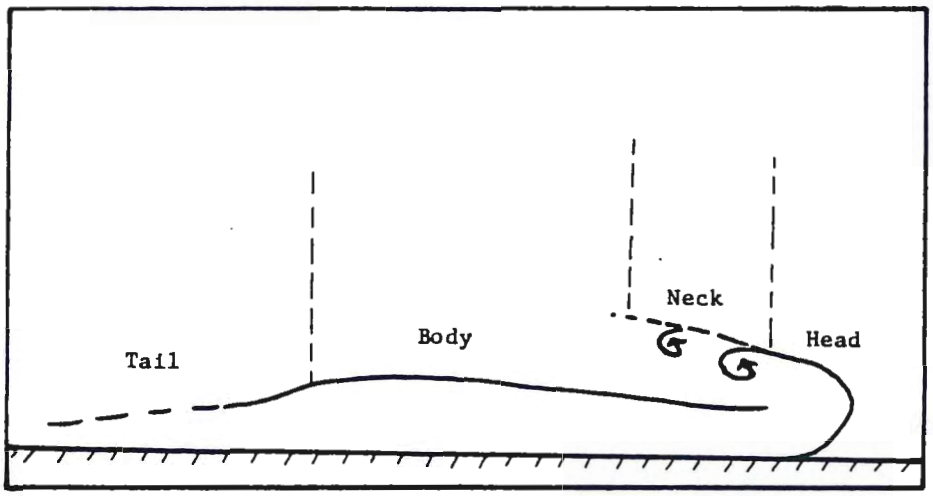

Figure 6.1 Schematic division of a turbidity current into head, neck, body and tail showing the flow pattern within and around the head (After Middleton and Hampton, 1973).

replaced by gravitational potential energy as the current moves downslope.

The turbidity current concept is both simple and purposeful in that it interprets each greywacke-siltstone-mudstone bed to be result of a single short-lived event (Walker, 1984). The concept is extremely purposeful because it suggests that the deposition of thousands of graded greywacke beds, alternating with shales, is the result of similar events. Once the beds have been deposited, they are unlikely to be eroded. According to Walker (1973), no similar volume of rock can be interpreted so simply. The turbidity model accounts for graded beds that lack evidence of shallow water reworking. This model also accounts for transported shallow water foraminifera in greywacke beds in bathyal or abyssal environments.

Sedimentation and Environment of Deposition

Pettijohn (1943) conducted the first study of Archean sedimentation in the Superior Province, and concluded that the regularly interbedded sandstones and shales were varves. Since then, many workers have used the turbidity current model to explain Archean sandstone and slate sequences, such as Goodwin and Shklanka (1967) at Bee Lake in Northwestern Ontario, and Walker and Pettijohn (1971) in the Minnitaki Lake area of Northwestern Ontario.

The importance of turbidity currents as the mode of transportation and deposition of greywackes and interbedded shales on the continental slope and on submarine fans is firmly established (Walker, 1975; Normark, 1978). Their importance in the resedimentation of volcanogenic detritus as volcanogenic greywacke in arc systems has also been documented (Ojakangas, 1972a, 1972b, 1985; Ayres, 1982; Sigurdsson, 1982a, 1982b). Ojakangas (1985) reported that sedimentation during Archean time was dominated by the resedimented facies association of greywacke, interbedded shale and conglomerate, possibly on submarine fans. Many Archean metasedimentary assemblages are indicative of deposition on submarine fans. Slumping processes with subsequent accumulation around the edges of rapidly growing explosive submarine volcanic edifices is possible and does not necessitate the presence of submarine fans (Ojakangas, 1985).

The great thickness of metasedimentary sequences found in the Canadian Shield reflects deposition in very deep subsiding troughs flanked by volcanic areas. The absence of a "shelf facies" in the

metasedimentary sequence suggests a steep coastal margin due to uplift in the source area and downwarp of the basin (Goodwin, 1968). In the proposed model, the presence of well-rounded boulders in the conglomerate and the angular nature of detrital sand grains suggests rapid erosion in an area of substantial relief. The detritus was probably transported to the basin margin by high velocity streams. There, the clastic sediments accumulated as temporary deposits on the slopes of unstable basin margins, later to be jarred loose and transported downslope as turbidity currents (Fig. 6.2). The turbidites were deposited in deep water, as they lack any features indicative of shallow agitated water such as ripples or medium-to large-scale cross-bedding.

The metagreywacke, slate and biotite schists of the Quetico Metasediments are characterized by moderate to poor sorting, subrounded to angular grains, and a high percentage of matrix. In addition, they contain sedimentary features attributable to turbidity current deposition. It is the author's intention to produce a depositional environment model for these metasediments, but a lack of conclusive paleocurrent data, and the general absence of long unbroken and continuously exposed stratigraphic sections due to isoclinal folding and cover makes the complete interpretation of the depositional environment of these rocks difficult.

Walker (1967), has proposed a set of criteria to indicate the proximality of the turbidity current by using the Bouma model. The Bouma model has been assembled from a large number of examples and

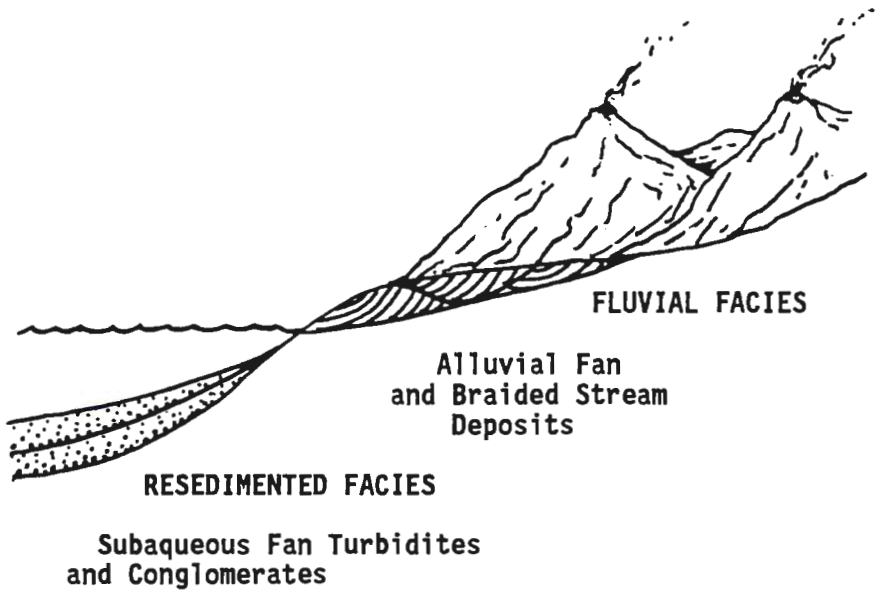

Figure 6.2 Model showing the common environments of deposition of some Archean sediments (After Ojakangas, 1985).

literally thousands of beds. It acts as a norm with which to compare individual beds, and as a framework with which to build general models of fan morphology. Walker (1967), distinguishes between proximal and distal sites based upon inferred flow regimes characterized as either upper or lower (Tables 2.2, 6.1). Walker considers upper flow regimes as proximal and lower flow regimes as distal. The majority of the beds observed in the Atikokan-Mine Centre region are "classical" facies "C" and "D" turbidites of Walker (1967), and Mutti and Lucchi (1972; Table 6.2). Facies "C" turbidites have a Bouma A base, whereas facies "D" turbidites have "base cut-out sequences" such as Bouma B, or DE. "Base cut-out" sequences are indicative of distal environments and are common in the western half of the study area. Also common in the western half of the study area are uniformly bedded slate (facies "E" and "G" of Walker, 1976; Mutti and Lucchi, 1972). Facies "E" has a lower sand/shale ratio and thinner beds than facies "D". Facies "G" beds are pelagic and hemipelagic shales, which form from very dilute suspensions (Walker, 1984).

In the eastern half of the study area, "classical" turbidites are in close spatial relationship with pebbly sandstones (facies "A4"-organized pebbly sandstone, and facies "B2"-massive sandstone without dish structure). It is difficult to explain the spatial relationship of fine and coarse sediments without a proper model. Thus, workers have turned to Normark's (1970) and Walker's (1973) slope-submarine fan-basin floor model to show the relationship between the various facies associations.

Table 6.1, Walkers's (1967) Comparison of Proximal to Distal Turbidites

Proximal Beds	Distal Beds
A) Beds thick.	-Beds thin.
B) Coarse-grained.	-Fine-grained.
C) Individual sandstone beds amalgamated to form thick beds.	-Beds not amalgamated.
D) Beds irregular in thickness.	-Beds parallel sided and regularly bedded.
E) Scours, washouts and channels common.	-Few small scours and no channels.
F) Mudstone partings rare, sand/silt ratio high.	-Mudstone layers between sandstone beds well developed, sand/silt ratio low.
G) Beds graded or crudely graded.	-Beds well graded.
H) Many AE sequences.	-Few AE sequences.
I) Laminations and ripples rare.	-Laminations and ripples common.
J) Scour marks are more common than tool marks.	-Tool marks are more common than scours.

Table 6.2

BASIC CLASSIFICATION OF TURBIDITE AND OTHER RESEDIMENTED FACIES, BASED UPON MUTTI AND RICCI-LUCCHI (1972) AND WALKER (1967, 1970)

BOUMA SEQUENCE NOT APPLICABLE	FACIES A	Coarse-grained sandstone and conglomerate
	A1	Disorganized conglomerate
	A2	Organized conglomerate
	A3	Disorganized pebbly sandstone
	A4	Organized pebbly sandstone
	FACIES B	Medium-fine to coarse sandstone
	B1	Massive sandstone with dish structure
	B2	Massive sandstone without dish structure
BEDS CAN REASONABLY BE DESCRIBED USING THE BOUMA SEQUENCE	FACIES C	Medium to fine sandstone "classical" proximal turbidites beginning with Bouma's division A.
	FACIES D	Fine and very fine sandstones, siltstones, classical distal turbidites beginning with Bouma's division B or C.
	C-D FACIES SPECTRUM	(can be described using the ABC index of Walker, 1967).
	FACIES E	Similar to D, but lower sand/shale ratios and thinner more regular beds.
BOUMA SEQUENCES NOT APPLICABLE	FACIES F	Chaotic deposits formed by downslope mass movements, e.g. slumps.
	FACIES G	Pelagic and hemipelagic shales and marls, deposits of very dilute suspensions.

Normark's (1970) general modern submarine fan model consists of three parts: a leveed valley on the upper fan, a mid-fan built up of suprafan lobes that periodically shifted position, and a flat lower fan without channels (Fig. 6.3). Walker (1973) introduced an integrated facies model for submarine fans in order to predict the distribution of "classical" turbidites and associated coarse clastic sediments. Normark and Walker have suggested that large submarine fans may have coalesced to form a continental rise. Figure 6.4 presents Walker's (1973) submarine abyssal plain fan model showing the relationship between various facies associations and paleocurrent directions.

"Classical" turbidites, as evident in the Quetico Metasediments, are spectacularly parallel bedded and unchanneled. They are assigned to the smooth fan environments, the smooth outer parts of suprafan lobes, lower fan and basin plain (Walker, 1984). Beds change from relatively coarse and thickly bedded with "A" bases (indicative of high velocity), to beds that are finer-grained, and thinner with common "B" or "D" bases. Increasing numbers of "B" or "D" bases is indicative of increased distance from the source.

Massive and pebbly sandstone units in the study area are commonly channelized and are hence assigned to the channelized fan environment. This facies typically occurs toward the inner fan channel. This fan facies is not common in the study area and is generally restricted to a small area a few kilometers west of the Highway 11B turnoff.

Along with "classical" turbidites and massive pebbly sandstone, other facies found in deep water include clast-supported conglomerate

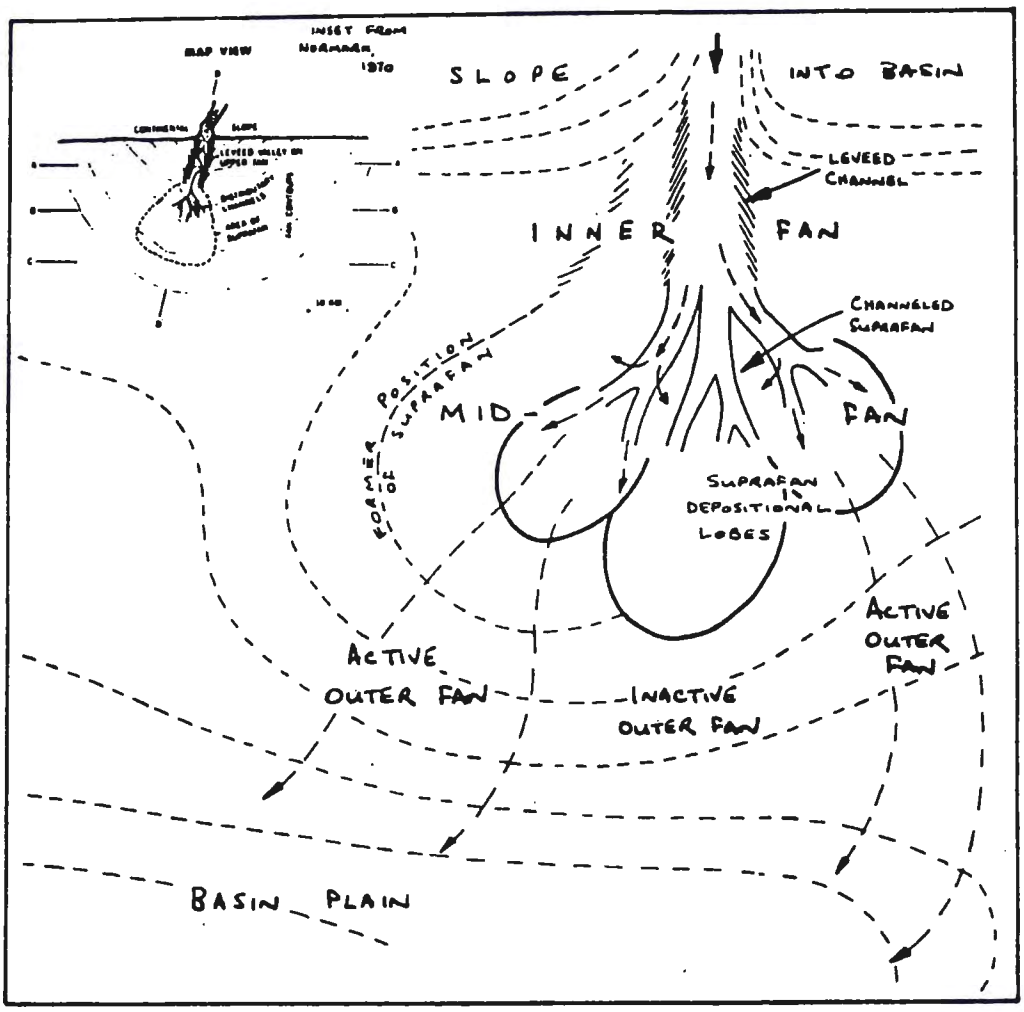

Figure 6.3 Idealized slope-fan-basin floor system showing relationships between the various facies associations, and possible paleocurrent directions. Zonation of the fan into Upper (inner), Middle and Lower (outer) segments is shown, with a suprafan developed in the middle fan area. The suprafan itself is subdivided into an upper channelized segment and a lower segment consisting of depositional lobes. Inset diagram is reproduced from Normark (1970), (From Walker and Mutti, 1973).

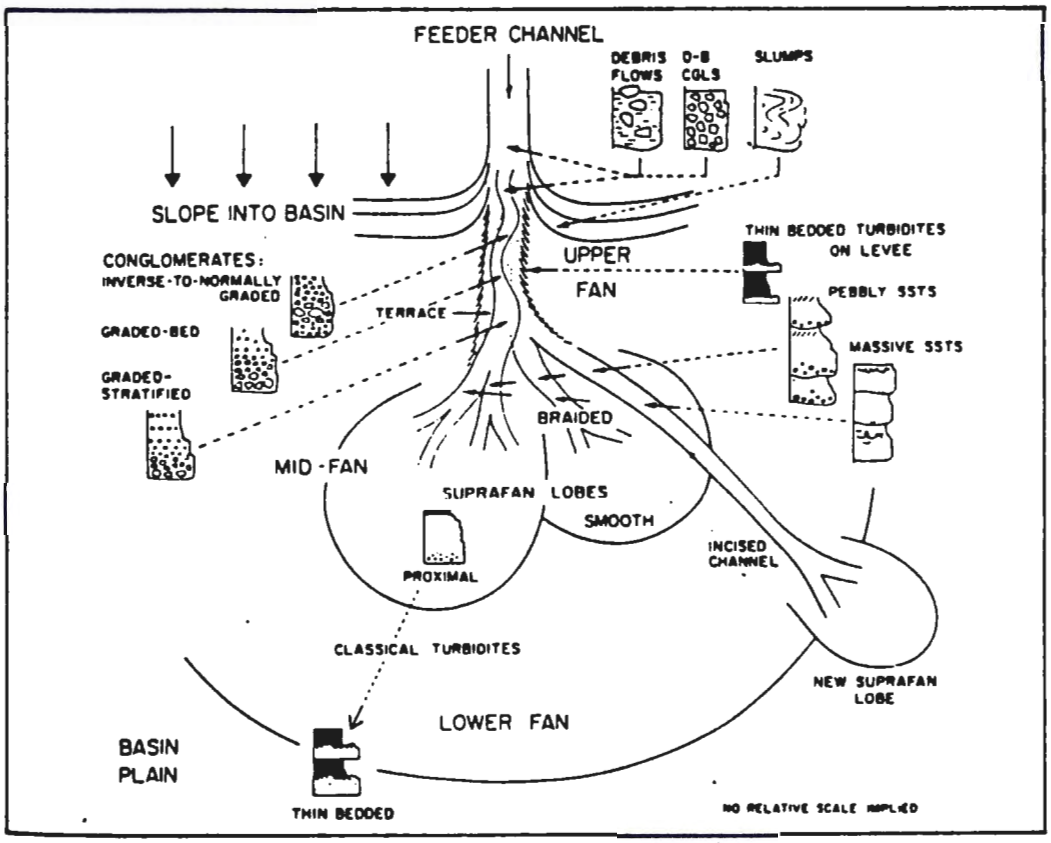

Figure 6.4 Submarine fan environment model illustrating where the various facies fit into the morphological parts of the fan (From Walker, 1973).

and chaotic matrix-supported conglomerate. These facies are not as common as the "classical" turbidites. One orthoconglomerate bed was observed 1.5 km west of the HWY 11B turnoff. In Walker's (1973) fan model, conglomerate (if supplied to the basin), tends to occur in the inner-fan or as lag in some of the distributary channels.

In the western half of the study area, interbedded metamorphosed siltstone and mudstone (slate) are much more common than to the east. Here Bouma sequences beginning with the lower "A" or "B" sequence are less common than to the east (Table 2.1, Table 2.2). The flow regime of a turbidity current depends upon initial velocity, distance travelled, and sediment load of the current. The interbedded metamorphosed siltstones and mudstones are likely Bouma "DE" beds, the product of turbidity currents in distal locations relative to their source. Most of the mudstones are probably beds which formed from the slow "rain-out" of hemipelagic mud over long periods between turbidity currents, taking centuries to form (Walker, 1984). Figure 6.5 provides the location of the six stratigraphic sections in the study area. Figures 6.6 to 6.11 illustrate the stratigraphic sections arranged east to west. These figures are diagrammatic and are not drawn to scale. Figure 6.12 is a bed-to-bed detailed study of one part of stratigraphic section 3; figure 6.13 is a bed-to-bed detailed study of a section of stratigraphic section 5. Note how the stratigraphic sections become more mud-rich to the west.

In addition to the previous lithologies, gross stratigraphic aspects such as progressive fining-up sequences may reflect location on

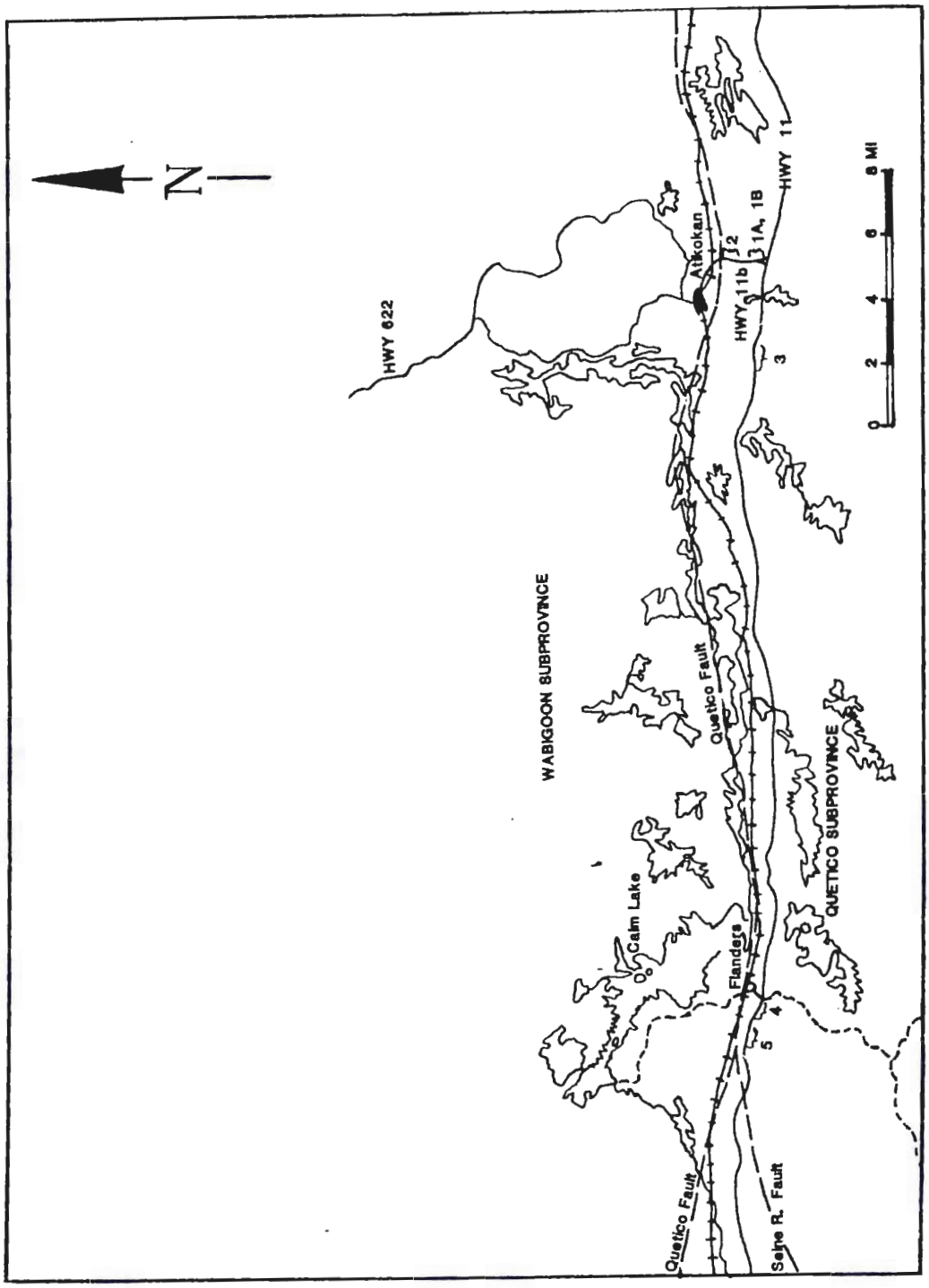

Figure 6.5 Map showing the location of stratigraphic sections 1A, 1B, 2, 3, 4 and 5.

Legend for stratigraphic sections 1A, 1B, 2, 3, 4, 5 and Figures 6.12 and 6.13.

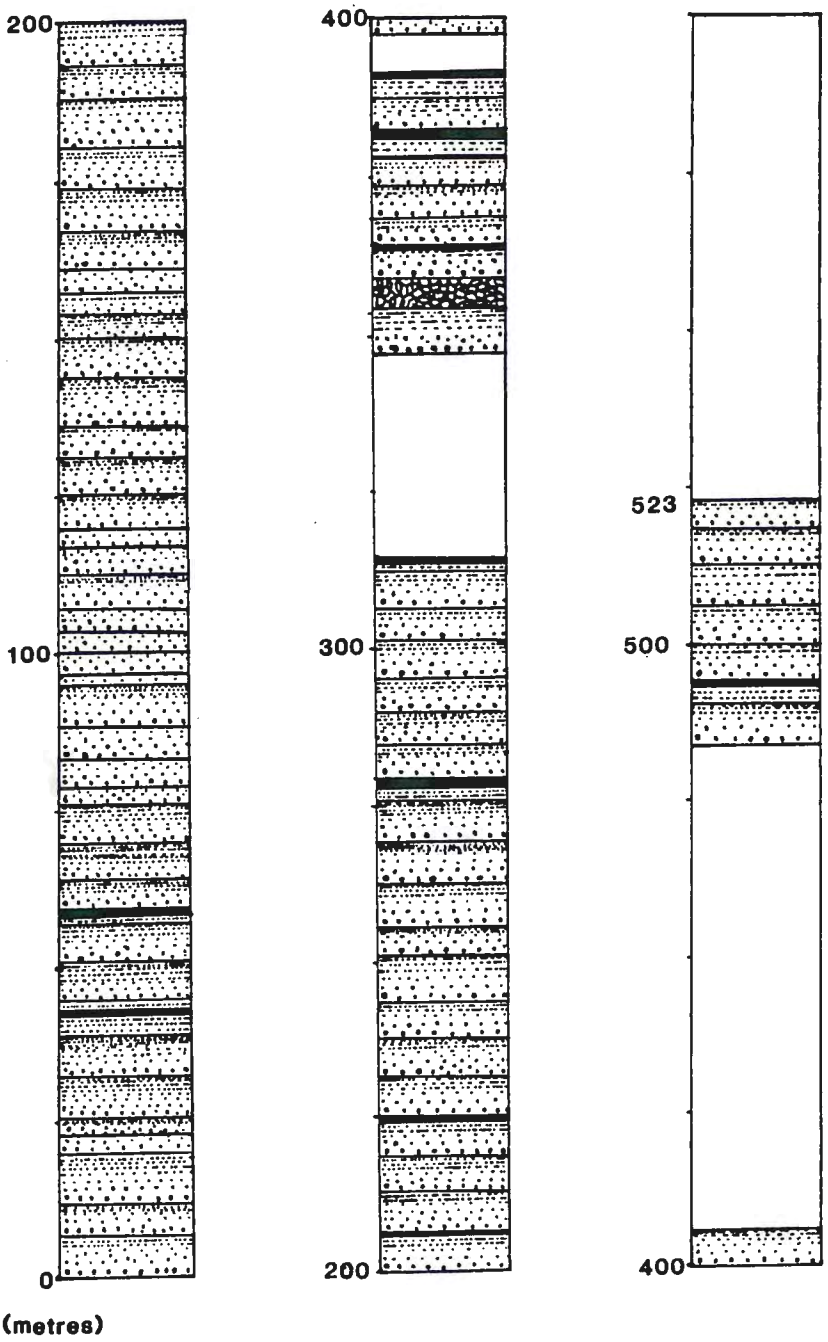

Figure 6.6 Details for stratigraphic section 1A, located along HWY 11B, immediately north of turnoff to Atikokan. The figure is diagrammatic and is not drawn to scale. Legend is on page 113a.

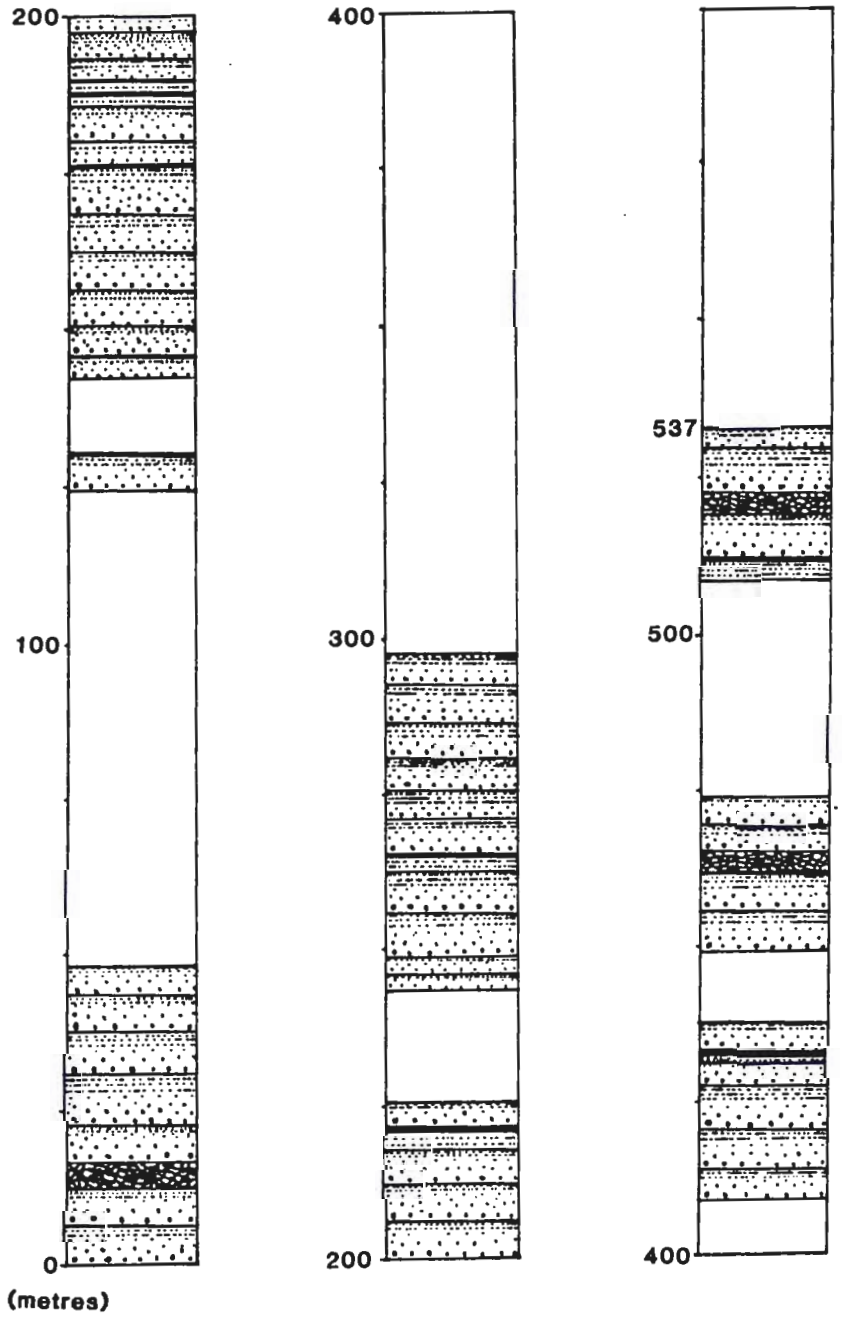

Figure 6.7 Details for stratigraphic section 1B, located on HWY 11B, 1.5 km north of turnoff to Atikokan. The figure is diagrammatic and is not drawn to scale. Legend is on page 113a.

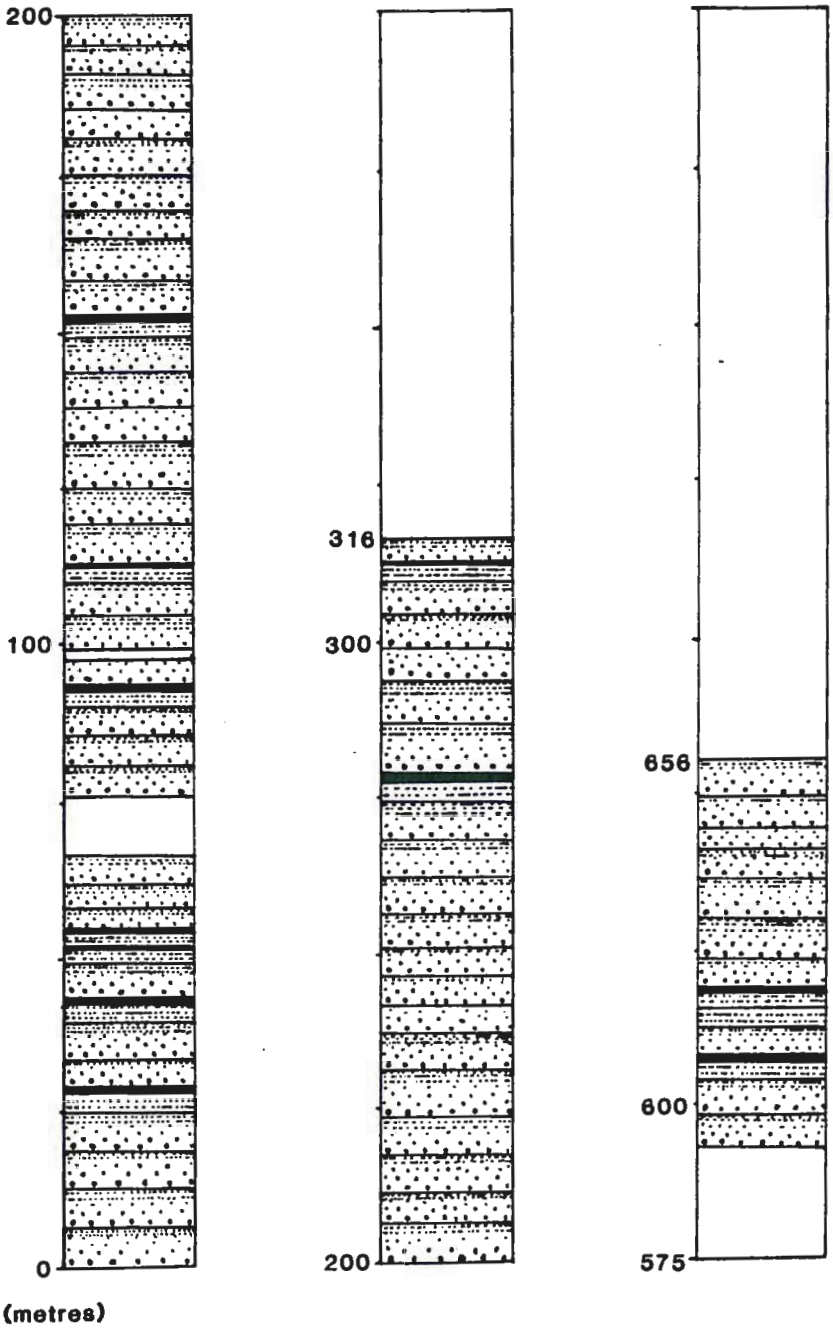

Figure 6.8 Details for stratigraphic section 2, located along HWY 11B, 3 km north of turnoff to Atikokan. The figure is diagrammatic and is not drawn to scale. Legend is on page 113a.

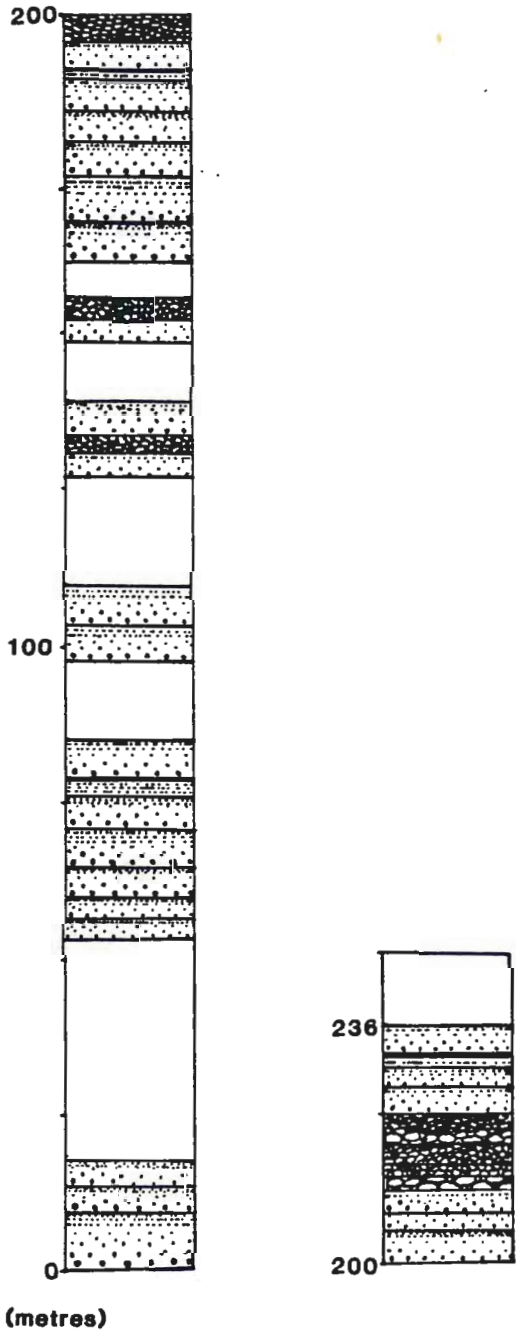

Figure 6.9 Details for stratigraphic section 3, located on HWY 11, 3 km west of the Atikokan turnoff. The figure is diagrammatic and is not drawn to scale. Legend is on page 113a.

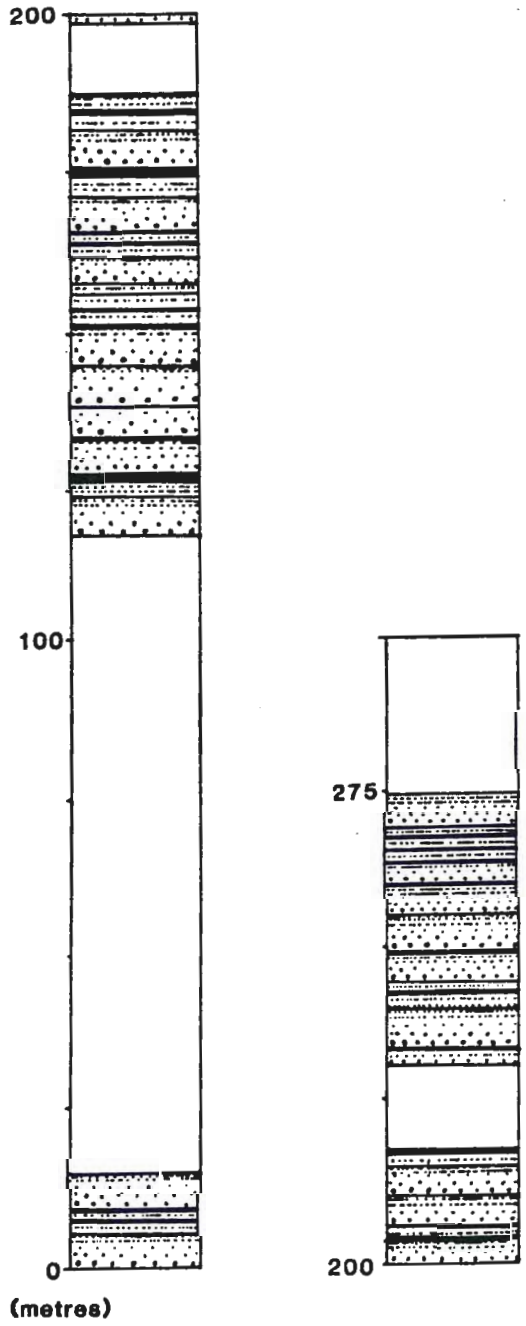

Figure 6.10 Details for stratigraphic section 4, located on HWY 11, 2 km east of where the Quetico fault crosses HWY 11. The figure is diagrammatic and is not drawn to scale. Legend is on page 113a.

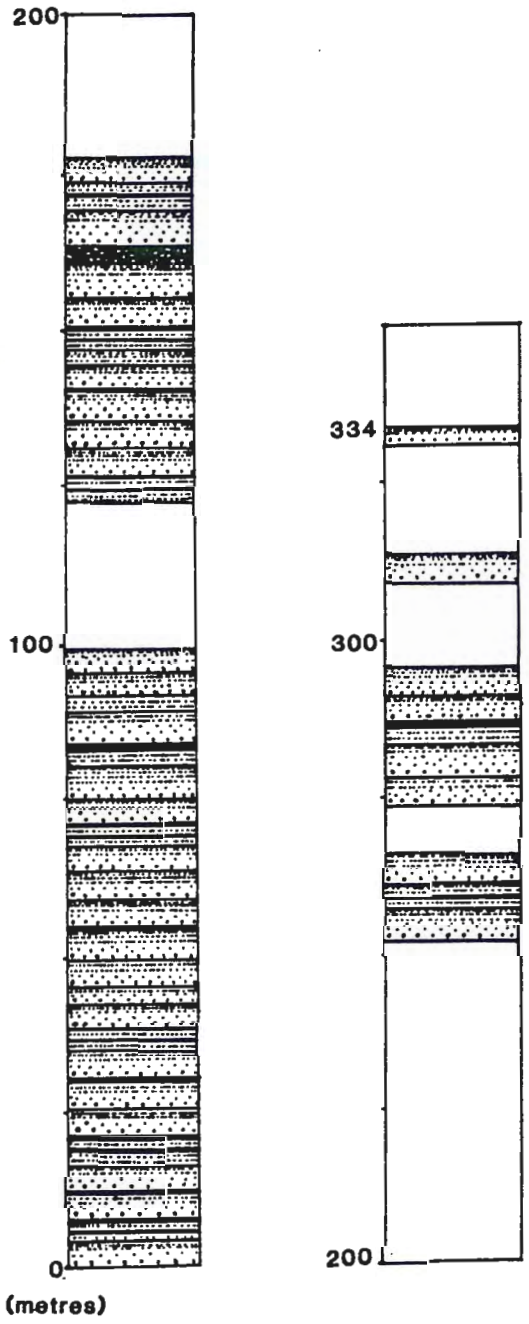

Figure 6.11 Details for stratigraphic section 5, located on HWY 11 immediately east of where the Quetico fault crosses HWY 11. The figure is diagrammatic and is not drawn to scale. Legend is on page 113a.

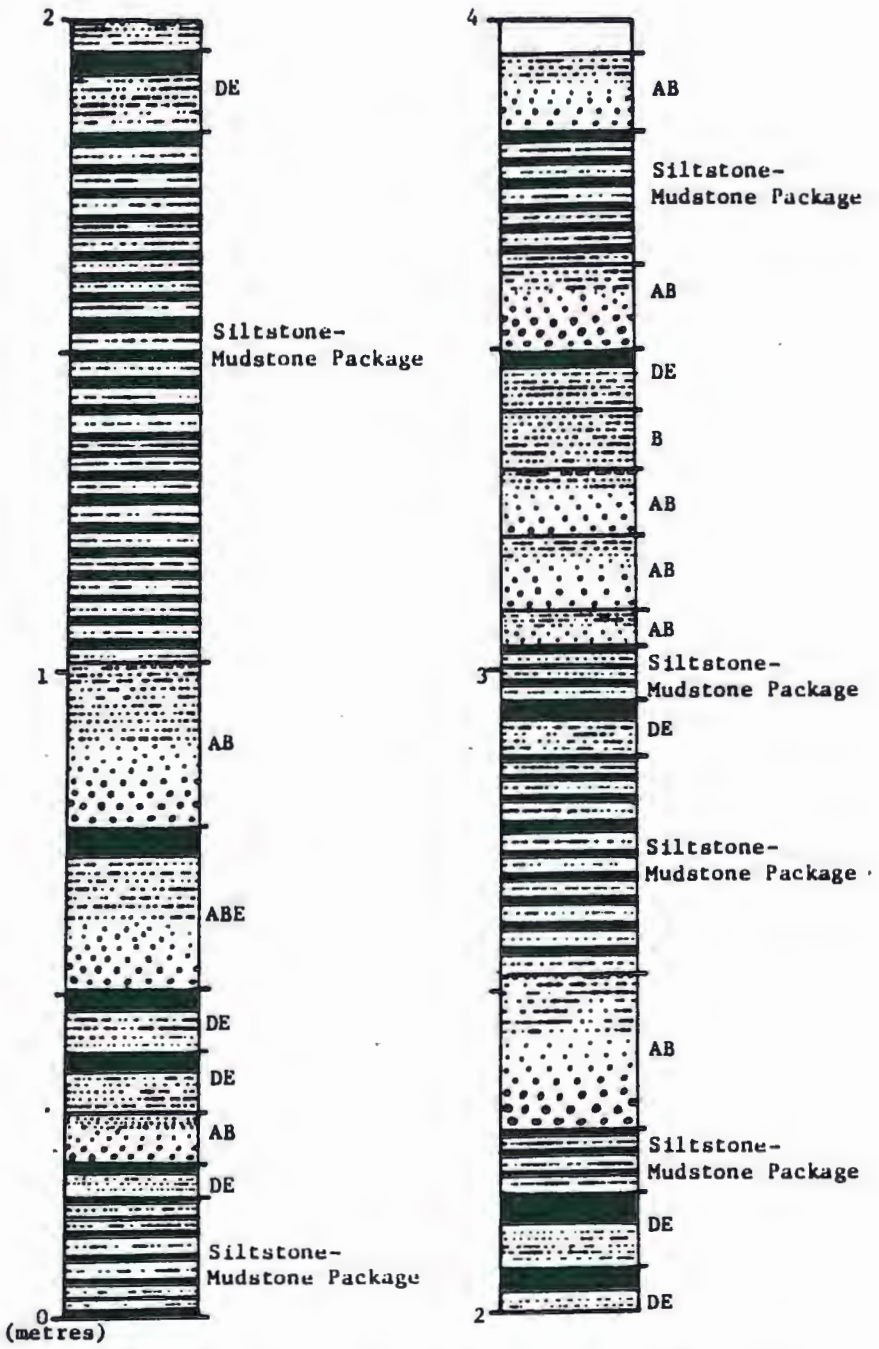

Figure 6.12 Detailed bed-by-bed study of a section statigraphic section 3, located on HWY 11, 3 km east of the junction of HWY 11B into Atikokan. Letters denote Bouma sequence present in each bed.

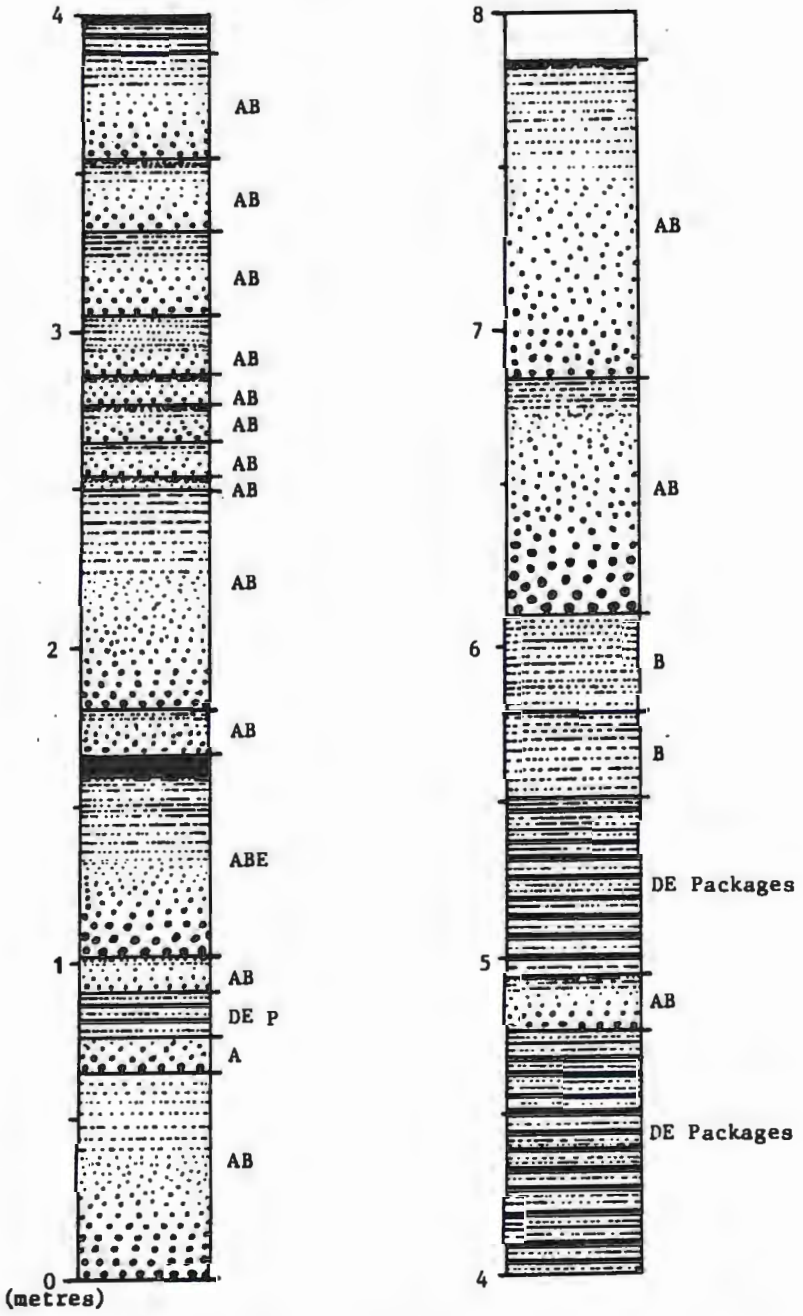

Figure 6.13 Detailed bed-by-bed study of a section of stratigraphic section 5, located on HWY 11, 1 km east of the gravel road to Gehl Lake. Letters denote Bouma sequence present in each bed.

the submarine fan as well as gross sedimentologic processes. Submarine fan progradation was a typical process; progradation would result in a succession passing from an initial outer-fan environment, through mid-fan and finally into inner-fan deposits. Progradation would result in the deposition of a series of "classical" turbidites that become more proximal in aspect upward. Localized thinning-up sequences were also identified in the field; Mutti and Ghibaudo (1972) interpreted them to represent gradual channel filling and abandonment, or lobe shifting from a lobe centre to a lobe-fringe environment, depositing thinner and finer beds from smaller flows. However, not all thin and fine beds are related to channel filling or lobe abandonment; silt-and mud-rich beds associated with coarse sand and pebbly material are often overbank deposits laid out along levees adjacent to main channels during flood stages. Several thinning-up sequences were observed along Highway 11B, and along Highway 11 near the Atikokan turnoff. Because the thinning-up sequences are spatially associated with coarse metasediments, they appear to be lobe abandonment or overbank deposits.

In the present study area, many reasonable diagnostic features of submarine fan facies were observed. The sediments in the study area were probably deposited on a suprafan lobe in a lower fan environment. The metamorphosed conglomerate and channelized pebbly sandstone, which are indicative of fan channels, are present only in an area east of the Highway 11B turnoff. The presence of channelized pebbly sandstone suggests the presence of a satellite lobe on the suprafan. Twenty to

30 km west of the HWY 11B turnoff, thin-bedded distal turbidites become increasingly common. These sediments consist of thousands of relatively thin (less than 1 cm thick) turbidite beds. The most likely environment for these undisturbed fine-grained beds is one that is quiet and deep, the lower fan or a basin plain.

The author wishes to emphasize that due to the structural complications of the study area, only a generalized interpretation has been attempted here. A predominantly distal fan environment has been proposed to explain the sedimentary history of the Quetico Metasediments in the study area, but the author would like to stress that that fans are not neccessary to explain the deposition history of "classical turbidites." Ojakangas (1985), suggests that volcaniclastic sediment in the Archean may have accumulated along narrow and unstable flanks of volcanic edifices. In turn, sudden events such as earthquakes were instrumental in triggering turbidity currents by which sediment was transported into the surrounding basins.

Chapter 7

PROVENANCE

According to Dickinson et al., (1983), and Dickinson and Suczek (1979), relative proportions of different types of terrigenous sand grains are guides to the nature of the source rock terrane. Sandstone compositions are influenced in part by the lithological characteristics of the provenance, the nature of the sedimentary process from source to deposition, weathering and diagenesis (Bhatia, 1983, Figure 7.1). Pettijohn et al., (1972, p. 237-244), advocate tectonism as the primary control of sandstone composition. McLennan (1984) cautions against using terrigenous sand components as guides to the nature of the source rock terranes during Archean time because of non-uniformitarianism. Relationships between tectonic setting and sandstone composition are based upon framework modes, but obtaining framework modes is difficult to do in rocks that are metamorphosed, and geochemistry is needed. No geochemistry was conducted by the author, but a geochemical study of the Quetico metasediments in an area 70 km east of Atikokan was conducted by Sawyer (1986).

When studying sandstone provenance, two important aspects are: 1) what is the primary source(s), and 2) what do the sedimentary rocks reveal about the overall tectonic relationship between the sedimentary belt and the surrounding source area. A thorough understanding of the significance of various modal components is necessary to delineate provenance sources. The emphasis in the determination of provenance will be on the metagreywackes and coarser pebbly metasandstones rather

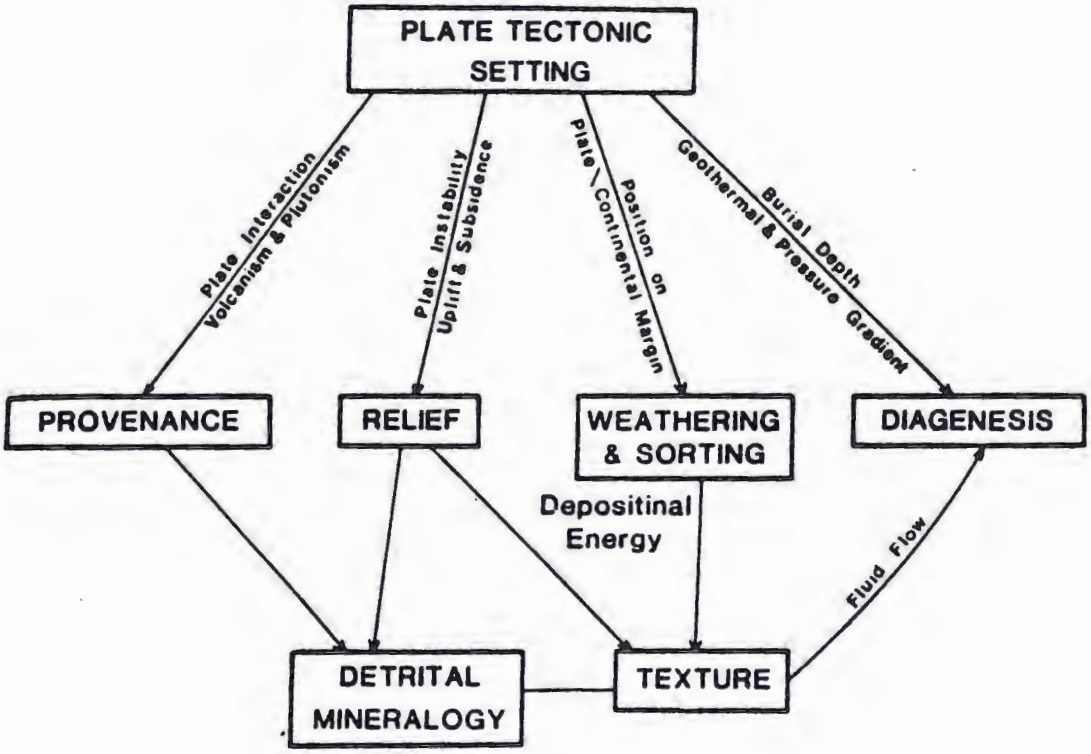

Figure 7.1 Relationships between attributes of the plate tectonic setting and compositional variables of sandstones (From Bhatia, 1983).

than on the slates, because sandstone petrography provides the best evidence of provenance because of the ease of grain identification. The most abundant grain type noted in the Quetico metasediments is common plutonic quartz, occurring as single undulose grains or as compound grains. The high percentage of common quartz both in terms of absolute abundance and relative proportion of framework grains, likely represents a traditional plutonic source. Some workers emphasize an origin of quartz from within volcanic belts. Ojakangas (1972), suggested that some modal quartz is derived from subvolcanic complexes. Ayres (1983), suggests a source from pyroclastic flows with quartz being concentrated by eruptive, weathering, hydraulic and reworking mechanisms. Some of the quartz may represent phenocrysts that were abraded and broken during transport and the scarcity of definite volcanic quartz indicates a plutonic source for some of the quartz. Schistose and stretched quartz represents a minor metamorphic provenance. Chert is present in significant amounts, especially in the orthoconglomerate, and may represent the erosion of cherty iron-formation.

Plagioclase (albite) is by far the dominant feldspar type noted, accounting for 94% of all the feldspar noted. The presence of significant quantities of plagioclase cannot be taken for evidence of solely a volcanic source because early Archean plutonic rocks are primarily sodium-rich varieties such as tonalite-trondhjemite (Taylor and McLennan, 1985). Some of the plagioclase may represent abraded phenocrysts and pyroclastic material but a substantial plutonic source

is still inferred.

Because orthoclase is rare in Archean granites, it is possible that some of the orthoclase may represent liberated phenocrysts from rhyolites or rhyodacites. However, a recent geochemical survey of the Quetico metasediments by Sawyer (1986), shows high LREE values (up to 50 ppm La). Late Archean potassic granites have been suggested as a source for the LREE in post-Archean metasediments by Taylor and McLennan (1981). The presence of late potassic granites with similar LREE patterns are common in Sawyer's study area and are therefore likely sources for the LREE in the Quetico metasediments. Jenner et al., (1981), conducted geochemical tests on the Archean Yellowknife Supergroup and concluded that granodiorite constitutes a significant provenance source for the metagreywackes in the Yellowknife Supergroup. Thus, it is possible that potassic granites are a definite yet minor provenance source for the Quetico metasediments.

Lithic fragments are common in all of the coarser metasediments of the Quetico Subprovince. The clasts are dominated by felsic and felsic-intermediate volcanic rocks. Intermediate to mafic volcanic clasts are present but in lesser quantities. The presence of these volcanic clasts is likely a reflection of the bimodal rhyodacite-basalt association typical of continental orogenic belts and island arc systems (Bass, 1961; Goodwin, 1968; Anhaeusser et al., 1968). Ojakangas (1985) reviewed chemical analyses of Archean metasediments and showed a striking chemical similarity to rhyodacites. The presence of abundant felsic to intermediate volcanic clasts in the metasediments

infers a major unconsolidated volcanic source where reworking took place rapidly. The paucity of felsic-intermediate pyroclastic units in greenstone belts is likely due to their rapid erosion and subsequent incorporation into greywackes and associated sediments (Ayres 1983; Ojakangas, 1985).

The presence of lesser amounts of mafic plutonic fragments (altered gabbro), hypabyssal mafic fragments and slate reaffirms the likelihood of a mixed provenance. Slate is possibly derived as rip-up clasts from the upper or middle fan.

Minor conglomerate beds in the study area are dominated by clasts of tonalite, porphyritic felsic volcanics, recrystallized chert, mafic volcanics, slate and schists. The matrix is similar in composition to coarse-grained metagreywacke and pebbly metasandstone. The metaconglomerate beds are excellent field indicators of the mixed provenance source for the Quetico metasediments.

Dickinson and Suczek (1979), showed that the mean composition of sandstones derived from different kinds of provenance terranes are controlled by plate tectonics and tend to lie on discrete fields on QFL and QmFLt diagrams (see Figure 7.2 for explanation of the components). Dickinson and others (1983), established three main classes of provenance, categorized as "continental blocks", "magmatic arcs" and "recycled orogens." Forty-one modal plots of the Quetico Metasediments are given in Figures 7.3 and 7.4. The QmFLt results indicate a mixed provenance in a setting where tonalite and its volcanic cover were being unroofed in dissected magmatic arcs. Dominantly felsic volcanism

may have continued nearby. The QFL results indicate a recycled orogenic provenance although the average value of the 41 point-counts lies near the dissected arc boundary. The average value for the QmFLt plots falls in the recycled orogenic zone due to high detrital quartz values. High detrital quartz values are due in part to the likelihood that much of the quartz is volcanic in origin. One expects to see high quartz values where some recycling of sediments took place especially in fluvial systems. In addition much of the detrital feldspar was too fine to be point counted as such and was included as matrix. Higher feldspar values might result in more plots in the dissected arc zone. It is possible however, that the QFL plot which indicates a recycled orogenic provenance, is correct. Older volcanic arcs may have been uplifted (by thrusting) and eroded after ocean-floor subduction and the ensuing collision of younger arcs with the main land mass had occurred. However, a magmatic arc origin still seems more likely. In either case much of the detritus was transported into the basin (Fig. 7.5) resulting in the deposition of greywackes of mixed volcanic and plutonic origin.

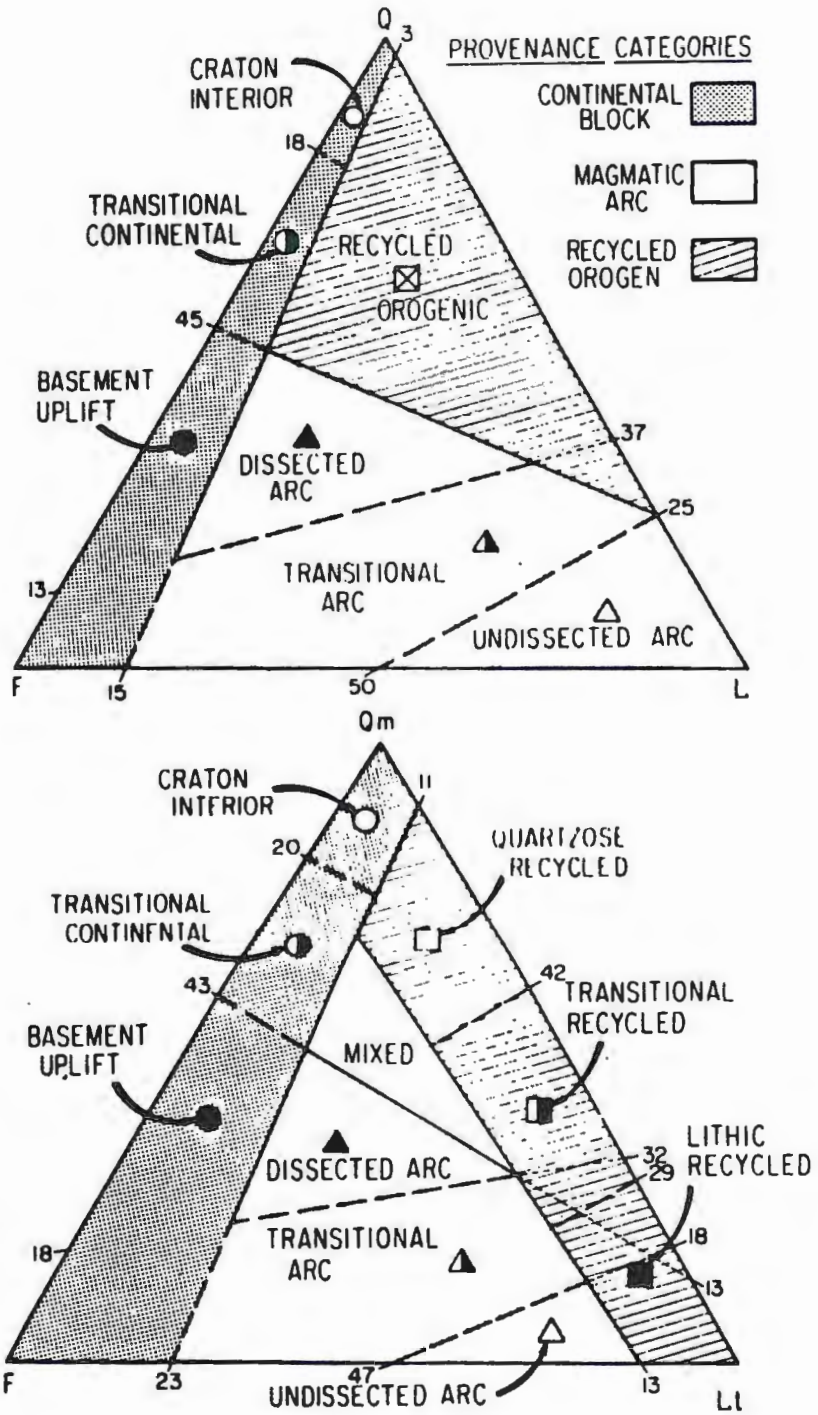

Figure 7.2 Subdivisions for the provenance zones of the QFL and QmFLt plot (From Dickinson and Suczek, 1979).

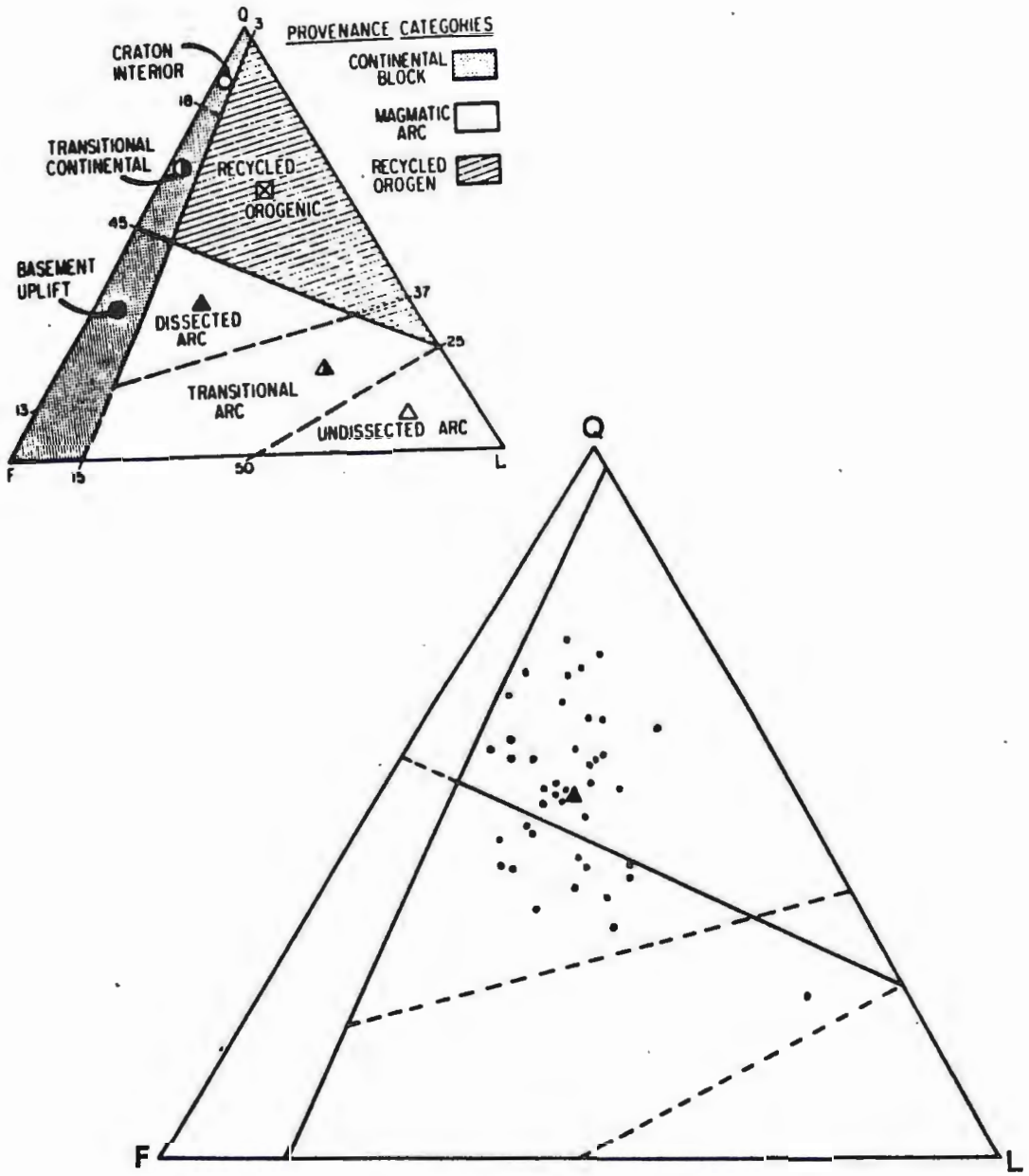

Figure 7.3 QFL plot for 41 framework modes of the Quetico metasediments showing provisional subdivisions according to inferred provenance type. The triangle located in the recycled orogenic subdivision represents the average value.

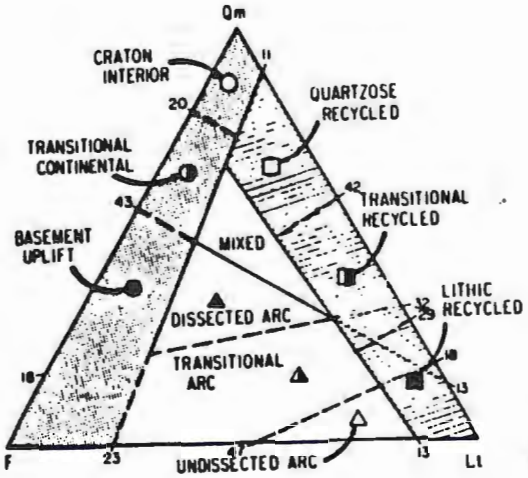

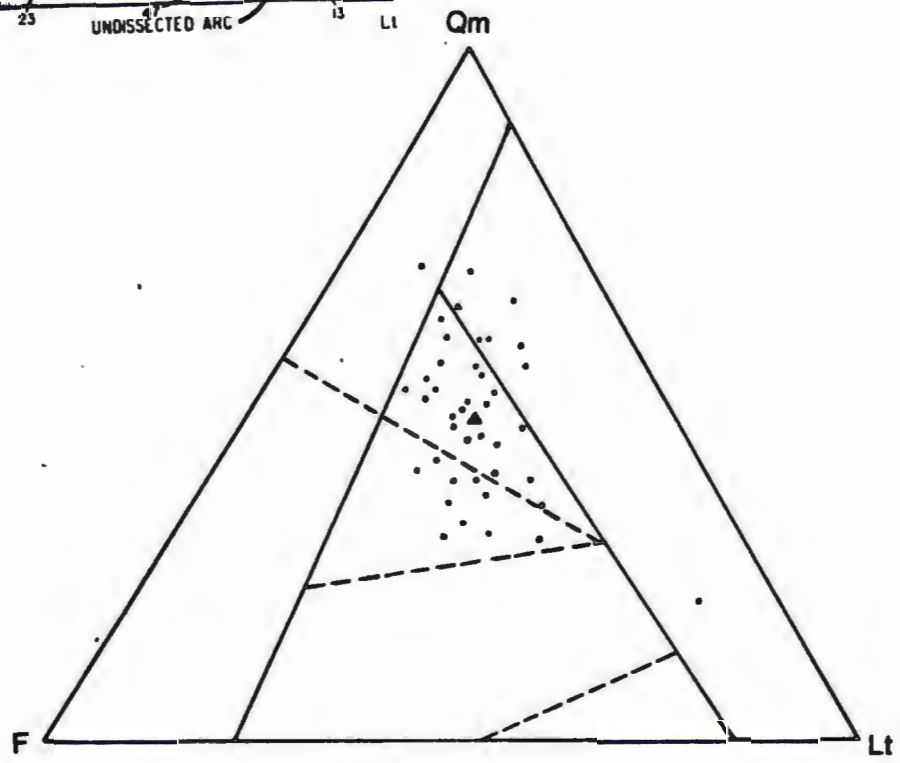

Figure 7.4 QmFLt plot for 41 framework modes of the Quetico metasediments showing provisional subdivisions according to inferred provenance type. The triangle located in the mixed subdivision represents the average value.

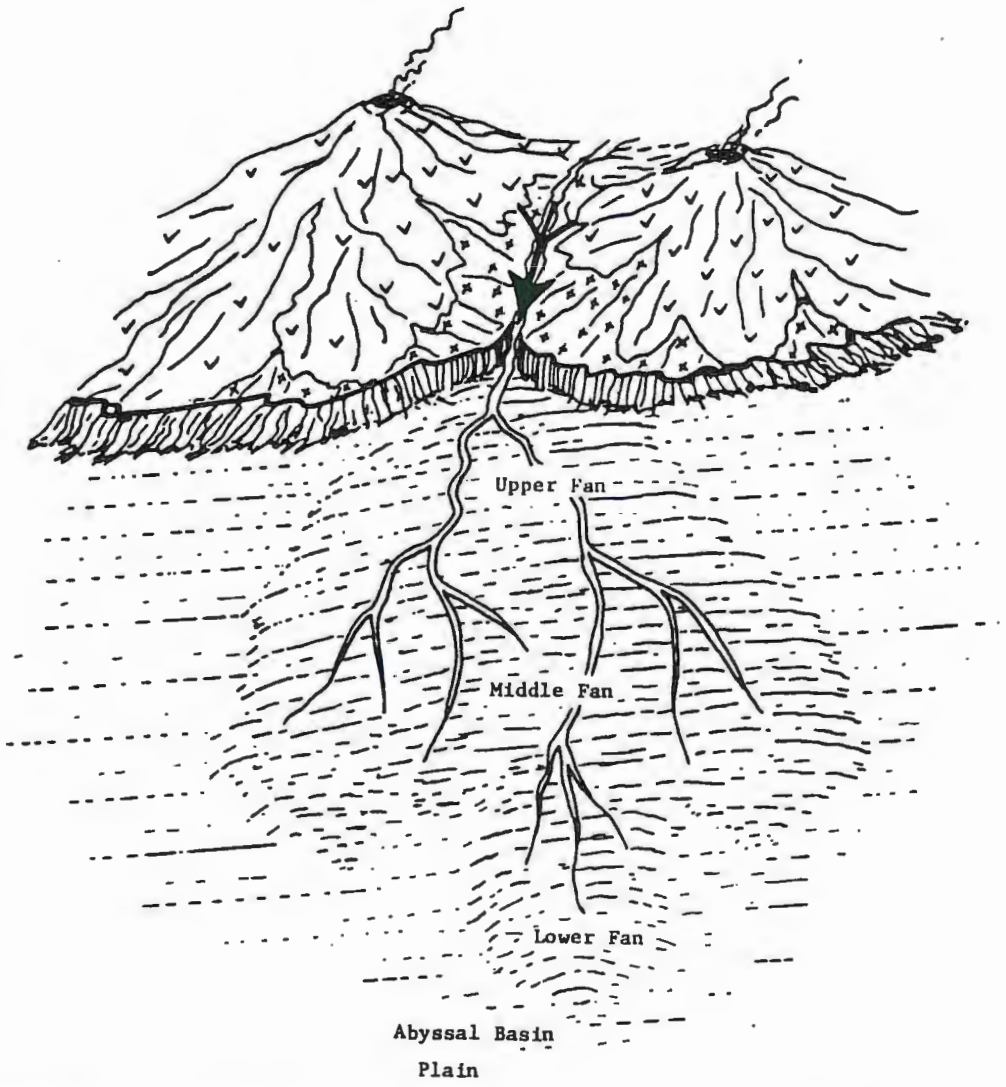

Figure 7.5 Summary model showing the Archean sediment sources as being dominantly felsic volcanic highlands and coeval felsic plutons. A smaller amount was eroded from mafic volcanics and possibly from felsic plutonic basement. Sediment was likely carried by fluvial processes to the shorelines and deposited in submarine fans or along the flanks of volcanic edifices.

Chapter 8

TECTONIC MODEL

In terms of rock types, sequences, and overall tectonic aspect, many Superior Province greenstone belts are similar to modern island arcs (Card, 1985). The Archean Superior Province has numerous linear metasedimentary and metavolcanic subprovinces of similar scale to Cenozoic arc-trench systems of the western Pacific. These aspects suggest an origin by accreting arcs (Blackburn, 1980; Langford and Morin, 1976). Successive lateral and vertical accretion of volcanic arcs and related sedimentary accumulations, accompanied and followed by plutonism, resulted in multi-stage crustal thickening and stabilization of the Superior Province (Card, 1985).

There were two major periods of Archean greenstone belt development in the Canadian Shield at 3.0 to 2.9 Ga and 2.8 to 2.7 Ga (Card, 1985). This greenstone belt development was by the accretion of magmatic island arcs. Sedimentary basins developed adjacent to the island arcs and received terrigenous sediment from felsic volcanic edifices and coeval volcanic plutons. Subvolcanic material, lithified volcanic rocks and perhaps minor amounts of basement entered the basin from dissected magmatic arcs. Sedimentation was spurred by a continuum of volcanism, uplift, erosion and repeated volcanism. The most widely cited evidence for the contemporaneity of volcanism and sedimentation in the Canadian Shield is the occurrence of volcanic interbeds in the sedimentary units as reported by numerous workers (Ojakangas, 1985). In the present study area, Stewart (1984) observed mafic to

intermediate tuff grading diffusely into conglomerate. The great thickness of the Quetico metasediments and their intimate association with mafic tuff indicates that contemporaneous volcanism and sedimentation took place in a very deep and subsiding trough, one that is likely flanked by a volcanic chain.

The metagreywackes and associated resedimented deposits in the study area may be partly epiclastic as well as volcaniclastic. Significant subaerial relief on volcanic edifices would have resulted in rapid erosion on the vegetationless hinterland. This erosion was probably accomplished first by sheetflow and rivers as described in a modern environment by Kuenzi et al., (1979). Ayres (1982a) later modelled this process for the Archean. Upon reaching the submarine fan or the edifice margin, slumping or turbidity currents would have resedimented most of the material into deeper water. The volcaniclastic lithic sands from the magmatic arc were then deposited in trenches, fore-arc or back-arc basins. The author prefers the back-arc or fore-arc regions because thick turbidites and pelagic sediment are common in these settings, and not in the narrow and comparatively sediment-starved trench system (Hallam, 1981).

Preliminary synthesis suggests that sedimentation took place on extending crust forming the Quetico basin during volcanism in adjacent terranes (Percival and Stern, 1984; Fig. 8.1). U-Pb zircon geochronology in the Wawa Subprovince indicates major volcanic activity between 2749 and 2696 Ma (Turek et al., 1982), followed by D_1 deformation at about 2696 Ma and deposition of alkaline volcanics at

2689 Ma. D_2 deformation, and intrusion of post-tectonic plutons took place at 2684 Ma (Corfu and Stott, 1985) to 2668 Ma (Krogh and Turek, 1982). In the Wabigoon Subprovince, volcanism occurred in the interval of 2755 to 2702 Ma, with post-tectonic plutons younger than 2695 Ma (Davis and Edwards, 1982). Preliminary isotopic dates indicate that volcanic and sedimentary sequences in some adjacent subprovinces are coeval (Davis and Edwards, 1982), and a similar trend is likely in this part of the Superior Province. Later closure of the basin during D_1 and D_2 events, as dated in adjacent belts, led to folding of the sedimentary pile and thickening of the weak crust. On the basis of metamorphic assemblage data, Percival (in Percival and Stern, 1984) concluded that metamorphism occurred as a result of heat transported to the higher structural levels by granitic plutons. During subsequent thermal relaxation, partial melts were extracted from lower crustal metasedimentary and tonalitic rocks, as well as from the mantle. The derived granites and diorites ascended to within 10 km of the surface producing a regional low-pressure aureole in the host rocks. Asthenospheric upwelling beneath a back-arc environment could have given rise to high heat flow and possible crustal melting to produce the intrusives (Percival and Sullivan, 1985). A chilled porphyritic dacite sill cutting biotite-grade Quetico metasediments yielded an imprecise U-Pb zircon age date of 2743 plus or minus 16 Ma (Percival and Sullivan, 1986). This dike provides a minimum age for sediment deposition. Figure 8.2 provides a tentative summary for correlation of the Wawa-Shebandowan, Quetico and Wabigoon Subprovinces.

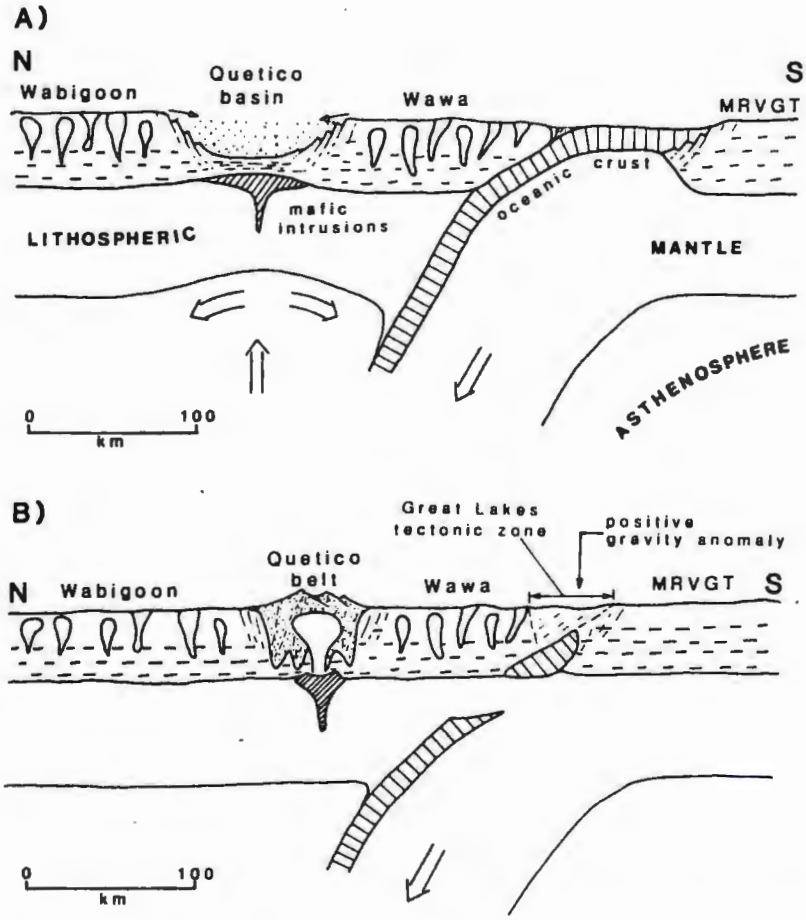

A- Sedimentary basin development (with clastic input from volcanic highlands), in response to lithospheric stretching in a tensional back-arc environment. Compensation by upwelling of asthenosphere causes elevated heat flow under developing linear basin.

B- Outboard collision between Wawa subprovince and a more southerly block (Minnesota River Valley Gneiss Terrane? (MRVGT)) results in intense deformation and metamorphism associated with weakened lithosphere (Le Pichon et al., 1982) beneath the Quetico belt. Partial melting of basement and metasedimentary gneiss produces buoyant granites which rise to within 10 km of the surface.

Figure 8.1 Back-arc basin analogue for the development of the Quetico belt between the Wabigoon and Wawa volcanic arcs. (From Percival and Stern, 1984).

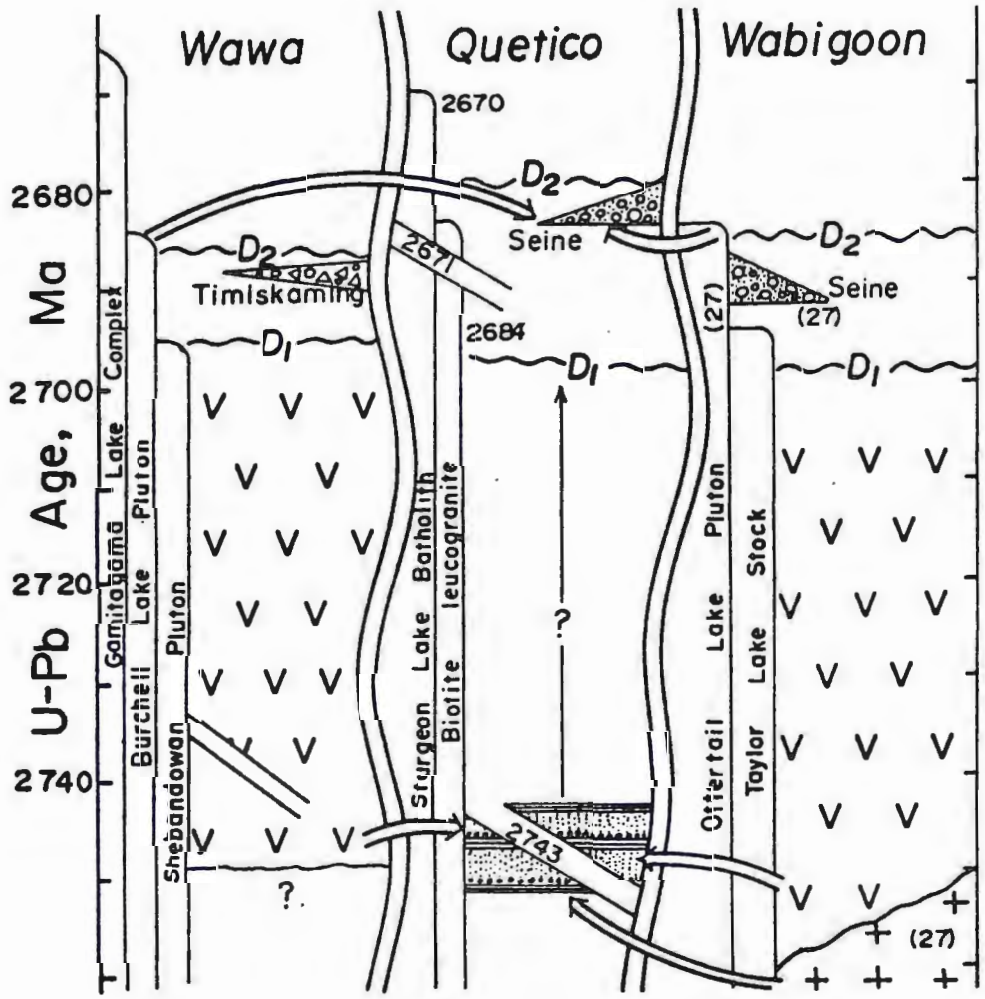

Figure 8.2 Age summary and tentative correlation diagram for the Wawa, Quetico and Wabigoon Subprovinces. Arrows crossing subprovince boundaries indicate sedimentary provenance (From Percival and Sullivan, 1986).

Chapter 9

CONCLUSIONS

1. The 20 to 100 km wide Quetico Subprovince, a typical metasedimentary subprovince of the Superior Province, consists of a 1200 km long Archean gneiss-granite superbelt between the the Wabigoon and the Wawa-Shebandowan Superbelts to the north and south, respectively.

2. Sedimentation on the Canadian Shield during Archean time was dominated by the resedimented (turbidite) facies association of greywacke, siltstone-mudstone and conglomerate. The metagreywackes, slates, conglomerates and biotite shists in the Atikokan-Mine Centre region display sedimentary features diagnostic of turbidite deposition.

3. In the northern part of the Quetico Subprovince along a marginal zone 1 to 2 kilometres wide, the metasediments are sub-greenschist to greenschist in metamorphic grade. The rocks have been deformed, progressively metamorphosed southward and migmatized toward a central axis so that the original textures and most of the sedimentary features have been obliterated. The core of the Quetico Subprovince is made up of metasedimentary remnants in the migmatite, amphibolite, shists, paragneisses and granitic intrusives, many of anatectic origin.

4. Metagreywacke is the most abundant metasedimentary rock observable

in the study area, commonly interbedded with slate, and uncommonly with pebbly metasandstone. The east-trending bedding is very pronounced and regular. The fine-to medium-grained metagreywacke is generally graded, and beds generally range in thickness from 15 to 40 cm in the eastern half of the study area but decrease in average thickness (8-12 cm) further to the west.

5. Bouma beds are generally of the AB, A, B, DE, and ABE type. In the eastern half of the study area near the town of Atikokan, the metagreywacke beds observed in four stratigraphic sections contain a higher percentage of basal A units than the greywacke beds observed further to the west. The Bouma sequences in the western half of the study area are typically of the B and DE type.

6. Areal variations in the relative proportions of metagreywacke, slate, pebbly sandstone and conglomerate, and in the character of Bouma cycles, indicate a proximal to distal facies relationship westward from Atikokan towards Mine Centre. This relationship may be useful in defining the geometry and scale of these submarine fans. In the study area, there is indication of the presence of a fan on the order of at least 40 km across its smallest dimension. Deposition of sediments throughout the Quetico Subprovince likely took place on a series of large submarine fans.

7. The bulk of the sediment in the metagreywacke and pebbly

metasandstone was probably derived from felsic to intermediate (dacitic) sources. Explosive felsic detritus as well as Archean tonalite-trondhjemite are essential components in the formation of Archean volcanic-and sedimentary-rich greenstone belts and perhaps in Archean gneiss terranes as well.

8. Significant plutonic detritus is also present as evidenced from petrographic studies. Cobbles to sand-sized grains of Na-rich plutonic clasts are expected in Archean greywackes because tonalite-trondhjemite was the most common plutonic rock type present in Early Precambrian terranes. These plutonic clasts may be basement rock fragments, but they are likely coeval plutonic bodies that intruded into the felsic volcanic edifices and were exposed as the accreting island arcs were dissected.

9. Although the majority of lithic fragments are felsic to intermediate volcanic in composition, and some are felsic plutonic, rarer fragments of mafic volcanic, chert, metasedimentary and hypabyssal mafic rocks indicate a mixed sourcs of detritus as indicated by QmFLt plots. A QFL plot of 41 point counts reveals a recycled orogenic source for the bulk of the sediments. The author suspects that the abundance of quartz (48% of all framework grains) observed in the metasediments, which normally testifies to much reworking, is due to appreciable amounts of volcanic quartz from explosive felsic island arcs.

10. The recognition of orthoclase in clasts with myrmekitic texture and in stained heels points to a minor potassic granitic source for some of the detritus. This minor source is significant because potassic granite is generally believed to be a very rare contributor to the Archean resedimented (turbidite) facies association of greywacke (Ojakangas, 1985).

11. The high percentage of angular clasts in the metasediments suggests the importance of rapid erosion of unconsolidated material on volcanic edifices. Rapid erosion in an area of high relief, with subsequent transportation of detritus by high velocity streams to the basin margin, was an important process during Archean time.

12. The reworked clastic material accumulated as temporary piles on the slopes of unstable basin margins in the surrounding volcanic-granitic terranes. The temporary clastic piles were destined to be jarred loose and transported downslope by turbidity currents into the depositional basin. While both fore-arc and back-arc basins are possible depositional environments, Percival and Stern (1984) have proposed that the Quetico Metasediments were deposited in a back-arc basin based upon tectonic analysis.

13. Analysis of heavy mineral assemblages reveals that the vast majority of the heavy minerals present (biotite, amphibole, apatite, and epidote) are metamorphic in origin. Zircon is the only clearly

detrital mineral present.

14. Preliminary U-Pb geochronology has provided an absolute time framework for deposition of the Quetico Metasediments. Zircons recovered from the Blalock pluton define a 2688 +4/-3 Ma minimum age for sediment deposition. The youngest detrital zircons from the Quetico Metasediments are in the range of 2700 +/-3 Ma; the oldest zircons are approximately 3004 Ma. These two dates apparently provide a timeframe for sediment deposition in the Quetico Subprovince. U-Pb analyses from adjacent greenstone and batholithic terranes have provided age dates that correlate with detrital zircons recovered from the Quetico Metasediments. These units must be regarded as possible sediment sources, but such correlations are still tentative.

15. The stratified rocks of the Quetico Subprovince possess the following fabric elements: an early (S_1) schistosity that is related to an early deformational event that produced recumbent folds, and (S_2), a dominant penetrative schistosity related to a second generation of upright folds. The dominant penetrative cleavage is axial planar to F_2 folds and subparallel to bedding. Lineations in the bedding planes indicate that S_2 fold axes strike to the east and plunge moderately or shallowly to the east and west. Along the western margin of the study area, kinks and small chevron folds are related to the folding of the S_2 schistosity around steeply dipping axial fold surfaces.

16. Tectonic interpretation of the Quetico Subprovince by several workers show that the Quetico basin developed in response to lithospheric stretching in conjunction with clastic input from volcanic highlands. Later closure of the basin during D_1 and D_2 events led to folding and thickening of the weak crust. During subsequent thermal relaxation, partial melts were extruded from the lower crustal portions to form the granitic core of the Quetico basin.

Bibliography

Anhaeusser, C.R., Roering, C., Vilgoen, M.J., and Vilgoen, R.P., 1968, The Barberton Mountain Land: A Model of the Elements and Evolution of an Archean Fold Belt: Annex. Trans. Geol. Soc. South Africa., 71, p. 225-253.

Ayres, L.D., 1978, Metamorphism in the Superior Province of Northwestern Ontario and its Relationship to Crustal Development: in Metamorphism in the Canadian Shield, Fraser, J.S., and Haywood, W.W. eds., Geol. Surv. Canada, Paper 78-10, p. 25-36.

-----, 1982a, Pyroclastic Rocks in the Geologic Record: in Ayres, L.D., ed., Pyroclastic Volcanism and Deposits of Cenozoic Intermediate to Felsic Volcanic Islands with Implications for Precambrian Greenstone Volcanoes: Geological Association of Canada, Short Course Notes, v. 2, p. 1-17.

-----, L.D., 1983, Bimodal Volcanism in Archean Greenstone Belts, as Exemplified by Greywacke Composition, Lake Superior Park, Ontario: Canadian Journal of Earth Sciences, v. 20, p. 1168-1194.

Bass, M.N., 1961, Regional Tectonics of Part of the Canadian Shield: Journal of Geology, v. 69, p. 668-702.

Bhatia, M.R., 1983, Plate Tectonics and Geochemical Composition of Sandstones: Journal of Geology, v. 91, p. 611-627.

Blackburn, C.E., 1980, Towards a Mobilist Tectonic Model for Part of the Archean of Northwestern Ontario: Geoscience Canada, v. 7, p. 64-72.

-----, 1981, Kenora-Fort Frances Sheet Map 2443 at 1:253,440: Ontario Dept. of Mines.

Blackburn, C.E., Bond, W.D., Breaks, F.W., Davis, D.W., Edwards, G.R., Poulsen, K.H., Trowell, N.F., and Wood, J., 1985, Evolution of Archean Volcanic-Sedimentary Sequences of the Western Wabigoon Subprovince and its Margins: A Review: in Ayres, L.D., Thurston, P.C., Card, K.D., and Weber. W. eds., Evolution of Archean Supracrustal Sequences: Geological Association of Canada, Special Paper 28. p. 89-117

Borradaile, G.J., 1982, Comparison of Archean Structural Styles in two Belts of the Canadian Superior Province: Precambrian Research, v. 19, p. 179-189.

Bouma, A.H., 1962, Sedimentology of Some Flysch Deposits: Amsterdam, Elsevier Publ. Co., 168 p.

Card, K.D., 1986, Tectonic Setting and Evolution of Late Archean Greenstone Belts of Superior Province, Canada: in Workshop on Tectonic Evolution of Greenstone Belts, eds., de Wit, M.J., and Ashwal, L.D., Lunar and Planetary Institute Technical Report 86-10, p. 74-76.

Card, K.D., and Ciesielski, A., 1986, DNAG#1. Subdivisions of the Superior Province of the Canadian Shield: Geoscience Canada, v. 13, p. 5-13.

Clari, P., and Ghibaudo, G., 1979, Multiple Slump Scars in the Tortonian Type Area (Piedmont Basin, Northwestern Italy): Sedimentology, v. 26, p. 719-730.

Corfu, F., and Stott, G.M., 1985, Geochronology and Tectonic History of the Shebandowan belt, Northwestern Ontario (abstr.), Institute of Lake Superior Geology, 32, p. 15-16.

Daly, R.A., 1936, Origin of Submarine Canyons: Amererican Journal of Science, v. 31, p. 410-420.

Davis, G.H. 1984, Structural Geology of Rocks and Regions: Library of Congress, John Wiley and Sons, New York, 492 p.

Davis, D. W., Corfu, F., and Krough, T.E., 1986, High Precision U-Pb Geochronology and Implications for the Tectonic Evolution of the Superior Province, in Workshop on Tectonic Evolution of Greenstone Belts, eds., de Wit, M.J., and Ashwal, L.D., Lunar and Planetary Institute Technical Report 86-10, p. 77-79.

Davis, D.W., and Edwards, G.R., 1982, Zircon U-Pb ages from the Kakagi Lake area, Wabigoon Subprovince, Northwest Ontario: Canadian Journal of Earth Sciences, v. 19, p. 1235-1245.

Davis, D.W., and Trowell, N.F., 1982, U-Pb Zircon ages from the Eastern Savant Lake-Crow Lake metavolcanic-metasedimentary belt, Northwestern Ontario: Canadian Journal of Earth Sciences, v. 19, p. 868-877.

Davis, D.W., Blackburn C.E., and Krough, T.E. 1982, Zircon U-Pb ages from the Wabigoon-Manitou Lakes region, Wabigoon Subprovince, Northwestern Ontario: Canadian Journal of Earth Sciences, v. 19, p. 254-266.

Davis, D.W., Poulsen, K.H., and Kamo, S.L., 1986, Geochronology of the Southern Rainy Lake Area, Northwestern Ontario. Thirty-second Annual Institute on Lake Superior Geology, Wisconsin Rapids,

Wisconsin, April 29-May 4, 1986, p. 21-22.

Dickinson, W.R., 1970, Interpreting Detrital Modes of Greywacke and Arkose: Journal of Sedimentary Petrology, v. 40, p. 695-707.

Dickinson, W.R., Beard, L.S., Brakenridge, G.R., Erjavec, J.L., Ferguson, R.C., Inman, K.F., Knepp, R.A., Lindberg, F.A., and Ryberg, P.T., 1983, Provenance of North American Phanerozoic Sandstones in Relationship to Tectonic Setting: Geological Society of America Bulletin., v. 94, p. 222-235.

Dickinson, W.R., and Suczek, C.A., 1979, Plate Tectonics and Sandstone Compositions: American Association of Petroleum Geologists Bulletin, v. 63, p. 2164-2182.

Dott, R.H. Jr. 1963, Dynamics of Subaqueous Gravity Depositional Processes: American Association of Petroleum Geologists Bulletin, v. 47. p. 104-128.

Dott, R.H. Jr., 1964, Wacke, Greywacke and Matrix-What Approach to Immature Sandstone Classification?: Journal of Sedementary Petrology, v. 34, p. 625-632.

Dutka, R.J.A., 1982, The Structure and Lithology of the Quetico Metasediments in the Atikokan Area: Unpublished B.Sc. Thesis, Lakehead University, Thunder Bay, Ontario, 102 p.

Fenwick, K.G., 1976, Geology of the Finlayson Lake Area, District of Rainy River: Ontario Division of Mines, Geoscience Report 145, 86 p.

Forel, F., 1885, Les Ravins Sous-lacustre des Fleuves Glaciaires: C. R. Acad. Sci., Paris, v. 101, p. 725-728.

Frantes, J.R., 1987, Petrology and Sedimentation of the Archean Seine Group Conglomerate and Sandstone, Western Wabigoon Belt, Northern Minnesota and Western Ontario: Unpublished M.Sc. Thesis, University of Minnesota, Duluth. 149 p.

Fumerton, S.L., 1980, Geology of the Righteye Lake Area, District of Rainy River: Ontario Geological Survey, Open File Report 5299, 91 p.

-----, 1981, Geology of the Calm Lake area, Districy of Rainy River: Ontario Geological Survey, Open File Report 5351, 119 p.

-----, 1982, Redefinition of the Quetico Fault near Atikokan, Ontario: Canadian Journal of Earth Sciences, v. 19, p. 222-224.

-----, 1986, Geology of the Righteye Lake Area, District of Rainy

River: Ontario Geological Survey Report 239, 57p.
Accompanied by Map 2464, Scale 1:31680 or 1 inch to 1/2 mile.

Goldich, S.S., and Peterman, Z.E., 1980, Geology and Geochemistry of the Rainy Lake Area: Precambrian Research, v. 11, p. 307-327.

Goodwin, A.M., 1968, Archean Protocontinental Growth and Early crustal History of the Canadian Shield: 23rd International Congress, Prague, Proceedings, v. 1, p. 69-89.

-----, 1972, The Superior Province, in Variations in Tectonic Styles in Canada, Price, R.A., and Douglas, R.J.W., eds., Geological Association of Canada, Special Paper II.

Goodwin, A.M., and Shklanka, R., 1967, Archean Volcano-Tectonic Basins: Form and Pattern: Canadian Journal of Earth Sciences, v. 4, p. 777-795.

Grout, F.F., 1925, The Coutchiching Problem: Geological Society of America Bulletin, v. 36, p. 351-364.

Hallam, A., 1981, Facies Interpretation and the Stratigraphic Record: W.H. Freeman and Company, Ltd., San Fransico, California. 292 p.

Harris, F.R., 1974, Geology of the Rainy Lake Area, District of Rainy River: Ontario Division of Mines, Geological Report 115, 94 p.

Hawley, J.E., 1930, Geology of the Spawe Lake Area with Notes on Some Iron and Gold Deposits of Rainy River District: Ontario Department of Mines, Annual Report for 1929, Volume 38, Part 1, p. 1-56.
Accompanied by map 38e, scale 1:47520 or 1 inch to 3/4 mile.

Heezen, B.C. and Ewing, M., 1952, Turbidity Currents and Submarine Slumps and the 1929 Grand Banks Earthquake: American Journal of Science, v. 250, p. 849-873.

Hendry, H.E., 1978, Cap des Rosiers Formation at Grosses Roches, Quebec-Deposits of the Mid-fan Region on an Ordovician Submarine Fan: Canadian Journal of Earth Sciences, v. 15, p. 1472-1488.

Hutton, C.O., 1950, Studies of Heavy Minerals: Bulletin of the Geological Society of America, v. 61:2, p. 635-716.

Jenner, G.A., Fryer, B.J., and McLennan, S.M., 1981, Geochemistry of the Archean Yellowknife Supergroup: Geochimica et Cosmochimica Acta, v. 45, p. 1111-1129.

Jolliffe, A.W., 1955, Geology and Iron Ores of the Steep Rock Lake: Economic Geology, v. 50, p. 373-398.

Kamineni, D.C., and Stone, D., 1983, The Ages of Fractures in the Eye-Dashwa Pluton, Atikokan, Canada: Contributions to Mineralogy and Petrology, v. 83, p. 237-246.

Kehlenbeck, M.M., 1976, Nature of the Quetico-Wabigoon Boundary in the de Courcey-Smiley Lakes Area, Northwestern Ontario: Canadian Journal of Earth Sciences, v. 13. p. 737-748.

-----, 1985, Folds and Folding in the Beardmore-Geraldton Fold Belt, Canadian Journal of Earth Sciences, v. 23, p. 158-191.

Krough, T.E., 1982, Improved Accuracy of U-Pb Zircon ages by the Creation of More Concordant Systems Using an Air Abrasion Technique: Geochimica et Cosmochimica Acta, v. 46, p. 637-649.

Krough, T.E., and Turek, A., 1982, Precise U-Pb Zircon Ages from the Gamitogama Greenstone Belt, Southern Superior Province: Canadian Journal of Earth Sciences, v. 19, p. 859-867.

Kuenen, Ph.H., 1950, Turbidity Currents of High Density: 18th International Geological Congress, London, Reports, Part 8, p. 44-52.

Kuenen, Ph.H., and Migliorini, C.I., 1950, Turbidity Currents as Cause of Graded Bedding: Journal of Geology, v. 58, p. 91-121.

Kuenzi, W.D., Horst, O.H., and McGehee, R.V., 1979, Effect of Volcanic Activity on Fluvial-Deltaic Sedimentation in a Modern Arc-Trench Gap, Southwestern Guatemala: Geological Society of America Bulletin, v. 90, p. 827-838.

Langford, F.F, and Morin, J.A., 1976, The Development of the Superior Province of Northwestern Ontario by Merging Island Arcs: American Journal of Science, v. 276, p. 1023-1034.

Lawson, A.C., 1888, Report on the Geology of the Rainy Lake Region: Geology and Natural History Survey of Canada, Annual Report, N.S., v. III, Part 1, 180 p.

-----, 1913, The Archean Geology of the Rainy Lake, Restudied: Geological Survey of Canada Memoir, 40, 115 p.

Lehto, D.A.W., 1974, Structural and Petrological Evolution of the Quetico Gneiss Belt in the Dog-Hawkeye Lakes area: Unpublished B.Sc. thesis, Lakehead University, Thunder Bay, Ontario, 92 p.

Le Pichon, X., Angelier, J., and Sibuet, J-C., 1982, Plate Boundaries and Extensional Tectonics: Tectonophysics, v. 81, p. 239-256.

Mackasey, W.O., Blackburn, C.E., and Trowell, N.F., 1974, A Regional

Approach to the Wabigoon-Quetico Belts and its Bearing on Exploration in Northwestern Ontario: Ontario Division of Mines, Miscellaneous Paper 58, 29 p.

McLennan, S.M., 1984, Petrological Characteristics of Archean Greywackes: Journal of Sedimentary Petrology, v. 54, p. 889-898.

McIlwaine, W.H., and Hillary, E.M., 1974, West Half of Spawe Lake Area, District of Rainy River: in Summary of Field Work, 1974, Ontario Division of Mines, MP 59, p. 65-69.

Middleton, G.V., 1967, Experiments on Density and Turbidity Currents III. Deposition of Sediment: Canadian Journal of Earth Science, v. 4, p. 475-505.

Middleton, G.V., and Hampton, M.A., 1973, Part 1, Sediment Gravity Flows: Mechanics of Flow and Deposition: in Turbidites and Deep Water, SEPM Pacific Section, Short Course, Middleton, G.V., and Bouma, A.H., eds., p. 1-38.

Moore, E.S., 1940, Geology and Ore Deposits of the Atikokan Area, District of Rainy River: Ontario Department of Mines, Annual Report for 1939, v. 48, part 2, p. 1-34.

Mutti, E., and Ghibaudo, G., 1972, Un Esempio di Torbiditi di Conoide Sottomarina Esterna: Le Arenarie di San Salvatore (Formazione di Bobbio, Miocene) nell' Appennino de Piacenza: Memorie dell' Accademia delle Scienze di Torino, Classe di Scienze Fisiche, Matematiche e Naturali, Series 4, No. 16, 40 p.

Mutti, E., and Ricci-Lucchi, F., 1972, Le Torbiditi dell' Appenino Settentrionale: Introduzione all' analisi di Facies: Memorie Soc. Geol. Italiana, v. 11, p. 161-199.

Normark, W.R., 1970, Growth Patterns of Deep Sea Fans: American Association of Petroleum Geologists, Bulletin, v. 54, p. 2170-2195.

-----, 1978, Fan-valleys, Channels and Depositional Lobes on Modern Submarine Fans: Characteristics for the Recognition of Sandy Turbidite Environments: American Association of Petroleum Geologists, Bulletin, v. 61, p. 912-931.

Ojakangas, R.W., 1968, Cretaceous Sedimentation, Sacramento Valley, California: Geological Society of America Bulletin, v. 79, p. 973-1008.

-----, 1972a, Archean Volcanogenic Greywackes of the Vermillion District, Northeastern Minnesota: Geological Society of America Bulletin, v. 83, p. 429-442.

-----, 1972b, Greywackes and Related Rocks of the Knife Lake Group and Lake Vermillion Formation, Vermillion District: in Sims, P.K., and Morey, G.B., eds., Geology of Minnesota: A Centennial Volume: Minnesota Geological Survey, p. 82-90.

-----, 1985, Review of Archean Clastic Sedimentation, Canadian Shield: Major Felsic Volcanic Contribution to Turbidite and Alluvial Fan-fluvial Facies Associations: in Ayres, L.D., Thurston, P.C., Card, K.D., and Weber, W., eds., Evolution of Archean Supracrustal Sequences, Geological Association of Canada, Special Paper, 28, p. 23-47.

Percival, J.A., 1983, Preliminary Results of Geological Synthesis in the Western Superior Province: in Current Research, Part A, Geological Survey of Canada, Paper 83-1A, p. 125-131.

Percival, J.A., and Stern, R.A., 1984, Geological Synthesis in the Western Superior Province, Ontario: in Current Research, Part A, Geological Survey of Canada, Paper 84-1A, p. 397-408.

Percival, J.A., Stern, R.A., and Digel, M.A., 1985, Regional Geological Synthesis of Western Superior Province, Ontario; Project 820006: in Current Research, Part A, Geological Survey of Canada, Paper 85-1A, p. 385-397.

Percival, J.A., and Sullivan, R.W., 1986, Age Constaints on the Evolution of the Quetico Belt, Superior Province, Ontario: in Workshop on Tectonic Evolution of Greenstone Belts, eds., de Wit, and Ashwal, L.D., Lunar and Planetary Institute Technical Report 86-10, p. 167-169.

Pettijohn, F.J., 1943, Archean Sedimentation: Geological Survey of American Bulletin, v. 54, p. 925-972.

Pettijohn, F.J., Potter, P.E., and Siever, R., 1972, Sand and Sandstone: New York, Springer-Verlag, 618 p.

Pirie, J., and Mackasey, W.O., 1978, Preliminary Examination of Metamorphism in parts of Quetico Metasedimentary Belt, Superior Province, Ontario: in Metamorphism in the Canadian Shield, Geological Survey of Canada, Paper 78-10, p. 37-48.

Poldervaart, A., 1955, Zircons in Rocks 1 Sedimentary Rocks: American Journal of Science, v. 253, p. 433-461.

Poulsen, K.H., 1982, Archean Tectonic Evolution at a Subprovince Boundary, Rainy Lake, Ontario: Geological Association of Canada, Program with Abstracts, v. 7, p. 74.

-----, 1984, The Geological Setting of Mineralization in the Mine Centre-Fort Frances area, District of Rainy River, Ontario:

-----, 1986, Rainy Lake Wrench Zone: An Example of an Archean Subprovince Boundary in Northwestern Ontario: in Workshop on Tectonic Evolution of Greenstone Belts, eds., de Wit, M.J. and Ashwal, L.D., Lunar and Planetary Institute Technical Report 86-10, p. 177-179.

Poulsen, K.H., Borradaile, G.J., and Kehlenbeck, M.M., An Inverted Archean Succession at Rainy Lake, Ontario: Canadian Journal of Earth Sciences, v. 17, p. 1358-1369.

Pye, E.G., and Fenwick, E.G., 1965, Atikokan-Lakehead Sheet, Kenora, Rainy River and Thunder Bay Districts, Ontario Dept. of Mines, Geological Compilation Series, Map 2065, Scale 1:253440 or 1 inch to 4 miles.

Sawyer, E.W., 1983, The Structural History of a Part of the Archean Quetico Metasedimentary Belt, Superior Province, Canada: Precambrian Research, v. 22, p. 271-294.

-----1986, The Influence of Source Rock Types, Chemical Weathering and Sorting on the Geochemistry of Clastic Sediments from the Quetico Metasedimentary Belt, Superior Province, Ontario: Chemical Geology, v. 55, p. 77-95.

Shklanka, R., 1972, Geology of the Steep Rock Lake Area, District of Rainy River: Ontario Department of Mines and Northern Affairs, Geological Report 93, 114 p. Accompanied by Map 2217, scale 1:1200 or 1 inch to 4 miles.

Sigurdsson, H., 1982a, Volcanogenic Sediments in Island Arcs: in Ayres L.D., ed., Pyroclastic Volcanism and Deposits of Cenozoic Intermediate to Felsic Volcanic Islands with Implications for Precambrian Greenstone Belt Volcanoes: Geological Association of Canada, Short Course Notes, v. 2, p. 221-293.

-----,1982b, Subaqueous Volcanic Sediments in Ocean Basins: in Ayres L.D., ed., Pyroclastic Volcanism and Deposits of Cenozoic Intermediate to Felsic Volcanic Islands with Implications for Precambrian Greenstone Belt Volcanoes: Geological Association of Canada, Short Course Notes, v. 2, p. 294-342.

Smith, W.H., and McInnes, 1897, Seine River Sheet, Thunder Bay and Rainy River Districts, Ontario: Geologic Survey of Canada, Map 560, scale 1 inch to 4 miles.

Smyth, H.L., 1891, Structural Geology of Steep Rock Lake, Ontario: American Journal of Science, 3rd Series, v. 42.

Stewart, R.W., 1984, The Structure and Lithology of the Quetico Metasediments in the Chub Lake-Little McCaulay Lake Area: Unpublished B.Sc. Thesis, Lakehead University, Thunder Bay, Ontario, 64 p.

Stone, D., Kamineni, D.C., Shanks, B., and Jackson, M., 1986, Atomic Energy of Canada Ltd. Open File 1221.

Tanton, T.L., 1926, Recognition of the Coutchiching near Steep Rock Lake, Ontario: Royal Society of Canadian Trans., Sec. 4, Series 3, 20, p. 39-49.

Taylor, S.R., and McLennan, S.M., 1981, The Rare Earth Element Evidence in Precambrian Sedimentary Rocks: Implications for Crustal Evolution: in Kroner, A., ed., Precambrian Plate Tectonics: Amsterdam, Elsevier, p. 527-548.

Taylor, S.R., and McLennan, S.M., 1985, The Continental Crust: its Composition and Evolution: Blackwell Scientific Publications Inc. Palo Alto, California, 312 p.

Turek, A., Smith, P.E., and Van Schmus, W.R., 1984, U-Pb Zircon Ages and the Evolution of the Michipicoten Plutonic-Volcanic Terrane of the Superior Province, Ontario: Canadian Journal of Earth Sciences, v. 21, p. 457-464.

Van Hise and others, 1905, Report of the Special Committee for the Lake Superior Region (pre-Cambrian nomenclature): Journal of Geology, v. 13, p. 89-104.

Walker, R.G., 1967, Turbidite Sedimentary Structures and their Relationship to Proximal and Distal Depositional Environments: Journal of Sedimentary Petrology, v. 37, p. 25-43.

-----, 1970, Review of the Geometry and Facies Organization of Turbidites and Turbidite-bearing Basins: in Lajoie, J., ed., Flysch Sedimentology in North America: Geological Association of Canada Special Paper 7, p. 219-251.

-----, 1973, Mopping-up the Turbidite Mess. A History of the Turbidity Current Concept: in Ginsberg, R.N., ed., Evolving Concepts in Sedimentology: Baltimore, John Hopkins University Press, p. 1-37.

-----, 1975, Generalized Facies Models for Resedimented Conglomerates of Turbidite Association: Geological Society of America Bulletin, v. 86, p. 737-748.

-----, 1976, Facies Model 2. Turbidites and Associated Coarse Clastic Deposits: Geoscience Canada, v. 3, p. 25-36.

-----, 1984, ed., Turbidites and Associated Coarse Clastic Deposits: Geoscience Canada, Reprint Series 1. Facies Models, Second Edition. p. 171-188.

Walker, R.G., and Mutti, E., 1973, Part IV, Turbidite Facies and Facies Associations: in Turbidites and Deep Water Sedimentation, SEPM Pacific Section Shoet Course, Middleton, G.V. and Bouma, A.H., eds., p. 119-158.

Walker, R.G., and Pettijohn, F.J., 1971, Archean Sedimentation: Analysis of the Minnitaki Basin, Northwestern Ontario, Canada: Geological Society of Canada Bulletin, v. 82, p. 2099-2130.

Wood, J., 1980, Epiclastic Sedimentation and Stratigraphy in the North Spirit Lake and Rainy Lake Areas: A Comparison: Precambrian Research, v. 12, p. 227-255.

Young, W.L., 1960, Geology of the Bennet-Tanner Area, Rainy River District, Ontario: Ontario Department of Mines, Annual Report for 1960, v. 69, p. 1-16. Accompanied by Map 1960b, scale 1:31680 or 1 inch to 1/2 mile.

APPENDIX

SAMPLE	LOCATION OF POINT-COUNTED SAMPLE
2B1	Sample taken on west side of HWY 11B, 300 metres north of turnoff to Atikokan.
3A1	Sample taken on west side of HWY 11B, 500 metres north of turnoff to Atikokan.
3A2	Same location as 3A1.
3A3b	Same location as 3A1.
3AZ	Same location as 3A1.
3BZ	Sample taken on west side of HWY 11B, 550 metres north of turnoff to Atikokan.
4A1	Sample taken on west side of HWY 11B, 700 metres north of turnoff to Atikokan.
4DZ	Sample taken on west side of HWY 11B, 900 metres north of turnoff to Atikokan.
4D1	Same location as 4DZ.
5C2	Sample taken on west side of HWY 11B, 1 km north of turnoff to Atikokan.
6A2	Sample taken on west side of HWY 11B, 1100 metres north of turnoff to Atikokan.
6C1	Sample taken on east side of HWY 11B, 1200 metres north of turnoff to Atikokan.
6C2	Same location as 6C1.
7A2	Sample taken on east side of HWY 11B, 1.5 km north of turnoff to Atikokan.
11AZ	Sample taken on south side of HWY 11, 1.5 km east of Kemuel L.
13A2	Sample taken on north side of HWY 11, 200 metres east of turnoff to Caribus Lake.
15C1	Sample taken on south side of HWY 11 at turnoff to Caribus L.
15CZ	Same location as 15C1.

SAMPLE	LOCATION OF POINT-COUNTED SAMPLES
19D1	Sample taken on south side of HWY 11, 900 metres east of gravel road leading to cottages on Lerome L.
24A1	Sample taken on north side of HWY 11, 200 metres west of gravel road leading to cottages on Lerome L.
24A2	Same location as 24A1.
27BZ	Sample taken on north side of HWY 11, directly across from gravel road leading to boat ramp at Lerome L.
29B1	Sample taken on north side of HWY 11, 600 metres west of gravel road leading to boat ramp at Lerome L.
30C1	Sample taken on south side of HWY 11, 1 km west of gravel road leading to boat ramp at Lerome L.
33AZ	Sample taken on north side of HWY 11, 1 km east of where the highway crosses Jackfish Creek.
35BZ	Sample taken on north side of HWY 11, 1 km west of where the highway crosses Jackfish Creek.
36CZ	Sample taken on north side of HWY 11, 1.5 km east of gravel road to Perch Lake Resort.
37BZ	Sample taken on south side of HWY 11, 500 metres west of gravel road leading to Perch Lake Resort.
41C1	Sample taken on north side side of Hwy 11, 100 metres east of gravel road leading to McCaulay Lake Resort.
44B1	Sample taken on north side of HWY 11, 200 metres west of gravel road to McCaulay Lake.
44C1	Sample taken on south side of HWY 11, 200 metres west of gravel road to McCaulay L.
45CZ	Sample taken on south side of HWY 11, 2 km west of gravel road to McCaulay L.
101BZ	Sample taken on south side of HWY 11, 1 km west of Flanders road.
101DZ	Sample taken on north side of HWY 11, 1200 metres west of Flanders road.

SAMPLE	LOCATION OF POINT-COUNTED SAMPLE
101EZ	Sample taken on north side of HWY 11, 1300 metres west of Flanders Road.
103BZ	Sample taken on north side of HWY 11, 2 km west of Flanders Road.
103C1	Sample taken on south side of HWY 11, 2 km west of Flanders Road.
103C2	Same location as 103C1.
104AZ	Sample taken on north side of HWY 11, 200 metres east of where Quetico Fault crosses the highway.
202I	Sample taken on south shore of the Seine River where it enters Calm L.
206I	Sample taken on south shore of the Seine River where it enters Banning L.